(12)

AD A138285

DNA-TR-81-270

THE MICROSTRUCTURE THEORY FOR THREE DIMENSIONAL PLASMA TRANSPORT

C.W. Prettie
S.Y.F. Chu
J.B. Workman
Berkeley Research Associates, Inc.
P.O. Box 983
Berkeley, California 94701

1 May 1983

Technical Report

CONTRACT No. DNA 001-81-C-0061

APPROVED FOR PUBLIC RELEASE;
DISTRIBUTION UNLIMITED.

THIS WORK WAS SPONSORED BY THE DEFENSE NUCLEAR AGENCY
UNDER RDT&E RMSS CODE B322082466 S99QAXHC00054 H2590D.

Prepared for
Director
DEFENSE NUCLEAR AGENCY
Washington, DC 20305

Destroy this report when it is no longer needed. Do not return to sender.

PLEASE NOTIFY THE DEFENSE NUCLEAR AGENCY, ATTN: STTI, WASHINGTON, D.C. 20305, IF YOUR ADDRESS IS INCORRECT, IF YOU WISH TO BE DELETED FROM THE DISTRIBUTION LIST, OR IF THE ADDRESSEE IS NO LONGER EMPLOYED BY YOUR ORGANIZATION.

UNCLASSIFIED

SECURITY CLASSIFICATION OF THIS PAGE (When Data Entered)

REPORT DOCUMENTATION PAGE		READ INSTRUCTIONS BEFORE COMPLETING FORM
1. REPORT NUMBER DNA-TR-81-270	2. GOVT ACCESSION NO. AD-A138 285	3. RECIPIENT'S CATALOG NUMBER
4. TITLE (and Subtitle) THE MICROSTRUCTURE THEORY FOR THREE DIMENSIONAL PLASMA TRANSPORT		5. TYPE OF REPORT & PERIOD COVERED Technical Report 6. PERFORMING ORG. REPORT NUMBER PD-BRA-83-295R
7. AUTHOR(s) C.W. Prettie S.Y.F. Chu J.B. Workman		8. CONTRACT OR GRANT NUMBER(s) DNA 001-81-C-0061
9. PERFORMING ORGANIZATION NAME AND ADDRESS Berkeley Research Associates, Inc. P.O. Box 983 Berkeley, California 94701		10. PROGRAM ELEMENT, PROJECT, TASK AREA & WORK UNIT NUMBERS Task S99QAXHC-00054
11. CONTROLLING OFFICE NAME AND ADDRESS Director Defense Nuclear Agency Washington, DC 20305		12. REPORT DATE 1 May 1983 13. NUMBER OF PAGES 130
14. MONITORING AGENCY NAME & ADDRESS(if different from Controlling Office)		15. SECURITY CLASS (of this report) UNCLASSIFIED 15a. DECLASSIFICATION/DOWNGRADING SCHEDULE N/A since UNCLASSIFIED

16. DISTRIBUTION STATEMENT (of this Report)

Approved for public release; distribution unlimited.

17. DISTRIBUTION STATEMENT (of the abstract entered in Block 20, if different from Report)

18. SUPPLEMENTARY NOTES

This work was sponsored by the Defense Nuclear Agency under RDT&E RMSS Code B322082466 S99QAXHC00054 H2590D.

19. KEY WORDS (Continue on reverse side if necessary and identify by block number)

SCENARIO	Gradient Drift
Plasma	Microstructure
Electrostatic	HANE
Stochastic	Ionosphere

20. ABSTRACT (Continue on reverse side if necessary and identify by block number)

Microstructure theory is a stochastic approach to plasma simulation which accounts for structures unresolved by sampling. A stochastic approach to plasma simulation is called for by the need to address a large range of plasma structure scale sizes in the simulation of high-altitude nuclear environments.

The microstructure approach to a 2-dimensional split-step numerical simulation of electrostatic plasma evolution is presented with comparison to

DD FORM 1 JAN 73 1473 EDITION OF 1 NOV 65 IS OBSOLETE

UNCLASSIFIED

SECURITY CLASSIFICATION OF THIS PAGE (When Data Entered)

20. ABSTRACT (Continued)

the classical split-step approach. The primary difference between the two approaches rests in the assumed dependence of the plasma conductivity upon plasma density statistics. Justification for the microstructure conductivity assumption from numerical experiments is presented. Numerical simulations of barium-like plasma clouds and nuclear clouds under the influence of radial winds are presented which illustrate physically realistic results. Numerical considerations are also discussed.

In extensions of microstructure theory from 2-dimensional plasma evolution to 3-dimensional transverse transport the nature of the correlation of plasma structure along magnetic field lines is a key consideration. For the case of complete correlation, i.e., correlation with a correlation coefficient of ±1, three-dimensional algorithms are developed and implemented in a version of SCENARIO. The algorithms are physically appealing in form, reflecting many of the expected attributes of gradient-drift phenomena. The results of a Cheyenne Mt. calculation are given. Schemes for developing algorithms for uncorrelated and partially correlated structure are also suggested.

PREFACE

The authors would like to explicitly acknowledge the technical guidance of Major Leon A. Wittwer of DNA/RAAE and the benefit of close interactions with Dr. Robert Stagat and Dr. Ralph Kilb of Mission Research Corporation in the development of the material presented in this report.

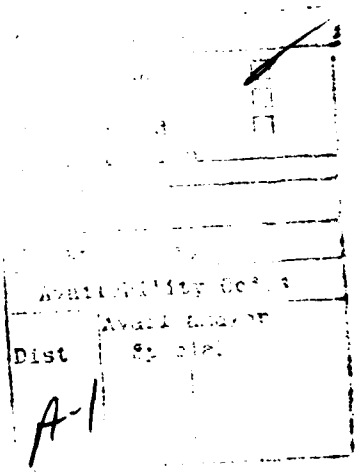

TABLE OF CONTENTS

LIST OF ILLUSTRATIONS

LIST OF ILLUSTRATIONS (Continued)

LIST OF ILLUSTRATIONS (Concluded)

SECTION 1

INTRODUCTION

The proper simulation of plasma transport in three dimensions is a crucial issue in the construction of a numerical model for the high altitude nuclear environment (HANE). As a rule, the digital simulation of the system of spatial equations, which describe the physics, requires that all fluctuations of the simulated quantities be resolved. In general, HANE simulations cannot meet this requirement because the range of relevant scale sizes can extend to six orders of magnitude. The practical limitations of computer storage and cost will, typically, constrain a three dimensional numerical code to a scale size range of one to one-and-one half orders of magnitude in each dimension. At this sampling rate, only the larger structures can be resolved. Historically, HANE plasma simulation algorithms, as employed in codes such as MELT, spatially resolve the large scales, but are forced to ignore a vast range of small scales. It is, of course, generally acknowledged that the small scales are important to satellite and IR systems effects modelling, but their interaction with the large scale flow has been generally neglected in codes such as MELT. The importance of small scale structure effects has motivated the development of a theory of microstructure generation and transport.

In recent years, a theory of microstructure generation and transport, based on the gradient drift mechanism, has been developed which is capable of addressing the scale size range problem in computer simulation. The numerical algorithms which derive from this microstructure theory have

been incorporated into the nuclear effects simulation SCENARIO code. In terms of general code architecture, SCENARIO may be viewed as an engineering version of MELT. The principal purpose of the code is to provide three-dimensional plasma environments for subsequent systems analysis of satellite communications effects. In the present context, the code is serving as a research vehicle for developing and applying the microstructure theory. This paper focuses upon the crossfield transport implemented in the code which represents the recent advances in the theory.

Microstructure theory can be regarded as the application of stochastic techniques to spatial simulation problems. The application of stochastic theory to the HANE plasma problem originated with research by Workman and Chu in 1975. Utilizing the principle of conservation of plasma power (the square of electron density), the early work tied the physical space numerical concepts into the Fourier space data base (as expressed in a power spectral density curve). The first theoretical and numerical model concentrated on the evolution of plasma scale size in Fourier space (Workman and Chu, 1978). This paper has stimulated other interesting research into the Fourier space evolution of plasma power, notably the outstanding experimental work by Pongratz and Fitzgerald (1981).

The early microstructure work was followed by the development of transport algorithms for the evolution of both mean plasma density and density variance. This modelling accounted for the effect of microstructure generation on gross plasma structures and flow (Workman, Chu, and Ferrante, 1979). The important concept of the flow of plasma power from macrostructure scales to

microstructure scales in a conserved manner was extensively developed in this work. The introduction of the "Haerendel velocity" approximation as a suitable vehicle for furthering the theoretical development was made by Workman in connection with the work.

A significant advance in the analytic development of microstructure theory towards a more formal and rigorous stochastic approach was undertaken by Stagat in 1979. The "smooth current" approximation in his work provided both a more complete statement of the Haerendel velocity model and, more important, laid the groundwork for a self consistent and elegant mathematical formulation of the general problem. Further developments (as reported in Stagat, et al., 1982) have formed the starting point for all subsequent work.

This paper is directed at recent developments in microstructure theory, but is organized, in its derivation of results from basic principles, to be a self contained document. That is, while the reader is encouraged to study the earlier work for the physical insight that has led to current theory, the objective here is to present a complete development of the work as it now stands.

The application of stochastic theory to the equations for the evolution of 2-dimensional plasmas, as discussed in Section 2, leads to further understanding of the implications of the "Haerendel velocity" and the "smooth current" or "smooth J" assumptions in terms of the correlation properties assumed between the stochastic quantities of the problem and in terms of the modifications to the effective conductivity that are assumed to be caused by microstructure. Two-dimensional algorithms are developed based on this theory and are applied to the 2-dimensional evolution both of a barium ion cloud and a nuclear plasma under the influence of radial heave winds.

In Section 3 the rigorous approach used to develop the 2-dimensional algorithms in Section 2 are extended to the problem of 3-dimensional transverse transport. The transverse transport aspects of 3-dimensional late-time HANE plasmas are very similar to the transport and evolution of 2-dimensional plasmas. Assumptions about the structure correlation properties in the parallel-to-the-field direction are needed in the 3-dimensional HANE problem to remove this dimension from the problem, but once this removal has been accomplished the two problems are nearly identical. Different transport algorithms arise from different assumptions and several possible assumptions are considered in Section 3. Algorithms based on one promising set of assumptions have been developed and implemented in a version of SCENARIO. Results from a trial run are presented.

Section 4 presents conclusions as well as other issues into which further extension of the theory is possible.

SECTION 2

MICROSTRUCTURE THEORY APPLIED TO 2-DIMENSIONAL PLASMA EVOLUTION

2-1 CLASSICAL SPLIT STEP ALGORITHM FOR 2-DIMENSIONAL PLASMA EVOLUTION

Classical modelling of 2-dimensional plasma evolution is performed using split-step algorithms that are characterized by the computational flow schematized in Figure 2-1. Two key steps seen in the figure are the potential solving step and the convection step. Given a specification for the spatially varying conductivity, the potential step finds the current flow and electric field patterns produced by plasma driving forces. The plasma motion is described by electron Hall drift ($E \times B$ motion) and thus electric field determination is equivalent to plasma velocity determination. Given the results of the potential equation solution, the plasma flow is known and can be used to advance plasma density parameters through an increment in time in the convection step. The changes in plasma density cause corresponding changes in the plasma conductivity which are provided to the potential solver through the conductivity relation for the start of the next split-step cycle.

For the classical case the conductivity relation is a simple proportionality and is, thus, not often singled out in classical split-step descriptions as it is in Figure 2-1. Portraying it as an explicit step in this instance provides an early insight into the importance this relation has in microstructure algorithms. Microstructure algorithms for plasma evolution can be regarded as an extension of the split-step scheme shown in Figure 2-1, as will be discussed

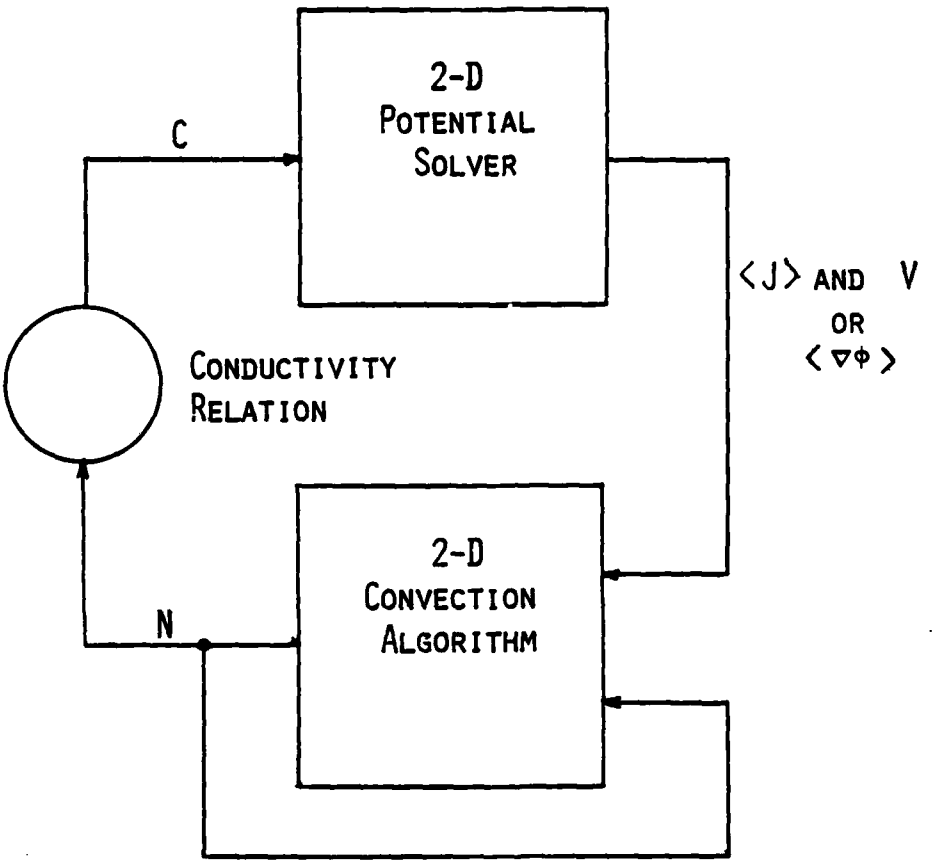

POTENTIAL Eq: $\nabla \cdot C \nabla \phi = \nabla \cdot C(V \times I_Z)$

CONVECTION Eq: $\partial_T N + \nabla \cdot NU = 0$

CONDUCTIVITY Eq: $C = eN/\mu B$

Figure 2-1. Classical 2-d split step algorithm for plasma evolution.

later. It is appropriate to discuss in this section the background of the relations behind the steps portrayed.

A key physical parameter in plasma evolution behavior is the plasma current density, J. Plasma currents are driven by imbalances between the forces acting on the electron fluid and the forces acting on the ion fluid. Currents are driven not only by the conventional electromagnetic field forces but also by neutral wind, pressure, gravity, and centrifugal acceleration forces. For the late time HANE plasma situation the electromagnetic field forces and the neutral wind forces frequently dominate plasma behavior. For the sake of simplicity this report will concentrate on these two forces. The results obtained, it should be noted, are easily generalizable to a more complete list of HANE forces.

The ionospheric current response to a combination of electric and neutral wind forces is approximated in this report with the relation

$$J = \frac{eN}{\mu B}\left(\frac{E}{B} + V \times i_z\right) \qquad (2.1)$$

where e is the electronic charge, N is the plasma density, μ is the ionic mobility through the neutral air background, V is the neutral wind, E is the electric field and B is the magnetic field intensity and where the magnetic field is assumed to be constant and directed in the z-direction. For the two-dimensional evolution problem the quantities N, E and V are assumed to vary only in the x- and y-directions. The quantity i_z represents the unit normal vector in the z-direction. Note that $eN/\mu B$ can be identified as the plasma conductivity.

The above current response is found from an evaluation of the difference between ion and electron fluxes in response to electromagnetic field and wind forces. The electron velocity is assumed to be essentially independent of the wind forces. The electron mobility in the background air is also assumed to be very high implying

$$U_e = E \times i_z/B \tag{2.2}$$

where U_e is the electron velocity.

The ion velocity is evaluated from the momentum or force balance equation. A force balance equation between the ion drag in a neutral gas and an imposed electric field produces the simple proportionality relation

$$U_i = \mu E \tag{2.3}$$

where U_i is the ion velocity and where again μ is the ionic mobility in the gas. If the neutral gas is not at rest but is moving with velocity V then the drag relation becomes

$$U_i - V = \mu E \tag{2.4}$$

Heuristically it is not expected that ions could differentiate between electromagnetic forces that are purely electrostatic and forces that include magnetic fields. This argument justifies use of the above expression for the more general case of having a magnetic field present with the electric field E in (2.4) substituted with $E + U_i \times B$ giving

$$U_i - V = \mu(E + U_i \times B) \tag{2.5}$$

Algebraic manipulation of this equation to isolate U_i produces the well known result

$$U_i = \frac{(\mu B)^2}{1 + (\mu B)^2} \frac{E}{B} \times i_z + \frac{\mu B}{1 + (\mu B)^2} \frac{E}{B}$$

$$+ \frac{\mu B}{1 + (\mu B)^2} V \times i_z + \frac{1}{1 + (\mu B)^2} V \qquad (2.6)$$

The ion velocity for large μB is essentially $E \times B/B^2$ and thus very close to the electron velocity. The small differences between the ion velocity and the electron velocity are the source of plasma currents. The difference between ion and electron velocity can be seen to be

$$U_i - U_e = - \frac{1}{1 + (\mu B)^2} \frac{E}{B} \times i_z + \frac{\mu B}{1 + (\mu B)^2} \frac{E}{B}$$

$$+ \frac{\mu B}{1 + (\mu B)^2} V \times i_z + \frac{1}{1 + (\mu B)^2} V \qquad (2.7)$$

which for large μB produces the approximate current relation presented earlier in the discussion.

As mentioned previously plasma motion is taken as synonymous to electron motion which is affected only by the electric field. The mechanism by which wind forces move a plasma irregularity must thus be through the electric fields it generates as there are no explicit wind terms in the electron velocity. The mechanism by which the wind generates electric fields is through the current that it drives. Where the wind current encounters gradients in density its flow is modified so that it is no longer divergenceless. Charge density source regions and sink regions are created which build up charge. This build up continues over the period of

typically milliseconds until the associated electric fields build up to a point where electrically driven currents bleed off the charge sources and sinks. The balance between the wind current produced charge sources and sinks and the electric field driven current is specified by the relation

$$\nabla \cdot C\, E/B = - \nabla \cdot CV \times i_z \tag{2.8}$$

where C, the conductivity, is given by $eN/\mu B$. Thus the plasma flow in response to applied wind forces is established through the creation of a polarization field which can be found through the above equation. The additional assumption that $\nabla \times E = -\partial B/\partial t = 0$ is made for late time electrostatic flow which facilitates solution for E in terms of a potential function, ϕ. The resulting relations are

$$\begin{aligned} E/B &= - \nabla\phi \\ \nabla \cdot C\nabla\phi &= \nabla \cdot C\, V \times i_z \end{aligned} \tag{2.9}$$

where C and V are known functions of x and y and where ϕ is to be found. The potential ϕ is found through these relations in the potential step algorithm.

The convection step algorithm uses the plasma continuity equation with the known plasma flow to update the plasma density. The continuity relation is given by

$$\frac{\partial N}{\partial t} + \nabla \cdot NU = 0 \tag{2.10}$$

where U is the plasma flow velocity given by $E \times i_z/B$. The continuity equation is basically a restatement of the conservation of electrons. The only source of local density changes is assumed to be variations of the fluxes into and

out of a region. The continuity expression can also be written in terms of the current density J

$$\frac{\partial N}{\partial t} + \nabla \cdot \left(\frac{J \mu B}{e} \times i_z + N V \right) = 0 \qquad (2.11)$$

This form of the continuity expression is sometimes more useful for microstructure transport considerations.

The background relations for a complete cycle of the split step algorithm have thus been presented. The relation between the local density and the plasma conductivity is obtained from the current relationship with applied electric field and wind forces. The plasma motion determined by the potential step is found by balancing the plasma charge buildup and depletion caused by wind current divergences with electric current flows produced by electric fields. The flow quantities calculated are then used with the conservation principle to update plasma densities. The next section discusses how these steps are modified to account for the presence of microstructure.

2-2 APPLICATION OF STOCHASTIC THEORY TO THE TWO-DIMENSIONAL SPLIT-STEP ALGORITHM

In the previous section a description of the classical split-step approach to the simulation of plasma evolution is presented. In this section the basic refinements provided by the application of microstructure theory to the plasma transport algorithms are discussed.

The application of microstructure theory to the plasma evolution problem is motivated by one primary concern, namely fine scale plasma structure. Fine scale plasma structure with sizes down to the order of 100 meters is produced over

spatial extents of hundreds of kilometers by high altitude nuclear explosions. Its location intensity and spatial characteristics are important for the prediction of satellite communications effects. Because of the complex and seemingly chaotic nature of the HANE structure, stochastic descriptions of it are used to predict satellite communications effects. Only a few statistics of the fine scale structure are required to provide reliable estimates of satcom system performance and these statistics are believed to be nearly constant over many kilometer regions.

It is virtually impossible to grid HANE numerical computations fine enough to resolve the fine-scale structure details because of storage limitations. Classical techniques merely grid as fine as costs and storage limitations permit and ignore the presence of plasma density and velocity fluctuations varying faster than the spatial Nyquist rate. These approaches do not specify where the very important fine scale density fluctuations exist and they ignore any possible effects of the fine scale structure on transport. Microstructure theory was developed to address these deficiencies in the classical techniques.

Microstructure theory treats the plasma evolution equations on a stochastic basis. Numerical algorithms are used with sampling grids that have roughly the same resolution as the classical problem and that cannot resolve the fine scale structure on a deterministic basis. Rather than ignore the presence of the fine scale fluctuations, the microstructure approach treats structure unresolved by the sampling grid on a stochastic basis and describes its characteristics through its statistics. (Structure unresolved by the sampling grid when approached on a stochastic basis is what is meant by the

term 'microstructure.') By adopting a stochastic approach to the problem, transport algorithms for structure location and intensity can be developed for satcom effects predictions; the influence of fine scale structure upon bulk plasma motion can be investigated; and an understanding of the implicit assumptions behind the classical approach can be developed.

Microstructure theory provides refinements to the classical plasma evolution algorithms which are evident in a comparison of Figure 2-1 with Figure 2-2, the latter of which illustrates the microstructure split-step algorithms. The potential solving steps of both algorithms are the same. Both produce plasma flow parameters for the convection step from the specified spatial dependence of conductivity. The fundamental difference between the two algorithms is that the conductivity specified for the microstructure algorithm is a function of multiple statistical parameters instead of the one parameter of plasma density used in the classical algorithm. Further, in order to supply the spatial dependence of these multiple parameters it is necessary for the microstructure convection algorithm to convect multiple statistical quantities.

The refinements to the classical algorithm provided by the microstructure approach are based upon the premises that fine scale structure changes the conductivity from the value determined by the mean plasma density in a cell and that by specifying statistical quantities in addition to the mean a better approximation to the actual conductivity may be obtained. Specifying one or two additional quantities requires a loss in the linear scale resolution which is small in comparison to the gain in the accuracy of bulk plasma convection and which is virtually inconsequental in view of the distinct advantage of being able to predict structure location and intensity.

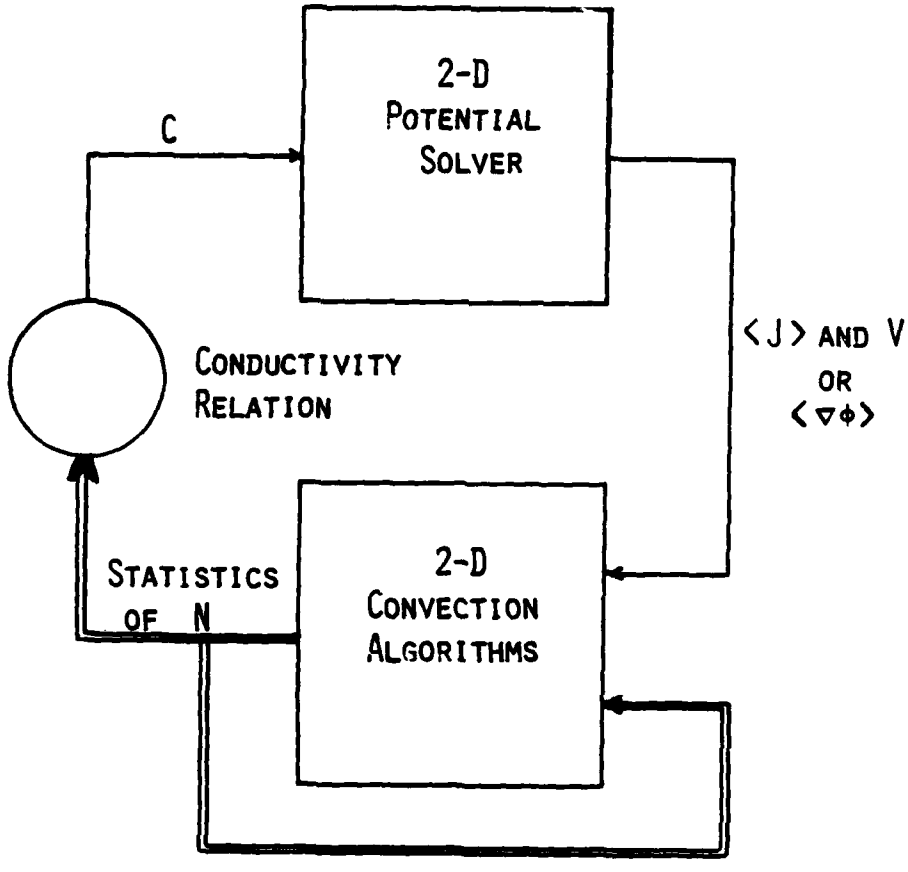

POTENTIAL EQ: $\nabla \cdot C \nabla \phi = \nabla \cdot C(V \times I_z)$

CONVECTION EQ: $\partial_T \langle F(N) \rangle + \nabla \cdot \langle F(N) U \rangle = 0$

THE TERM $\langle NU \rangle$ IS OBTAINED FROM $\langle J \rangle$.

DETERMINING $\langle F(N)U \rangle$ REQUIRES ASSUMPTIONS ABOUT CORRELATION BETWEEN ϕ, J AND N.

CONDUCTIVITY GIVEN IN TERMS OF STATISTICS OF N

Figure 2-2. Microstructure 2-d split step algorithm for plasma evolution.

In the microstructure approach the basic quantities of plasma density, plasma velocity, electrostatic potential and plasma current are treated as stochastic processes which are interrelated and advanced through time with the classical differential equations understood in a stochastic sense. The driving force of the neutral wind is taken to be deterministic. The stochastic quantities are assumed to have homogeneous statistics over each cell. The statistics are treated as inhomogeneous over the simulation dimension and it is the spatial dependence of the statistics that the approach tries to predict.

In the potential equation and in the convection equations for the statistics the stochastic quantities are strongly coupled together. As a result the nature of the correlation between them is important for characterizing their evolution. Currently the correlation properties between plasma quantities are not predicted quantities. They are determined instead through basic assumption (justified perhaps through physical intuition and to some extent by numerical investigation).

It is perhaps surprising that the classical algorithm, which simply ignores the presence of fine-scale fluctuations, can be justified from a microstructure perspective by making the simple assumption that the electric field and the density fluctuations are uncorrelated. This assumption allows the conductivity relation for the mean current $\langle J \rangle$ to be derived straightforwardly by taking the expectation (denoted by angle irons $\langle\ \rangle$) of both sides of the current relation (Eq. 2.1) presented in Section 2.1:

$$\begin{aligned} \langle J \rangle &= \frac{e}{\mu B} \langle N \frac{E}{B} \rangle + \frac{e}{\mu B} \langle N \rangle V \times i_z \\ &= \frac{e\langle N \rangle}{\mu B}\left(\frac{\langle E \rangle}{B} + V \times i_z\right) \end{aligned} \tag{2.12}$$

The latter form of this equation has incorporated the assumed uncorrelated nature of the fluctuations of the density N and the electric field E.

The mean plasma density <N> is seen to play the same role as the density N does in the classical conductivity relation. The convection relation for the mean plasma density <N> can also be found to be the same as that for the classical density by taking the expectation of the continuity equation

$$\left\langle \frac{\partial N}{\partial t} \right\rangle = \frac{\partial \langle N \rangle}{\partial t} = \langle \nabla \cdot N\, E \rangle \times i_z/B$$

$$= \nabla \cdot \langle N \rangle \langle E \rangle \times i_z/B \tag{2.13}$$

Thus, microstructure theory can justify the classical convection algorithms under the assumption that the density and the electric field are uncorrelated and by making a correspondence between the classically specified density and the mean density.

It may be of further interest to note that microstructure theory techniques can be applied to predict the convection of the variance of the plasma fluctuations using a similar assumption. If both N and N^2 are assumed to be uncorrelated with the electric field then it is found that $\langle N^2 \rangle$ is convected with the same velocity as <N> and consequently the plasma variance Σ^2 moves with the same velocity as <N>. To illustrate the convection velocity of $\langle N^2 \rangle$ note

$$\frac{\partial N^2}{\partial t} = 2N \frac{\partial N}{\partial t} = -2N\, E \times i_z \cdot \nabla N/B$$

$$= -\nabla \cdot N^2\, E \times i_z/B$$

and, thus,

$$\left\langle \frac{\partial N^2}{\partial t} \right\rangle = \frac{\partial \langle N^2 \rangle}{\partial t} = -\langle \nabla \cdot N^2 \, E \times i_z/B \rangle$$

$$= -\nabla \cdot \langle N^2 \rangle \langle E \rangle \times i_z/B \qquad (2.14)$$

where the last expression incorporates the assumed uncorrelated nature between N^2 and E. The convection velocity of $\langle N^2 \rangle$ is thus $\langle E \rangle \times i_z/B$ which is the same as the convection velocity of $\langle N \rangle$.

Thus microstructure theory can be applied to the plasma evolution problem with assumptions that result in not only the convection of density in a classical-like manner but also the convection of structure. The structure convection under these assumptions is somewhat trivial in that it moves with the same velocity as the mean plasma density but the exercise is worthwhile for understanding the relationships between classical and other microstructure convection techniques.

Alternative assumptions about the correlation between stochastic quantities lead to alternative conductivity relations. Early in the development of the microstructure approach for SCENARIO, Workman utilized the "Haerendel velocity" assumption for plasma transport. Stagat developed identical two-dimensional transport relations utilizing the "smooth current density" approximation. Couched in terms of microstructure theory these transport relations are the immediate consequence of assuming that the inverse of plasma density is uncorrelated with the current density. The conductivity relation is thus found by

$$\frac{J}{N} = \frac{e}{\mu B}\left(\frac{E}{B} + V \times i_z\right)$$

and

$$\left\langle \frac{J}{N} \right\rangle = \langle J \rangle \langle 1/N \rangle = \frac{e}{\mu B}\left[\frac{\langle E \rangle}{B} + V \times i_z\right]$$

giving

$$\langle J \rangle = \frac{e}{\mu B} \langle 1/N \rangle^{-1}\left[\frac{\langle E \rangle}{B} + V \times i_z\right] \qquad (2.15)$$

For the SCENARIO algorithms the statistic $1/\langle 1/N \rangle$ replaces the mean plasma density $\langle N \rangle$ used in the classical conductivity algorithm. In general this statistic can be shown to be less than or equal to the mean density with larger differences reflecting the presence of more intense structure. Note that this conductivity relation thereby reflects an implicit assumption that microstructure modifies conductivity. This conductivity relation and others similar to it will be discussed in further detail in the next section.

The convection algorithms for the mean density is straightforwardly obtained by taking the mean of the continuity equation in its current density form as presented in the previous section, namely Eq. (2.11), i.e.,

$$\frac{\partial N}{\partial t} = -\nabla \cdot \left(\frac{\mu B}{e} J \times i_z + N V \right)$$

yielding in the mean

$$\frac{\partial \langle N \rangle}{\partial t} = -\nabla \cdot \left(\frac{\mu B}{e} \langle J \rangle \times i_z + \langle N \rangle V \right) \qquad (2.16)$$

This expression for the convection of mean density is applicable regardless of the correlation assumption because of the absence of product terms of stochastic quantities in the stochastic continuity equation as given in the above form. Differences in the mean density transport and evolution can thus be attributed directly to differences in the mean current density pattern. Current density patterns, of course, reflect differences in conductivity dependences produced by different correlation assumptions.

An effective plasma transport velocity can be defined such that the convection equation for the mean density can be written as follows:

$$\frac{\partial \langle N \rangle}{\partial t} = -\nabla \cdot \langle N \rangle \, U_{eff}$$

where

$$U_{eff} = \frac{\mu B}{e \langle N \rangle} \langle J \rangle \times i_z + V \tag{2.17}$$

For the SCENARIO approach the effective velocity can be written in terms of the electric field as

$$U_{eff} = U_{ave} + F_c \, W \tag{2.18}$$

where U_{ave} is the average plasma velocity defined by

$$U_{ave} = \langle E \rangle \times i_z / B = -\langle \nabla \phi \rangle \times i_z \; ; \tag{2.19}$$

where W is the average ion-neutral slip velocity defined by

$$W = V - U_{ave} \; ; \tag{2.20}$$

and where F_c is a normalized structure intensity parameter varying from zero in structureless regions to near one in highly structured regions defined by

$$F_c = 1 - \frac{1}{\langle N \rangle \langle 1/N \rangle} \tag{2.21}$$

The continuity equation when written in this format shows the effective transport velocity for the mean plasma to be between the average plasma velocity as determined from the potential equation and the neutral wind velocity. The equation indicates that the more highly structured regions tend to move more with the neutral wind than with the average plasma velocity. This observation has been made in past works by Workman and Staqat. When comparison is made to classical transport velocities it should be kept in mind that this tendency is partially offset by the fact that the highly structured regions will be regions of lower conductivity

and U_{ave} will consequently be less coupled to the neutral wind. When investigating the differences in mean plasma transport for alternative conductivity models it may thus be advisable to use the current density form of the continuity equation and to compare current densities.

The motion and growth of structure in the SCENARIO approach can be described through the equation for the plasma variance Σ^2. This equation is derived from equations describing the convection of $\langle N^2 \rangle$ and $\langle N \rangle$ as follows:

$$\frac{\partial \Sigma^2}{\partial t} = \frac{\partial (\langle N^2 \rangle - \langle N \rangle^2)}{\partial t}$$

$$= \frac{\partial \langle N^2 \rangle}{\partial t} - 2\langle N \rangle \frac{\partial \langle N \rangle}{\partial t}$$

$$= -\nabla \cdot \langle N^2 U \rangle + 2\langle N \rangle \nabla \cdot \langle N U \rangle \qquad (2.22)$$

The mean flux of N^2 can be found by multiplying the flux expression for N in terms of the current by N and by then taking the mean. The flux expression for N and the subsequent operations to find $\langle N^2 U \rangle$ are:

$$N U = \frac{\mu B}{e} J \times i_z + N V$$

$$N^2 U = \frac{\mu B}{e} NJ \times i_z + N^2 V$$

$$\langle N^2 U \rangle = \frac{\mu B}{e} \langle NJ \rangle \times i_z + \langle N^2 \rangle V$$

$$= \frac{\mu B}{e} \langle N \rangle \langle J \rangle \times i_z + \langle N^2 \rangle V \qquad (2.23)$$

In the latter expression another correlation assumption is made in the SCENARIO approach that the plasma density is also uncorrelated with the current density. For Σ^2 the resulting expression is

$$\frac{\partial \Sigma^2}{\partial t} = -\nabla \cdot \left\{ \frac{\mu B}{e} \langle N \rangle \langle J \rangle \times i_z + \langle N^2 \rangle V \right\} + 2\langle N \rangle \nabla \cdot \left\{ \frac{\mu B}{e} \langle J \rangle \times i_z + \langle N \rangle V \right\} \tag{2.24}$$

An expression for the convection of Σ^2 in terms of only Σ^2 and $\langle N \rangle$ is desirable for use in numerical algorithms. With some algebraic manipulation the terms involving $\langle N^2 \rangle$ can be removed from the above equation yielding

$$\frac{\partial \Sigma^2}{\partial t} = -\nabla \cdot (\Sigma^2 V - \langle N \rangle^2 U_{eff}) - U_{eff} \cdot \nabla \langle N \rangle^2 \tag{2.25}$$

where U_{eff} is again the effect transport velocity of the mean plasma density as defined above in equation (2.18).

In the above format, the equation is physically enlightening. The equation describes the variance as a compressible fluid with an effective motion given by

$$V - \frac{\langle N \rangle^2}{\Sigma^2} U_{eff}$$

and with a source term given by

$$U_{eff} \cdot \nabla \langle N \rangle^2$$

The source term demonstrates a behavior that is related to the gradient drift growth of structure.

Unlike the convection equations for $\langle N \rangle$ and $\langle N^2 \rangle$ equation (2.25) cannot be put into a form where the entire right-hand side is a divergence operation on a flux. This feature of the equation reflects the physical behavior of gradient drift growth of structure. The total Σ^2 in a numerical simulation need not remain constant because of this growth term. However it should be noted that numerical algorithms which convect Σ^2 with the above equation and

$\langle N \rangle$ with its convection relation do come close to conserving the total $\langle N^2 \rangle$ within the simulation. This fact is important when considering which systems of statistics should be used for microstructure algorithms, e.g., choice of the system of $\langle N \rangle$ and Σ^2 versus the system of $\langle N \rangle$ and $\langle N^2 \rangle$. Further numerical considerations are discussed in Section 2-4.

Thus it has been demonstrated that the plasma evolution equations can be considered on a stochastic basis in order to accommodate the presence of fine-scale structure. Algorithms can be derived which predict the location of microstructure and its influence upon plasma evolution. These algorithms are dependent upon the assumptions made about which quantities are uncorrelated. The classical plasma evolution algorithms set forth in the previous section can be justified from a stochastic standpoint if the electric field fluctuations, and hence the velocity field fluctuations, are assumed uncorrelated with the plasma density fluctuations. It is observed earlier in this section that the classical approach can be extended to predict the location of structure. Using the extended classical approach structure is found to be frozen in. For SCENARIO an alternative set of stochastic variables are assumed to be uncorrelated, specifically, the density and its inverse both are assumed to be uncorrelated with the current density fluctuations. Using the SCENARIO approach plasma structure is found to move with a slightly different velocity than the mean density and to grow with movements through density gradients. Justification for the SCENARIO approach comes from conductivity measurements of structured regions, a topic that is discussed further in the next section.

2-3 MICROSTRUCTURE CONDUCTIVITY AND CLOSURE RELATIONS

As seen in the previous section the essential difference between classical techniques and SCENARIO microstructure techniques is contained within the conductivity relation between the mean current and the electric field. This difference can be seen by comparing equations (2.12) (classical) and equation (2.15) (SCENARIO). The refinements provided by the microstructure approach are based upon the premise that fine scale structure alters the conductivity from the value determined from the mean plasma density in a cell and that by specifying additional statistics of the plasma fluctuations the conductivity estimate can be improved. This section investigates the relations which prescribe the conductivity in terms of plasma density statistics and their motivation.

The stochastic potential equation (the stochastic version of equation (2.9)) is a relation between the deterministic neutral wind, V, and the stochastic quantities of plasma density N and electric field potential, ϕ:

$$\nabla \cdot (N\nabla\phi) = \nabla \cdot (N\, V \times i_z) \qquad (2.26)$$

The quantities N, ϕ and V are functions of spatial coordinates x and y. The quantities N and ϕ are also inhomogeneous and the potential solving step finds their spatially varying statistics for the given neutral wind flow. The numerical approach to the potential solving step is to spatially grid the problem to a resolution such that the spatial variation of the statistical descriptors are well resolved in the sampling grid. To a good approximation the stochastic fluctuations can be treated as homogeneous within a sampling cell. By ascribing an effective conductivity to each cell, as determined from solutions of the potential

equation with homogeneous processes, the spatially varying nature of the problem can be treated using classical techniques. The stochastic potential problem of interest thereby becomes the determination of the effective conductivity of a region with homogeneous statistics. (The correlation properties of the current with certain functions of the plasma density are also of interest for higher order moment convection but little work has been done in this area.)

In many respects the homogeneous stochastic potential problem for structured plasmas is related to a problem that should be found in other areas of physics and engineering, namely, the problem of finding the conductivity of a homogeneous aggregate of materials with each material having a different conductivity. The problem of finding the electrical conductivity of a slab of earth in which copper-rich pebbles are found is an example of a similar problem and there are potentially many other problems that would be of interest in related fields. Yet, to the author's knowledge the problem has not been extensively studied which may be somewhat surprising since the problem can also be thought of as the static equivalent to the problem of propagation through inhomogeneities.

Solutions to the stochastic potential equation are difficult to obtain even for the case of homogeneous statistics. There are two special situations in which solutions are available and both involve structure stratification. These cases are random density profiles stratified with gradients parallel to the wind, Figure 2-3, and stratified with gradients perpendicular to the wind, Figure 2-4. Because of the somewhat limited nature of the configurations which have analytical solutions the application of numerical techniques

has proven useful for extending understanding of stochastic potential equation solutions.

Consider the first situation in which an analytical solution exists as illustrated in Figure 2-3. This situation could easily arise in the simulation of smooth barium ion clouds that have steepened to a point where the actual density gradients are unresolvable by the sampling grid and thus must be treated as microstructure. With the wind applied so that currents are driven along the contours of constant density, there are no electric field fluctuations produced. The electric field is constant and independent of the density fluctuations. The average current in the cell is consequently given by

$$\langle J \rangle = \frac{e}{\mu B} \langle N \rangle \left(\langle E \rangle / B + V \times i_z \right) \tag{2.26}$$

and the conductivity is thus proportional to the mean electron density. This situation corresponds to classical conductivity relations.

The other situation with analytical solution has random density fluctuations with gradients perpendicular to the wind as shown in Figure 2-4 and is similar to the situation in late-time barium clouds in which long sheets have developed parallel to the wind. In this situation the density is constant in the direction of the wind and consequently the wind driven current in the perpendicular direction is also constant in the wind direction. Since the wind current is divergence free it can be concluded that the current is constant. Since the current is constant it is uncorrelated with the fluctuations in the density. As shown in Section 2-2 this fact leads to a conductivity that is proportional to $1/\langle 1/N \rangle$. This form of the conductivity is basically the form used in SCENARIO with some further approximation.

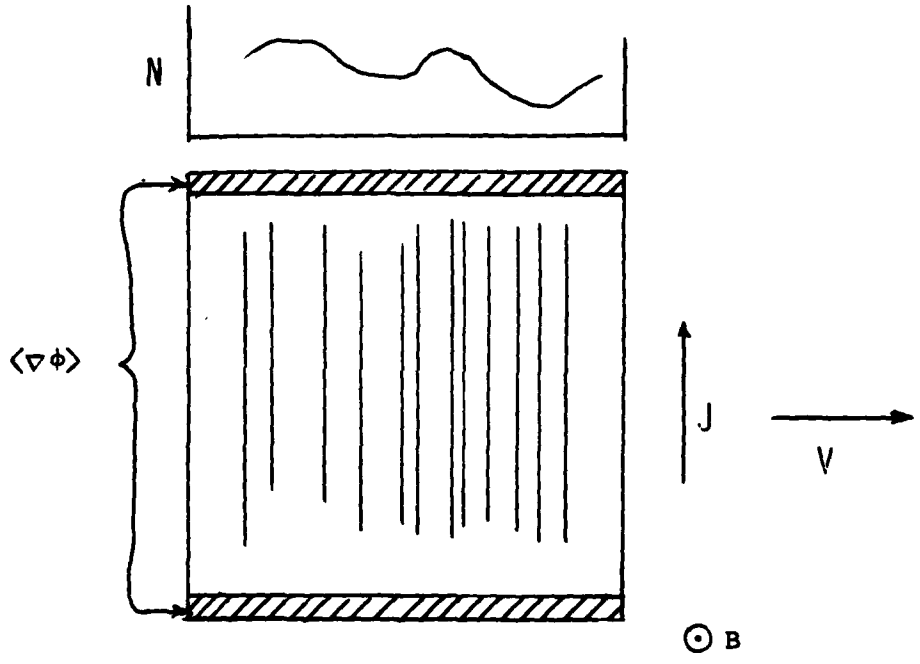

- ALLOWS SOLUTION WITH ϕ BEING INDEPENDENT OF N
- $\langle J \rangle = N \ (\langle \nabla \phi \rangle + V \times I_z)$
- $C = \langle N \rangle$
- THIS FORM OF CONDUCTIVITY ARISES WHENEVER N AND $\nabla \phi$ ARE UNCORRELATED

Figure 2-3. Structure stratified with gradients parallel to the winds.

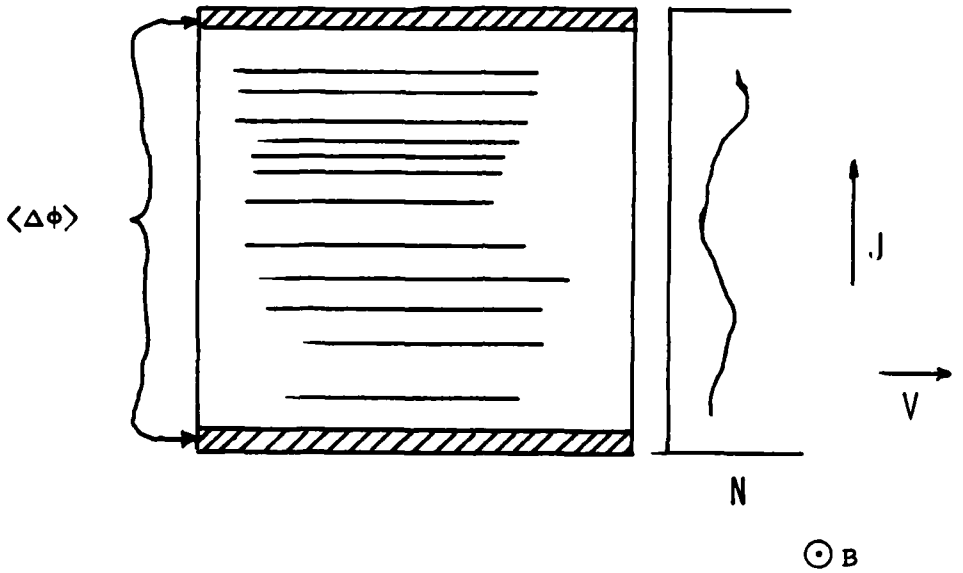

- ALLOWS SOLUTION WITH J = CONSTANT. THUS J AND N INDEPENDENT
- $J = \langle 1/N \rangle^{-1} (\langle \nabla \phi \rangle + V \times I_Z)$
- $C = \langle 1/N \rangle^{-1}$
- THIS FORM OF THE CONDUCTIVITY ARISES WHENEVER J AND 1/N ARE UNCORRELATED

Figure 2-4. Structure stratified with gradients perpendicular to the wind.

Since analytical solutions to the homogeneous stochastic potential equation are so limited numerical calculational results have been used to investigate the applicability of the various conductivity expressions. Calculational results provide the mean potential drop plus wind driver across a cell and the current density at the cell boundary. The ratio of these two is the mean conductivity.

Shown in Figure 2-5 is one geometry that has been numerically investigated. The figure shows the upper half of a symmetric problem of five sheet-like structures. The geometry is similar to the stratified case investigated analytically but to investigate the effect of the striation tips upon the problem the sheets are terminated within the calculational boundary. From the potential equation solution for this problem it is possible to evaluate the conductivity ratio on a column by column basis and to compare the results with the columnar statistics such as $\langle N \rangle$ and $1/\langle 1/N \rangle$--although it should be remembered that it is the average of these columnar ratios that should be used for the effective cell conductivity. A comparison of the numerically derived conductivity ratio and the columnar statistics is shown in Figure 2-6. The figure shows the statistical ratio $\langle N \rangle^3/\langle N^2 \rangle$ in addition to the quantities $\langle N \rangle$ and $1/\langle 1/N \rangle$. It can be seen that on a columnar basis the statistic $1/\langle 1/N \rangle$ provides a generally closer estimate to the calculated conductivity than the statistic of $\langle N \rangle$. In addition the statistic $\langle N \rangle^3/\langle N^2 \rangle$ also gives a respectable approximation to the numerical result. The average of all the columnar results is given in Table 2-1. The tabulated results show the expected

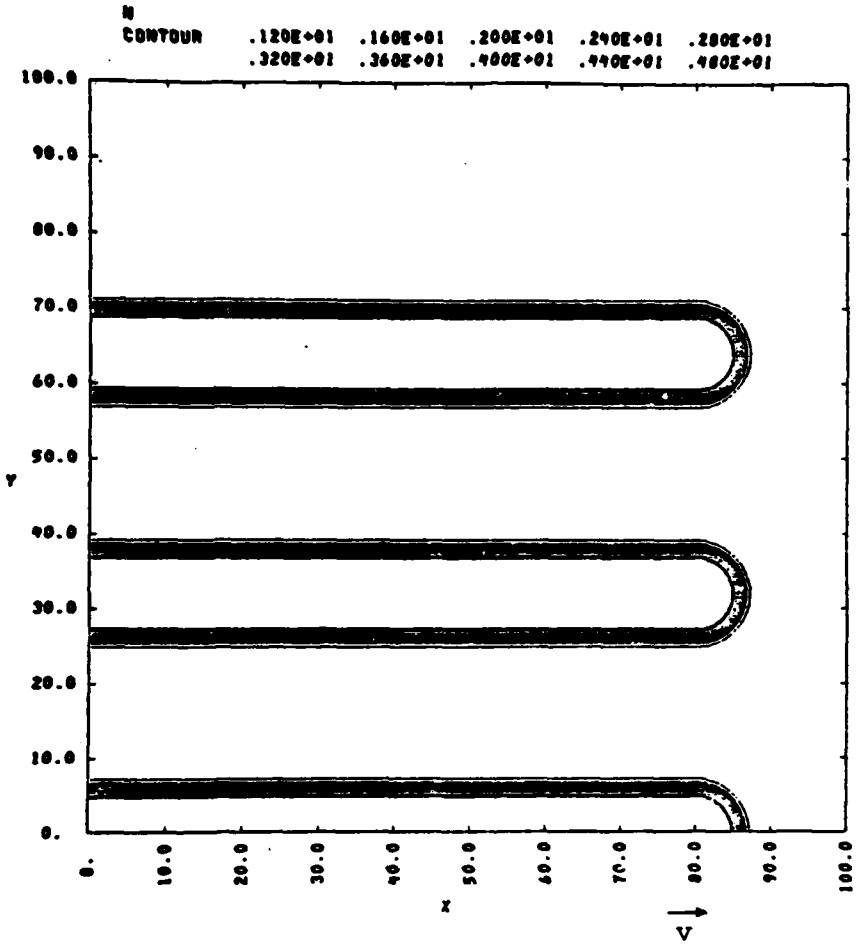

Figure 2-5. Five finger geometry is assumed about the x-axis. The neutral wind is horizontal and directed toward the right. There are 200 × 200 samples in the above figure.

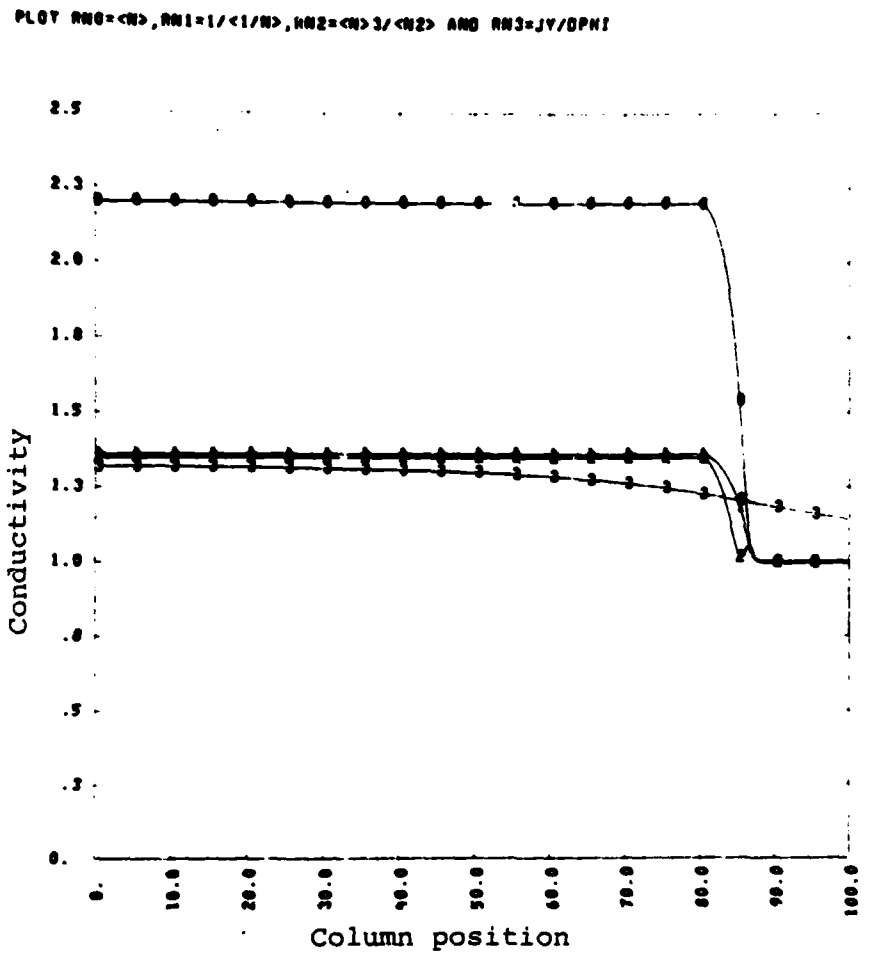

Figure 2-6. Mean columnar conductivity (3) versus position. Also shown are the columnar mean density (0), the inverse of the columnar mean inverse density (1), and the asymtotic closure approximation to (1) used in 3-dimensional SCENARIO routines (2).

Table 2-1. Comparison of Numerical Conductivity Calculational Results with Statistical Estimators

	FINGERS	RODS	GAUSSIAN
CLASSICAL $\langle N \rangle$	1.000	1.000	1.000
SCENARIO $\langle 1/N \rangle^{-1}$	.647	.682	.964
ASYMPTOTIC CLOSURE $\langle N \rangle^3 / \langle N^2 \rangle$	.640	.634	.966
NUMERICAL RESULT C	.632	.726	.982

result that the 1/<1/N> SCENARIO conductivity provides a better estimate to the actual conductivity than the classical <N> value. Note that the current pattern the magnitude of which is shown in Fig. 2-7 is not smooth everywhere in the cell because of the presence of the striation tips. Nevertheless, it appears that it is not crucial that the current be constant for the conductivity result to apply.

In the above numerical example the structure is highly stratified in the direction that favors the SCENARIO conductivity form. To remove the effects of structure elongation from the conductivity comparison the conductivity for a random distribution of nearby cylindrical rods as shown in Figure 2-8 was calculated. The results tabulated in Table 2-1 indicate the expected result that the conductivity does not agree quite as well as the previous case with the 1/<1/N> SCENARIO value. It is surprising perhaps that they are still much closer to the SCENARIO value than the classical value. Thus use of the SCENARIO conductivity approximation seems to be justified for structured regions in general so long as the density flucturations are not strongly stratified with gradients parallel to the wind.

The numerical conductivity examples shown in Figures 2-5 and 2-7 can be closely described as two dimensional shot noise processes (Papoulis, 1965, p. 288) in that they consist of a random placement of similar shapes. Numerical conductivity calculations have also been performed for one likely alternative type of stochastic process, namely, the two-dimensional Gaussian process.

One member of a two-dimensional Gaussian process ensemble with isotropic power law power spectral density is shown in Figure 2-9. The power law dependence used to generate the figure is proportional to $(k_x^2 + k_y^2 + A)^{-3/2}$

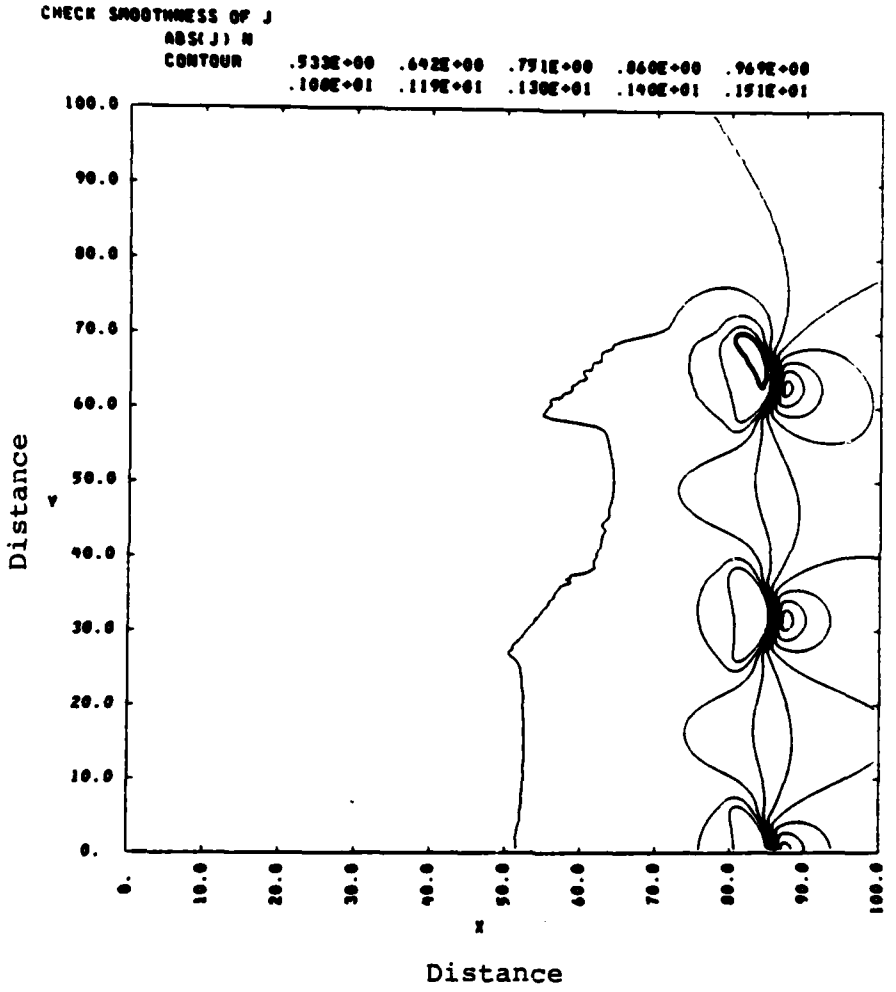

Figure 2-7. Contours of magnitude of current density resulting from five finger potential calculation.

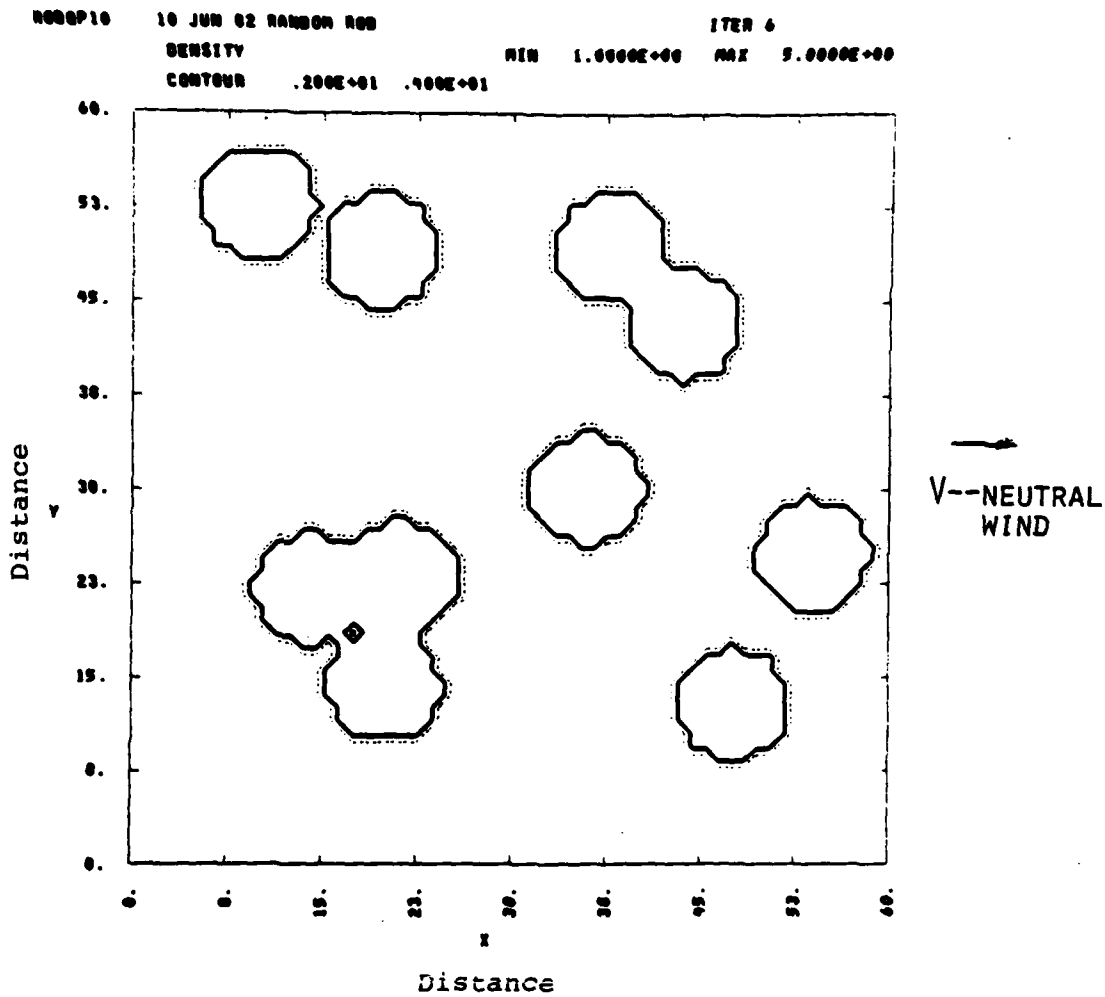

Figure 2-8. Geometry of random rod calculation. Grid sampling is 60 × 60.

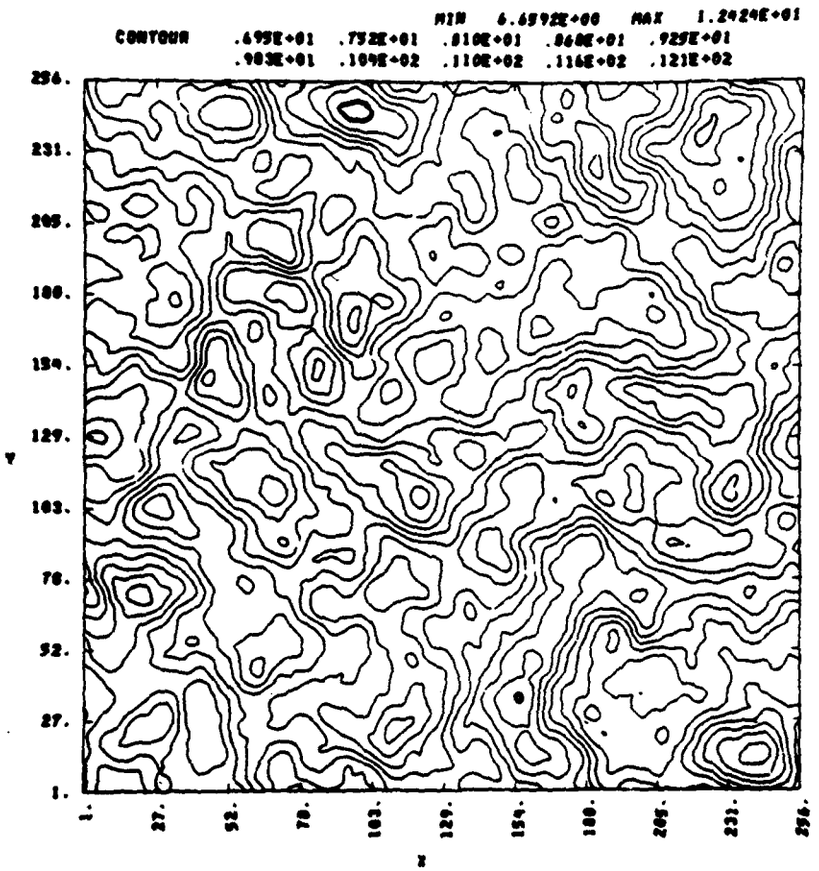

Figure 2-9. Constant value contours for stochastic pattern calculation. Member of isotropic Gaussian ensemble with k_r^{-3} spectrum.

where k_x and k_y are the wavenumbers in the horizontal and vertical directions and where A is a constant related to the outer scale. This power law dependence produces the k^{-2} 1-d in situ fluctuation spectrum expected from many structuring processes.

The isotropic process may be appropriate for weakly structured regions of plasma. As structure grows through the gradient drift instability the non-isotropic two-dimensional shot noise process probably becomes a better descriptor because of the manner in which structure tends to form elongated finger-like regions.

The process shown in Figure 2-9 is weakly structured and has a r.m.s. density to mean density ratio of only 19%. The results of the potential caclulation for this case are shown in Figure 2-10. Periodic boundary conditions have been used. The conductivity resulting from the calculation has been compared with other statistical descriptors for the conductivity in Table 2-1. The results show that the numerically calculated conductivity is basically a compromise between the classical and SCENARIO conductivities. Note that the asymptotic closure conductivity is found to be very close to the SCENARIO conductivity. The results, thus, show that the SCENARIO and asymptotic closure conductivity approximations are no worse (and only marginally better) than the classical conductivity for the case of weak isotropic Gaussian structure.

In all three numerical conductivity evaluations the statistic $\langle N\rangle^3/\langle N^2\rangle$ is seen to provide an approximation that is of comparable quality as the $\langle 1/N\rangle$ approximation. This conductivity relation has been labelled the asymptotic closure relation and it has been used extensively in the SCENARIO algorithms to be presented. It is instructive perhaps to discuss the origin of its name.

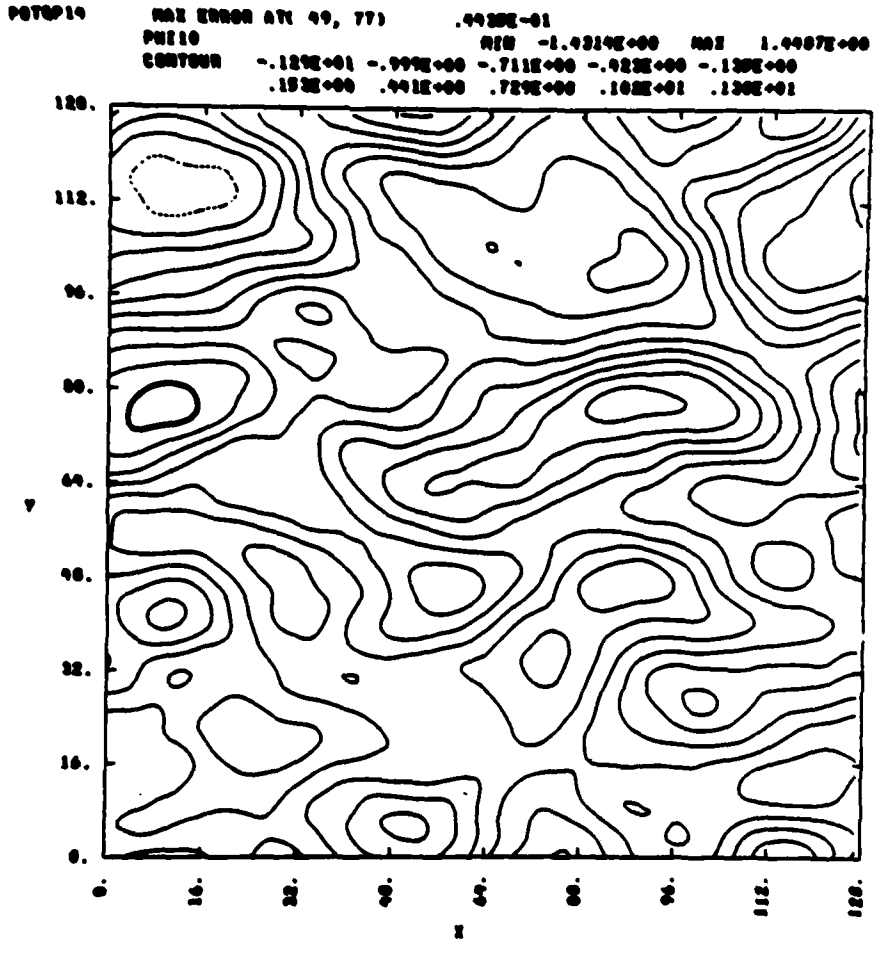

Figure 2-10. Contours of constant potential for isotropic Gaussian k_r^{-3} case.

The term closure relation originates in past work which attempted to explicitly calculate the statistic $\langle 1/N \rangle$. This work recognized that the statistic $\langle 1/N \rangle$ can be convected from initial conditions and flow patterns in the same manner as $\langle N \rangle$ is convected. Where the convection of $\langle N \rangle$ requires knowledge of $\langle 1/N \rangle$, the convection $\langle 1/N \rangle$ requires, analogously, $\langle 1/N^2 \rangle$. The statistic $\langle 1/N^2 \rangle$ can also be convected provided $\langle 1/N^3 \rangle$ is known and in general the statistic $\langle 1/N^p \rangle$ can be convected provided that $\langle 1/N^{p+1} \rangle$ is known, for all $p > 0$. Numerical treatments of the problem require a relation which terminates this infinite regression and this relation was appropriately called the closure relation. Techniques were also developed in this early work which did not convect $\langle 1/N \rangle$ specifically but instead approximated it in terms of other statistics and the label 'closure relation' was expanded to accommodate these relations. A closure relation is thus any relation between known statistics to approximate the unknown statistic in the problem, including $\langle 1/N \rangle$.

The statistic $\langle 1/N \rangle$ is directly evaluatable from the first order statistics of N. Ideally, one could evaluate all the positive moments of N and then apply the statistical moment theorem to find the first order probability density function and the statistic $\langle 1/N \rangle$. In practice, however, $\langle 1/N \rangle$ is approximated in one of two ways. First, by assuming a multi-parameter first order density, such as the "two-level variable epsilon" densities used in past work and by then using the known statistics to determine the density parameters; the first order density and $\langle 1/N \rangle$ can be found. Alternatively, a relation for $\langle 1/N \rangle$ in terms of the known statistics can be stated specifically with a family of first order density functions being implicitly assumed. The

asymptotic closure relation is a closure relation of the latter type that was formulated such that for both large and small amounts of structure the result would 'asymptote' to the value of $1/\langle 1/N \rangle$. Its simple form in terms of first and second moments make the relation attractive for numerical use.

The asymptotic closure approximation was originally developed as and may be thought of as an approximation to $1/\langle 1/N \rangle$. However, since the statistic $1/\langle 1/N \rangle$ is itself only an approximation to the conductivity it is conceivably more straightforward to regard the asymptotic closure relation as an alternative approximation to conductivity. In this vein it is felt that future work should concentrate more on developing good approximations to the conductivity rather than on developing good closure approximations to $\langle 1/N \rangle$.

2-4 NUMERICAL CONSIDERATIONS

A reasonable question is which of the myriad statistical parameters should be used as convected quantities in microstructure algorithms. In the past work, the choice of parameters was somewhat ad hoc. Recently, however, methods for making choices between parameter sets have been developed.

In order to perform a microstructure calculation the convection of at least two statistical parameters is required. The number of statistical quantities convected in a calculation could, in principle, be quite large. It should be kept in mind, however, that the motivation for using additional parameters must be to improve conductivity estimates. To this end it remains to be demonstrated that significant improvements in conductivity estimates over that provided by a two-parameter set using the asymptotic closure relation can be made by using three or four parameter sets. Because of

the advantage of reduced storage requirements it is felt that sets with only two statistical parameters should be used for convection unless an improvement in conductivity estimates can be demonstrated with larger sets. Thus one method for choosing parameter sets is to choose sets with only two members.

It might be thought that the set of the mean density $\langle N \rangle$ and the mean square density $\langle N^2 \rangle$ is a reasonable parameter set. Indeed, past work (Stagat, et al., 1982) used combinations of statistics including these two for their numerical algorithms. Recent numerical considerations have revealed that it is desirable to choose statistical parameters that are, in a sense, orthogonal. It is desired that the values that the parameters can take should be independent of each other. For the $\langle N \rangle$ $\langle N^2 \rangle$ set the parameter values are not independent of each other because the mean square $\langle N^2 \rangle$ must be greater than the mean squared $\langle N \rangle^2$. The closely related set comprised of the mean, $\langle N \rangle$, and the variance Σ^2 has been found to be more desirable for use. The fact that the variance Σ^2 can take values independent of $\langle N \rangle$ and the related fact that it is less susceptible to numerical noise when it is explicitly convected make the $\langle N \rangle$ Σ^2 set preferable to the $\langle N \rangle$ $\langle N^2 \rangle$ set.

The nature of the numerical pitfalls associated with the $\langle N \rangle$ $\langle N^2 \rangle$ set can be illustrated by a classical calculation of structure convection. A barium cloud problem has been simulated using the $\langle N \rangle$ $\langle N^2 \rangle$ pair and using the classical conductivity proportional to $\langle N \rangle$. From the discussion of Section 2-2 it is known that all the quantities $\langle N \rangle$ $\langle N^2 \rangle$ and Σ^2 should convect with the same velocity.

However explicit numerical calculations performed in two different frames of reference bring out important issues.

The problem has been initialized with a Gaussian spatial distribution of mean density and with microstructure levels with r.m.s. values of 3% of the mean. The initial values of $\langle N \rangle$ and $\langle N^2 \rangle$ are shown in Figures 2-11 and 2-12. With a neutral wind blowing in a horizontal direction toward the right in the figures, the cloud has been allowed to evolve 300 seconds in both a frame at rest and in a frame moving at 50 meters per second horizontally toward the right (1/2 the neutral wind velocity). The only source of difference in the two runs is that all the x-component velocity values used in the moving frame convection step have been reduced by 50 meters per second from the values used in the rest frame calculation. Figures 2-13, 2-14 and 2-15 respectively show the mean density, mean squre density and the variance for the rest frame calculation and Figures 2-16, 2-17 and 2-18 respectively show the corresponding results from the moving frame.

Comparisons of the resulting values of $\langle N \rangle$ and $\langle N^2 \rangle$ indicate small (roughly 5%) differences which by themselves are not unreasonable and are thoroughly acceptable. In contrast, a comparison of the resulting values of Σ^2, as determined from $\langle N^2 \rangle - \langle N \rangle^2$, shows a striking disagreement in magnitude and morphology. Further, neither of the results agree with the theoretically indicated dependence which specifies that the r.m.s. fluctuation level to mean density ratio is a constant 3%. Perhaps the most serious error is that the results from both frames of reference show regions where Σ^2 is negative.

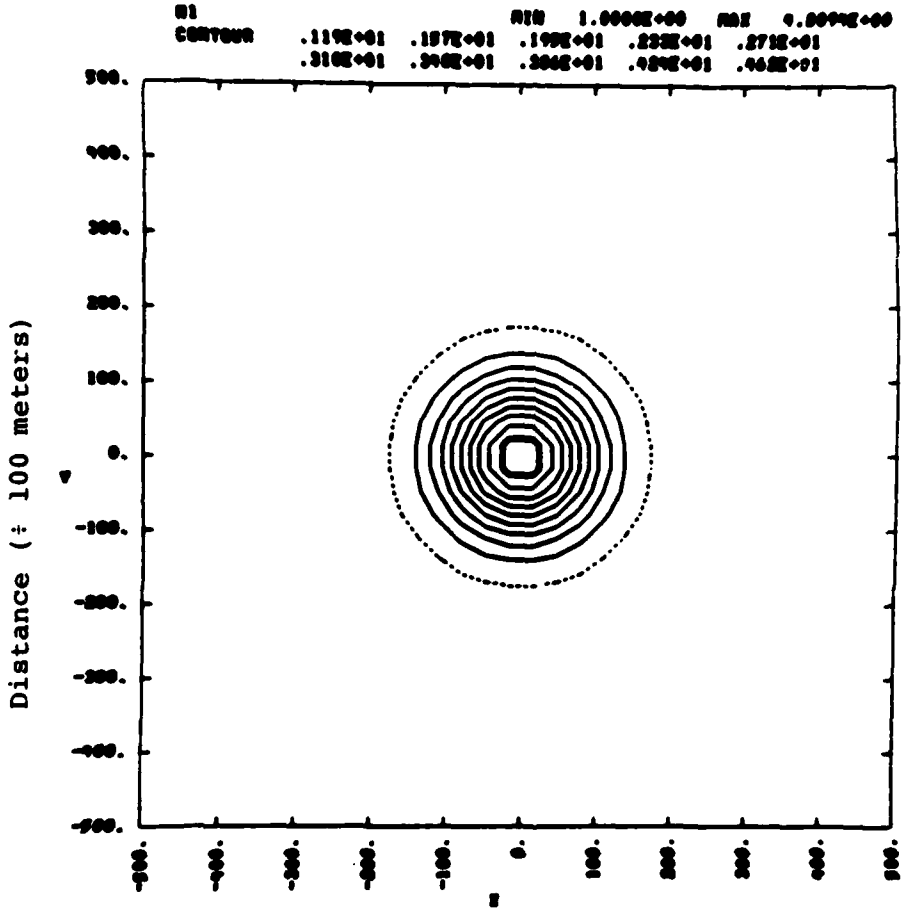

Figure 2-11. Initial density in an <N> $\langle N^2 \rangle$ barium cloud calculation. The wind is horizontal and toward the right at 100 m/s.

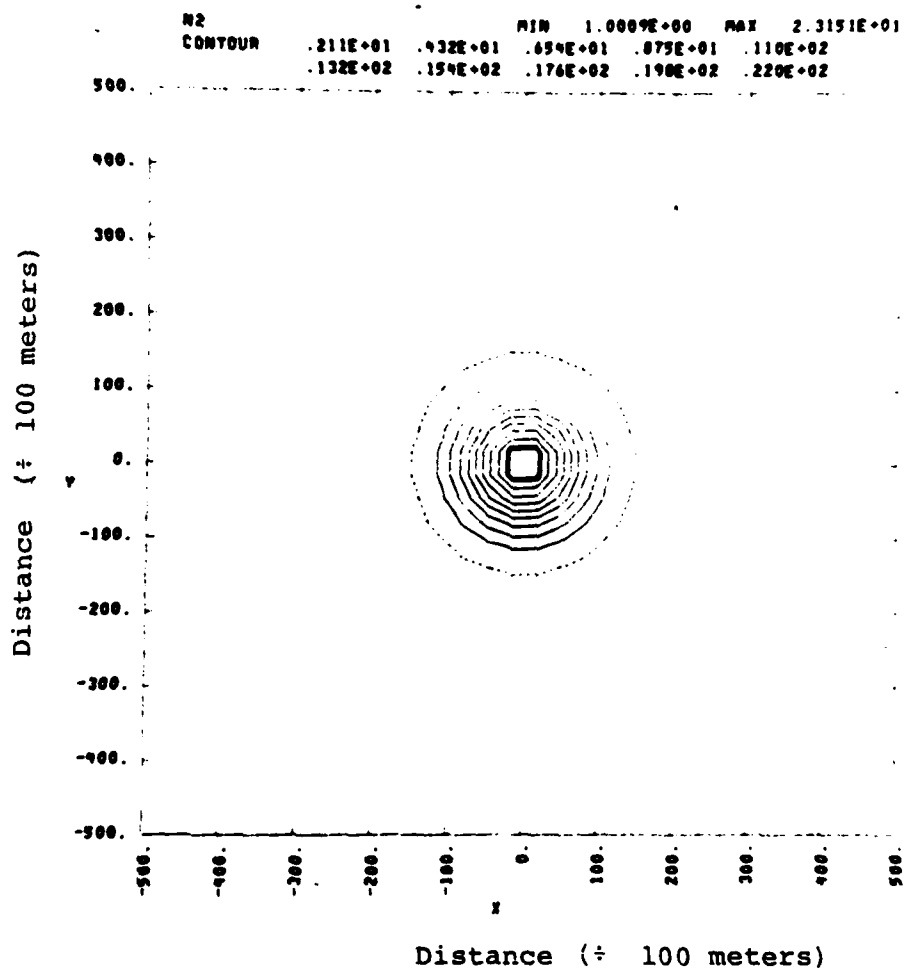

Figure 2-12. Initial density mean of N^2. The r.m.s. density is 3% of the initial density.

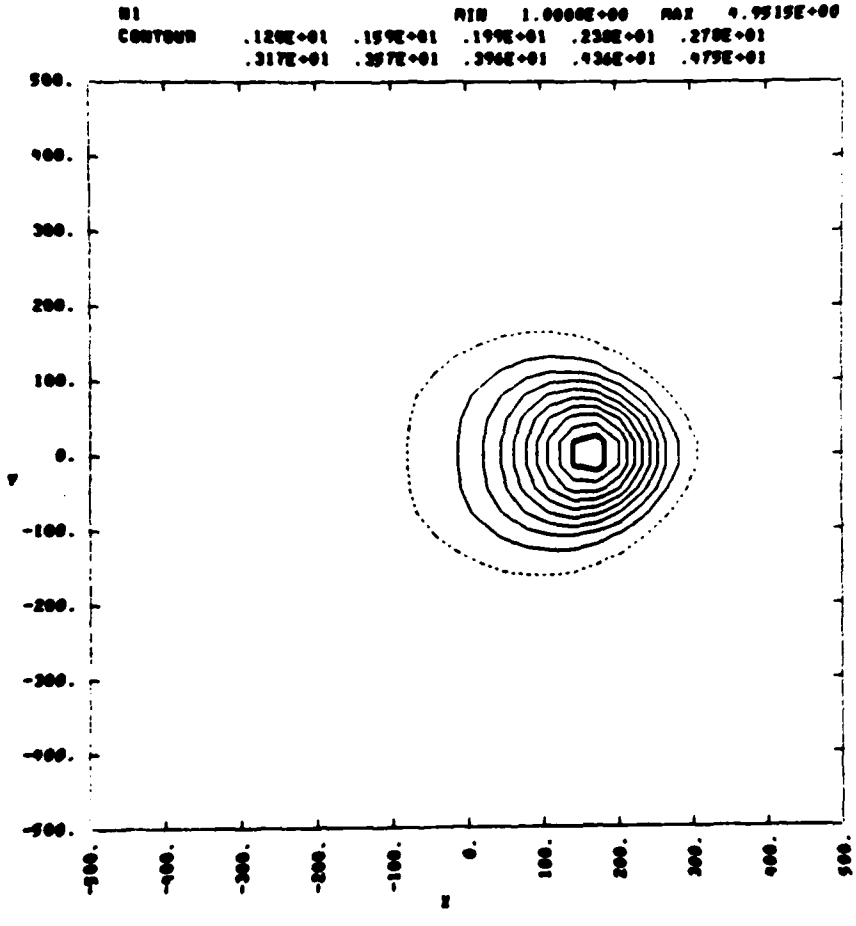

Figure 2-13. Mean density after 300 seconds in stationary frame of reference. The plasma evolution has been simulated using <N> to approximate the conductivity.

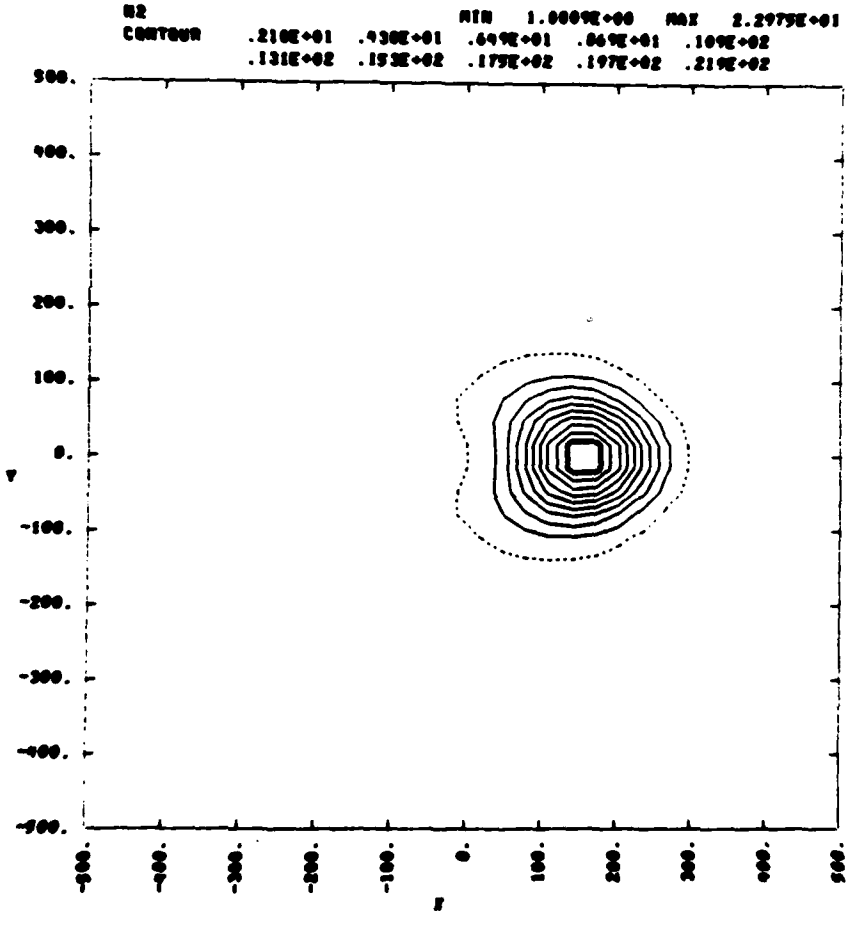

Figure 2-14. Mean of N^2 after 300 seconds in stationary frame of reference. This quantity has been convected numerically with the same velocity as N.

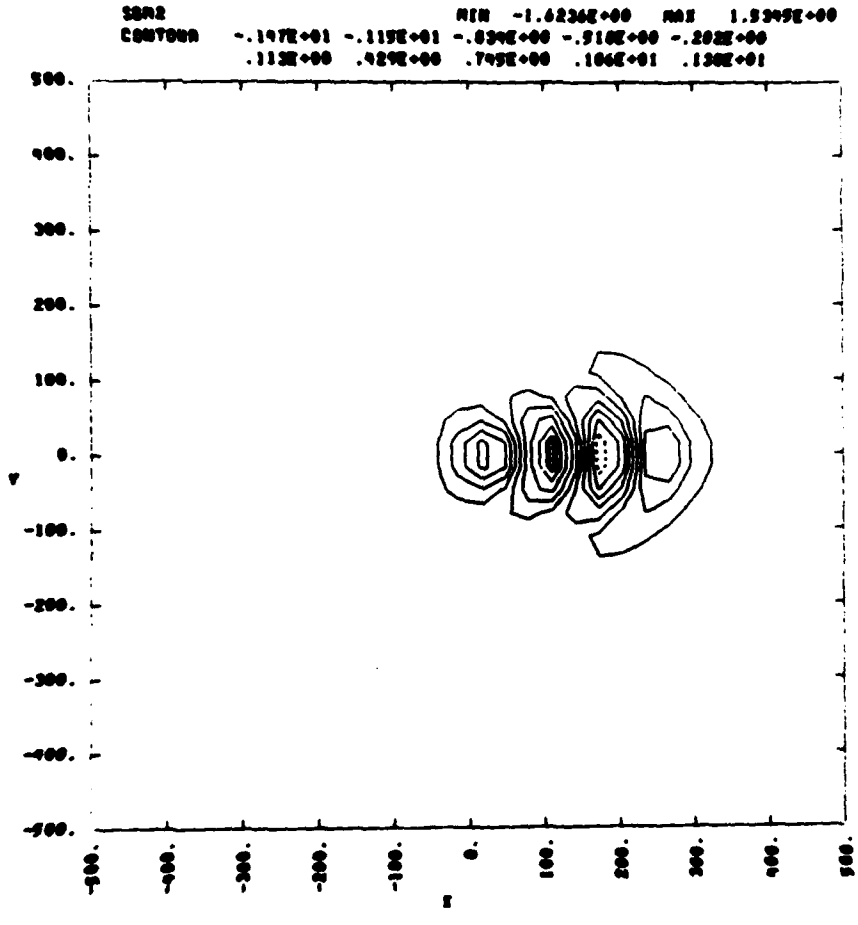

Figure 2-15. The variance implied by mean of N^2 minus the square of the mean of N calculated in the stationary frame at 300 seconds. Note that significant regions of negative variance are implied.

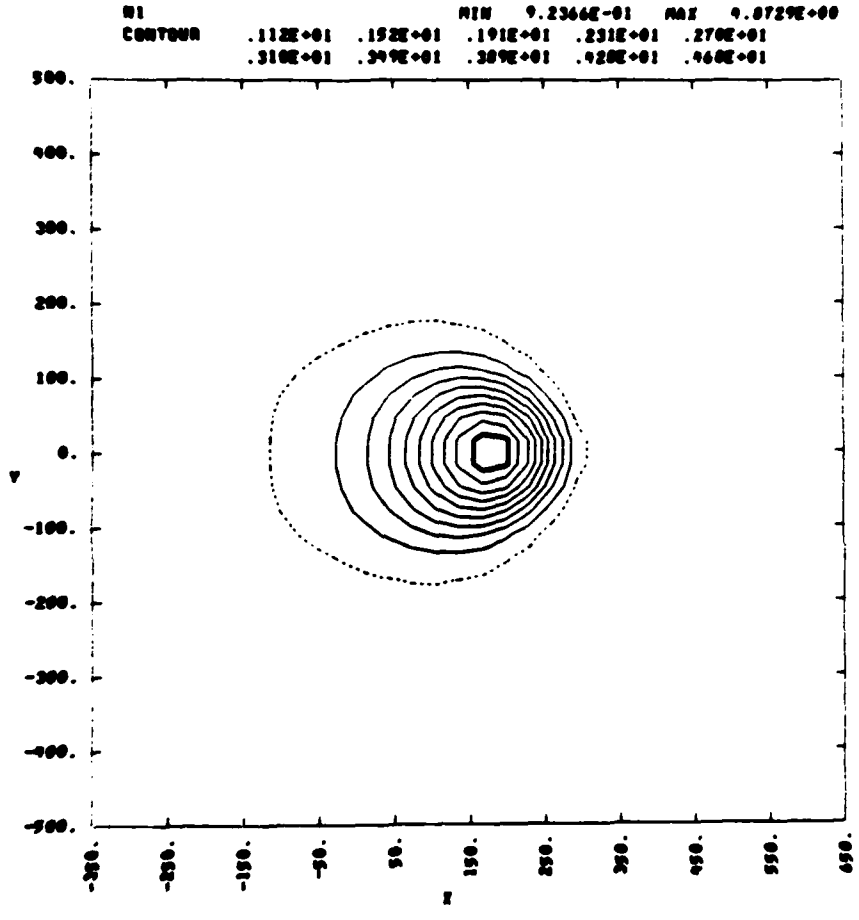

Figure 2-16. Mean density after 300 seconds in translating frame of reference. The frame of reference is moving 50 meters per second in the direction toward the 100 meter per second wind.

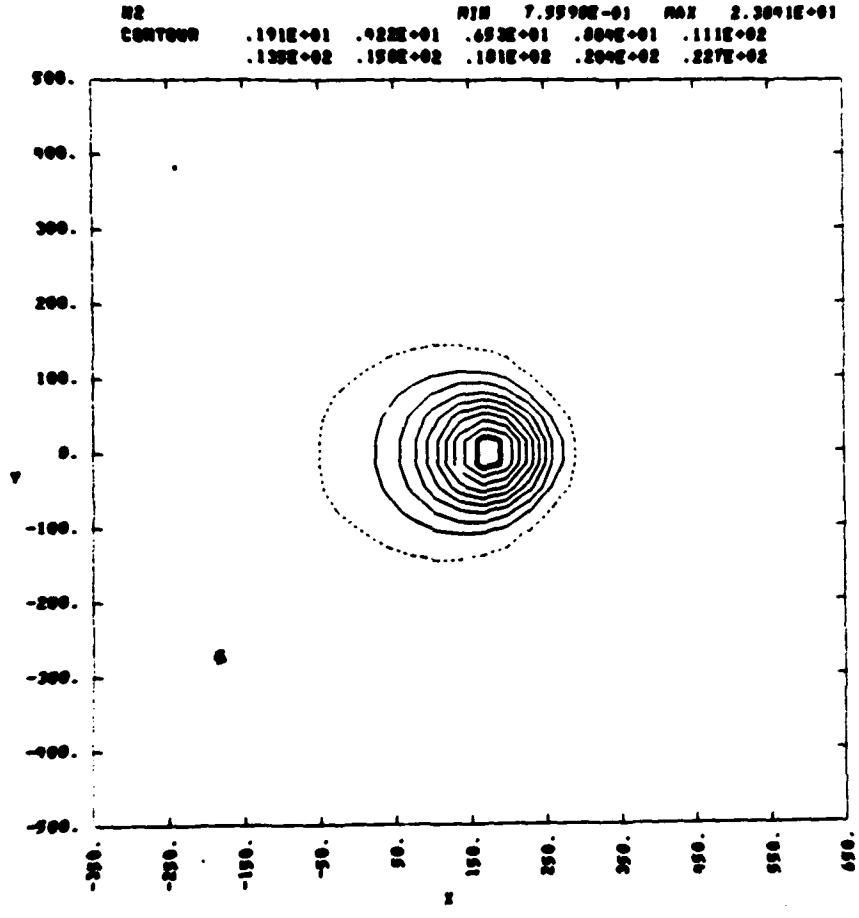

Figure 2-17. Mean of N^2 after 300 seconds in translating frame of reference.

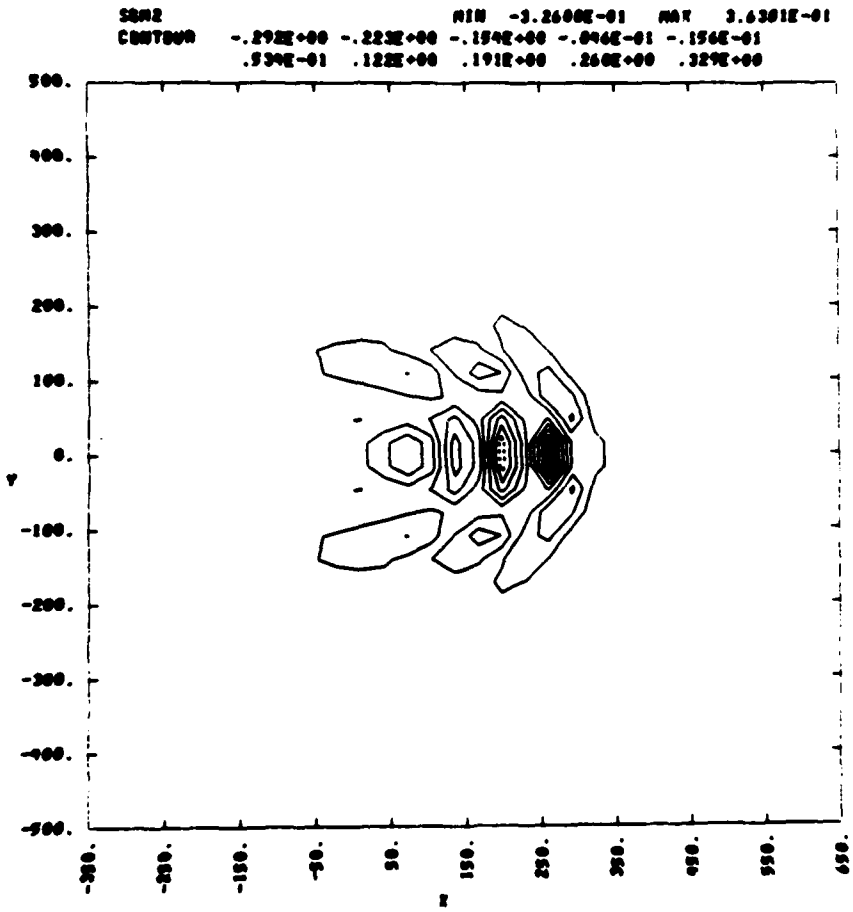

Figure 2-18. The variance implied by mean of N^2 minus the square of the mean of N calculated in the translating frame of reference. The regions of negative variance are morphologically different from those of a stationary frame indicating numerical difficulties with convecting $\langle N \rangle$ and $\langle N^2 \rangle$.

The cause of the erroneous behavior of the calculated variance can be attributed to the fact that the 5% fluctuations in $\langle N \rangle$ and $\langle N^2 \rangle$ become greatly exaggerated because of the approximate cancellation of the two numbers in the Σ^2 calculation. For calculations in which structure dependent conductivity values are used in place of the classical conductivity the value of Σ^2 is very important in the determination of the plasma flow and further evolution of Σ^2. Convecting $\langle N \rangle$ and $\langle N^2 \rangle$ explicitly and then using $\Sigma^2 = \langle N^2 \rangle - \langle N \rangle^2$ can produce even more unrealistic results because the large inaccuracies in Σ^2 resulting from each time step will feedback into the calculation through the conductivity values and the associated flow fields.

The major pitfalls associated with the $\langle N \rangle$ $\langle N^2 \rangle$ convection set are avoided if $\langle N \rangle$ and Σ^2 are explicitly convected. For the classical conductivity example above, use of the $\langle N \rangle$ Σ^2 convection set would produce acceptable results. The convection of Σ^2 is numerically no different from the convection of $\langle N^2 \rangle$ and consequently the variations of the results between the two frames of reference would have the same 5% level. This variation in the important Σ^2 parameter is acceptable and argues strongly for the use of 'orthogonal' statistics as convection parameters.

Arguments for the use of $\langle N \rangle$ and $\langle N^2 \rangle$ as convection parameters are that both of these quantities are conserved quantities and that by convecting them numerical inaccuracies can be guarded against by using conservation checks. The variance parameter is in general not a conserved quantity as mentioned in Section 2.2. However, mere conservation checks

do not guarantee accuracy as graphically pointed out by the above example. Indeed use of the $\langle N \rangle \Sigma^2$ convection set has been observed to come much closer to conserving the quantity of $\langle N^2 \rangle$ than an $\langle N \rangle \langle N^2 \rangle$ calculation which adjusts $\langle N^2 \rangle$ so that Σ^2 is kept non-negative. Also by not convecting a conserved quantity, conservation can serve as a numerical quality check. Furthermore, since it is basically Σ^2 and not $\langle N^2 \rangle$ that is of interest to satcom systems analysts, assuring the conservation of $\langle N^2 \rangle$ is much less important than assuring the accuracy of Σ^2.

2-5 BARIUM CLOUD EXAMPLE

A numerical calculation of the two-dimensional evolution of an ionospheric barium cloud has been performed using a microstructure algorithm implemented with the asymptotic closure conductivity approximation. The problem geometry and initial values are the same as those used for the numerical example discussed in Section 2-4. The barium cloud is represented as an enhancement in the mean density with a Gaussian spatial dependence. The mean density at the enhancement peak has a value of 5 and the background density has a value of 1. The Gaussian spatial dependence has an e-folding radius of 10 kilometers. Microstructure is assumed to exist everywhere with an r.m.s. level of 3% of the mean. Plots of the initial density and variance are shown in Figures 2-19 and 2-20. The plot grid of 50 kilometers by 50 kilometers is indicative of the spatial region sampled by a 32 by 32 grid. The mean density and the variance of the density are convected using the SCENARIO equations presented in Section 2-2. The wind is assumed to be horizontal and to the right with a 100 meter per second speed.

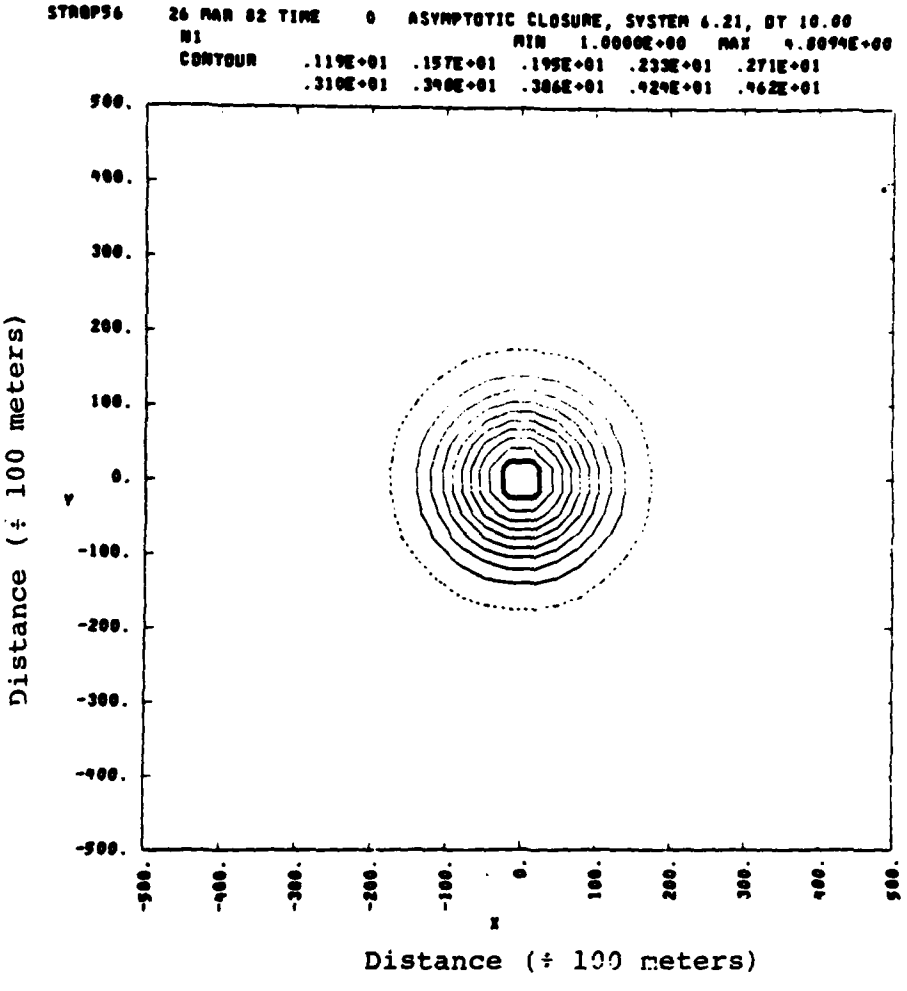

Figure 2-19. Initial mean density for a barium cloud simulation using the $\langle N \rangle \Sigma^2$ pair. The wind is horizontal and toward the right at 100 meters per second.

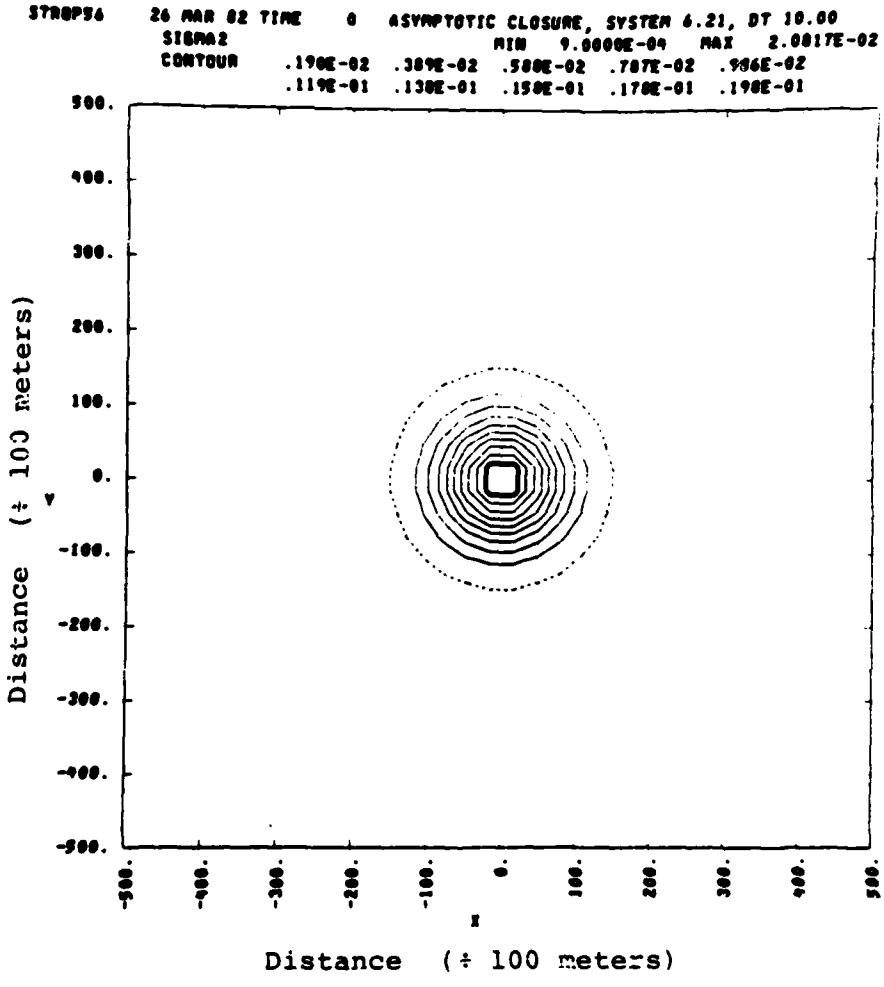

Figure 2-20. Initial variance in the barium cloud simulation. The standard deviation is 3% of the mean density.

The results of the first potential step calculation are illustrated in Figure 2-21. Because of the free space boundary conditions used in the solution the grid boundaries do not affect the motion of the plasma. The newly developed free space boundary condition algorithm avoids many of the deficiencies associated with previous potential solving algorithms.

The split step algorithm has been used to advance the density and variance values through time. Essentially a ten second interval has been used for each complete time step. The predicted values at 300 and 510 seconds using a calculation with a stationary frame of reference are shown in Figures 2-22 thru 2-25. The figures show the physically appealing result that the plasma structure region moves to the trailing (right-most) edge of the barium cloud and grows. This behavior is in good agreement with experimental observation. The growth rate indicated also seems to be realistic if one believes that barium cloud structures are produced by gradient drift amplification of irregularities in the ambient and barium Pedersen conductivity and that these levels have initially a 1% r.m.s. to mean density ratio. The time at which significant structure has been first observed in barium radio propagation data is typically 10-20 minutes. The winds observed in these observations produced an ion-neutral slip velocity of roughly the same magnitude as that observed in the numerical simulation. The numerical simulation data indicates a variance growth rate of doubling every 100 seconds. At this rate the structure variance becomes comparable to the square of the mean density level at roughly 16 minutes which can be considered to be in good agreement with observations.

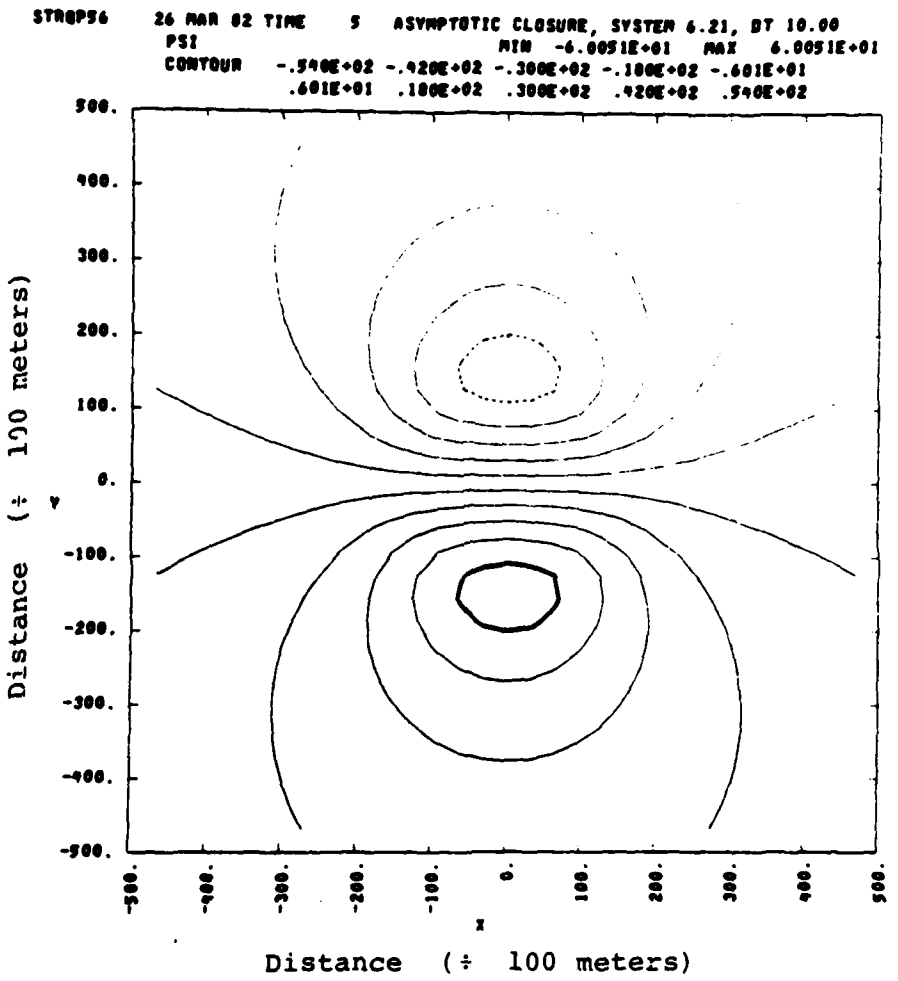

Figure 2-21. Results of the first potential solution step. Free space boundary conditions have been implemented.

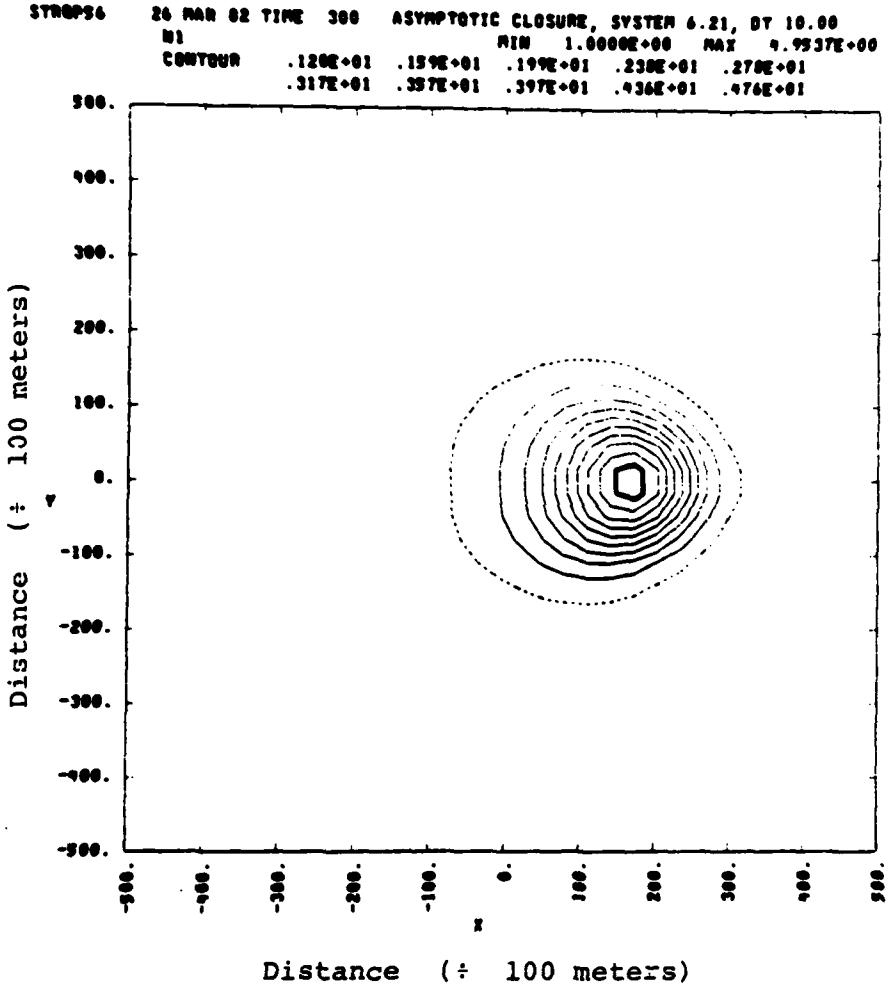

Figure 2-22. Mean density at 300 seconds.

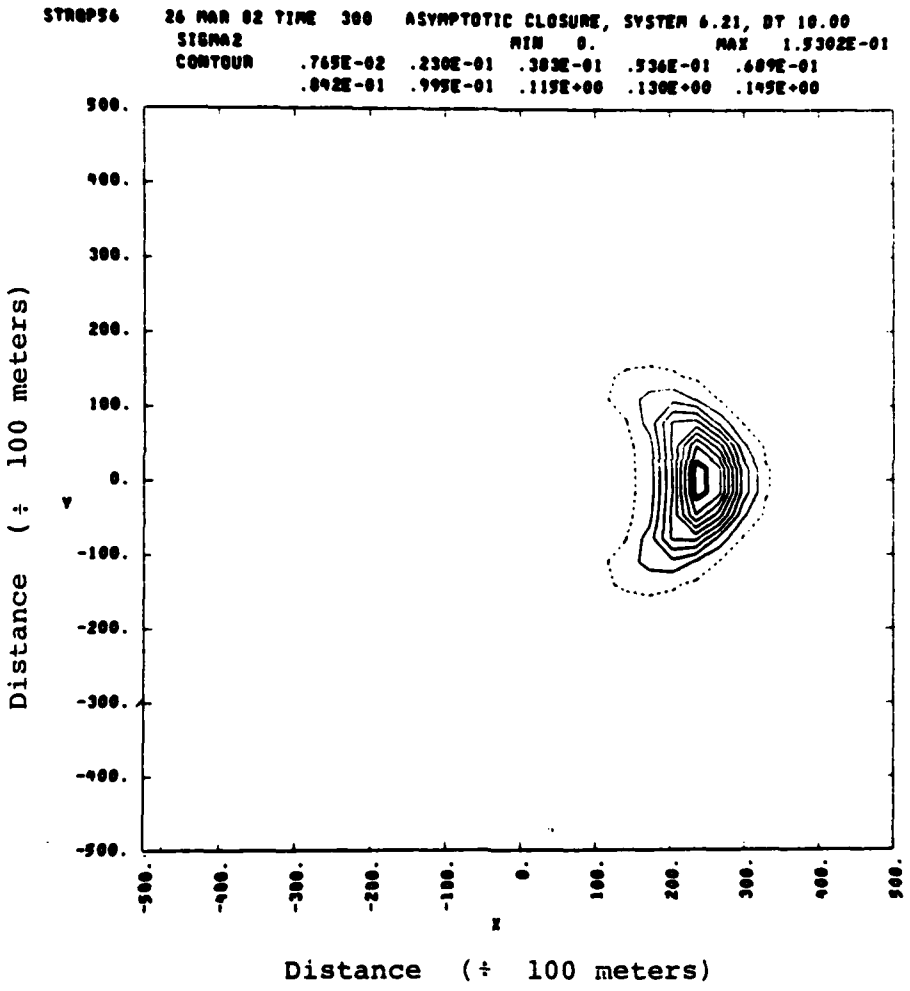

Figure 2-23. Variance at 300 seconds.

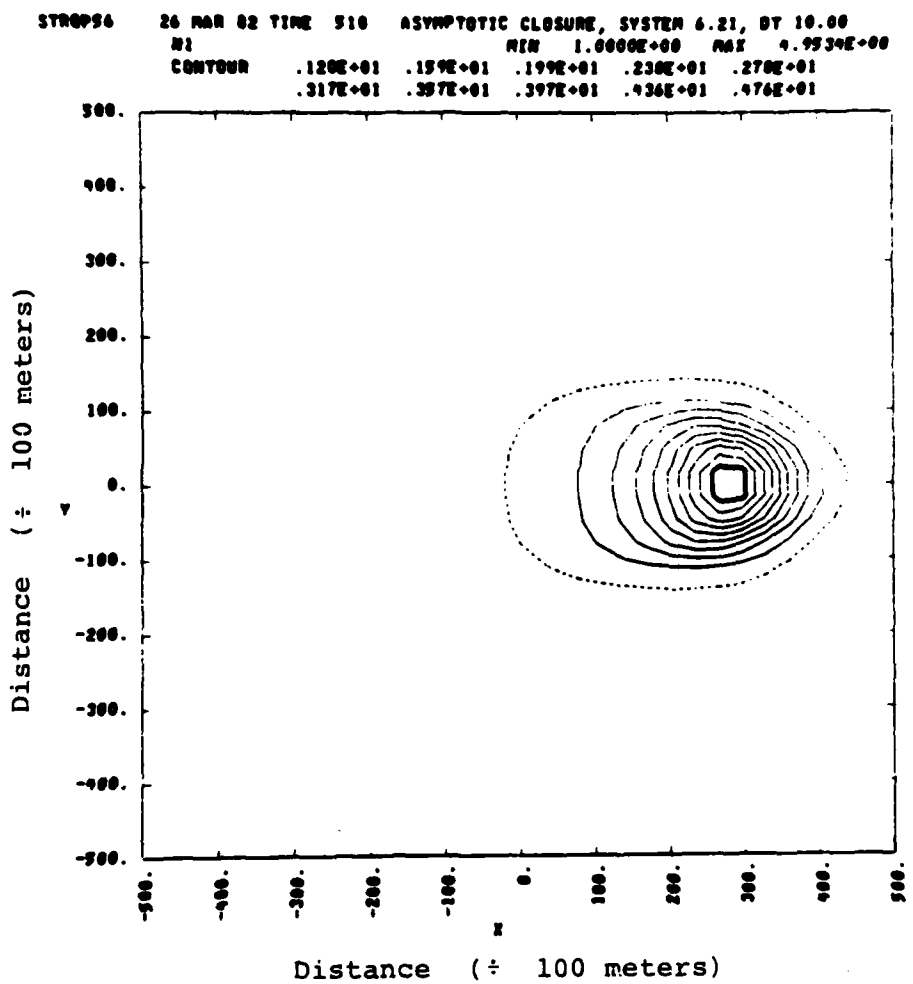

Figure 2-24. Mean density at 510 seconds.

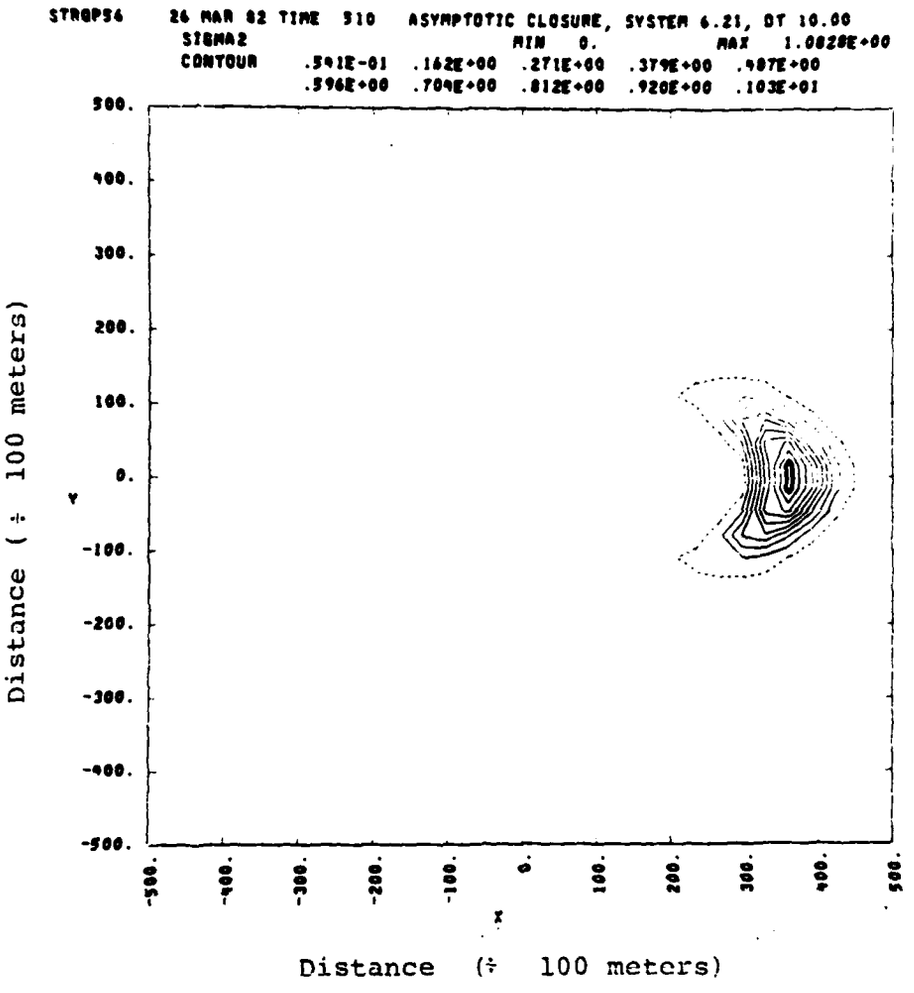

Figure 2-25. Variance at 510 seconds.

The above split-step calculation has also been performed for a translating frame of reference. The reference frame is assumed to move at one half of the wind velocity. Figures 2-26 thru 2-29 show the mean and variances predicted at 300 and 510 seconds. At 300 seconds the mean and variance are similar to those predicted in the rest frame calculations although there are small differences in the mean and the peak variance is nearly 50% greater. By 510 seconds the mean is developing a slightly different appearance from the rest frame calculation. The variance at 510 seconds is a factor of 2 greater. In view of the exponential growth of structure these differences are not very significant. The differences do however illustrate that microstructure calculations are more sensitive to numerical errors than classical calculations and emphasizes the importance of the numerical considerations of Section 2-4. It should be noted however that in spite of the marked differences in the variance values, the variance growth rates are roughly the same as those of the rest frame calculation and can also be considered to be in agreement with observed data.

2-6 TWO-DIMENSIONAL AXIALLY SYMMETRIC BOMB EVOLUTION WITH RADIAL HEAVE WINDS

The two-dimensional techniques presented in Section 2-2 can also be applied to the case of nuclear bomb plasma evolving under the influence of axisymmetric radially directed heave winds. The effective driver of plasma structure from high altitude nuclear detonations is the Pedersen conductivity weighted heave wind (see Section 3-1). For high latitude bursts this heave wind typically consists of two dominant components. One component is a poleward

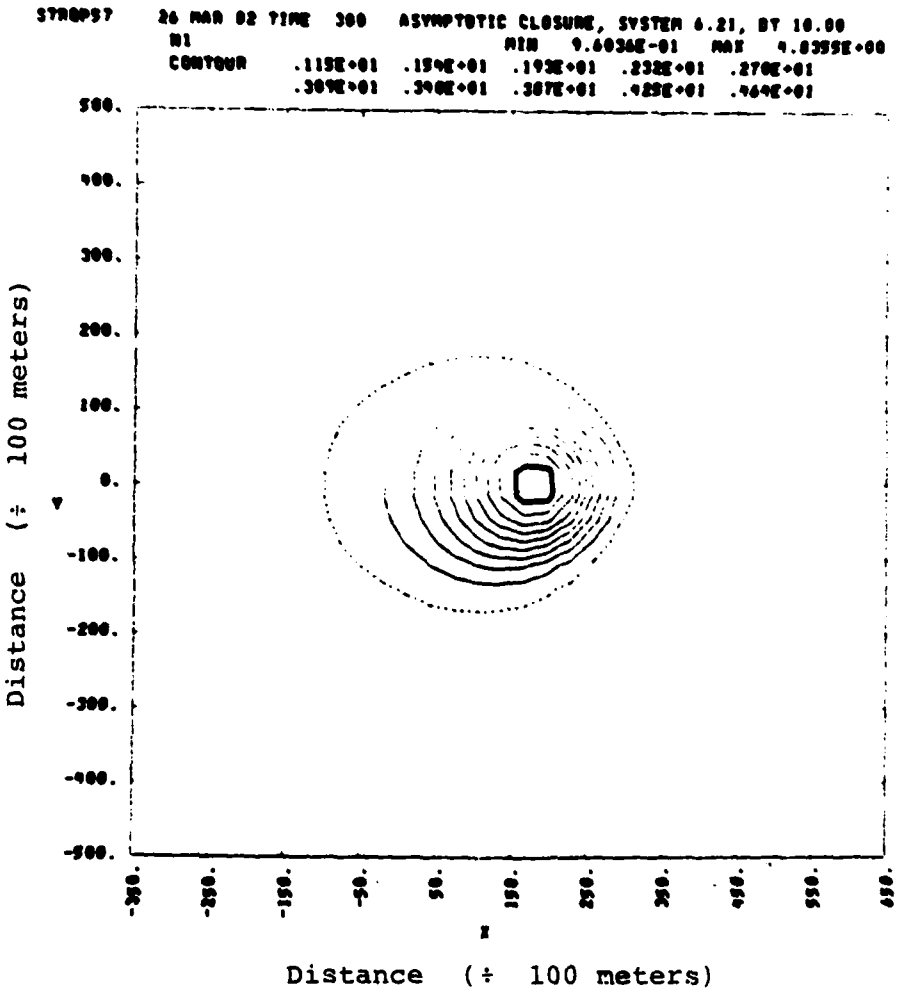

Figure 2-26. Mean density at 300 seconds in translating frame of reference.

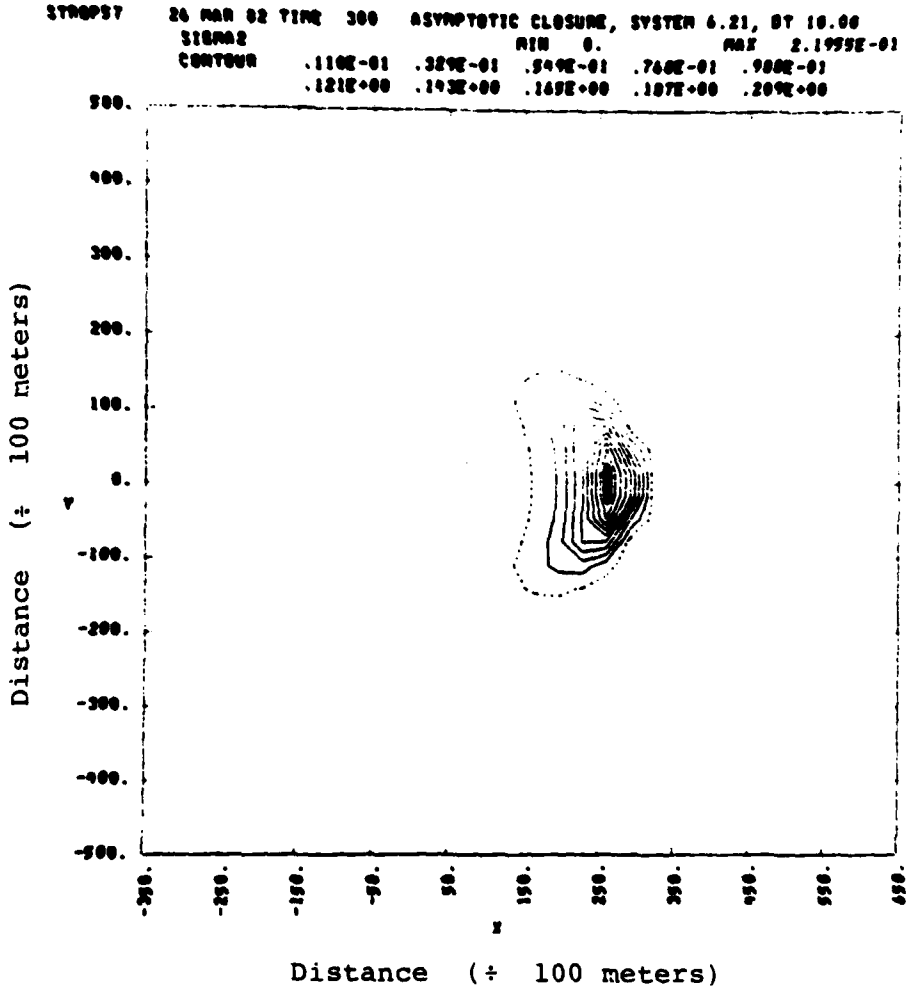

Figure 2-27. Variance at 300 seconds in translating frame of reference.

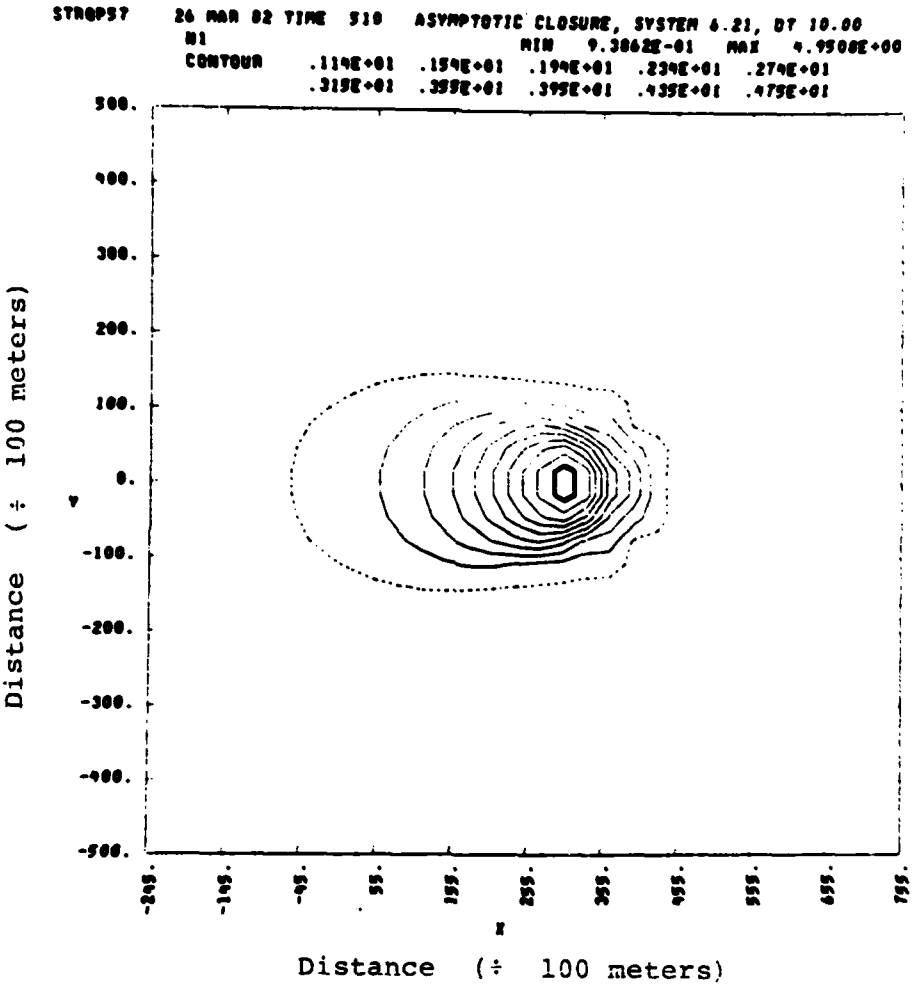

Figure 2-28. Mean density at 510 seconds in translating frame of reference.

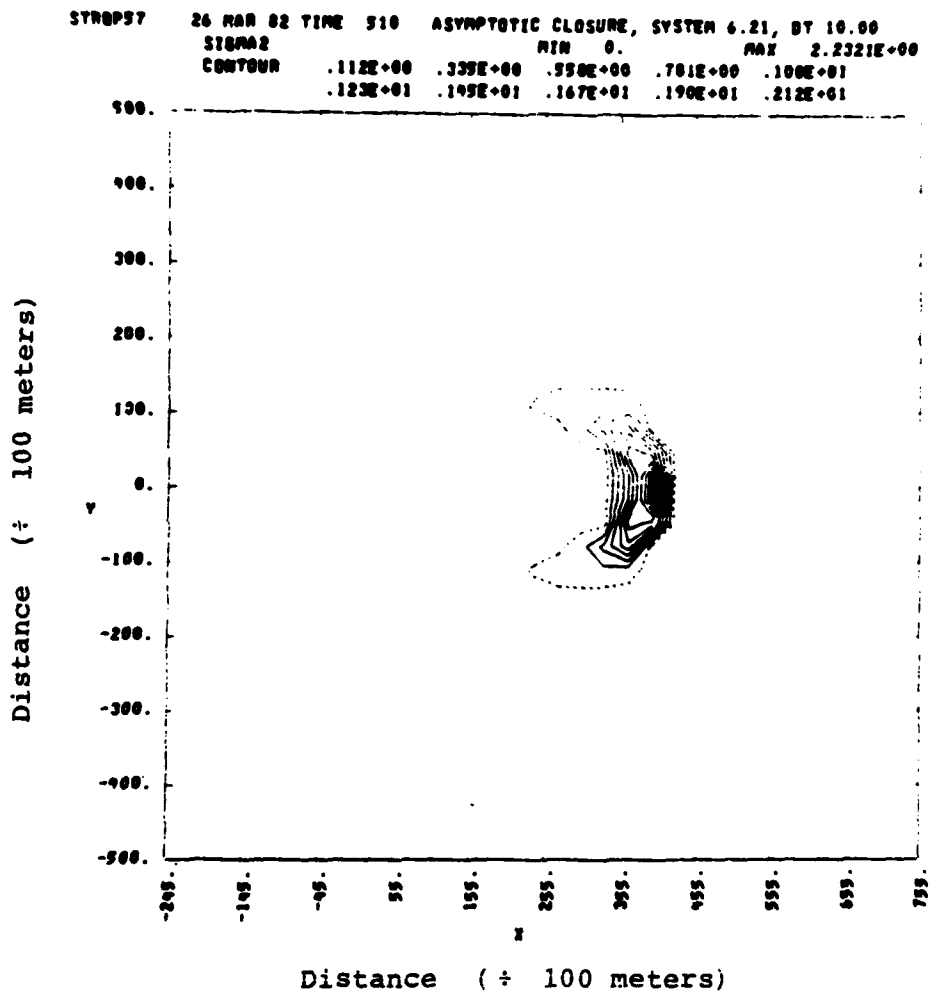

Figure 2-29. Variance at 510 seconds in translating frame of reference.

directed constant wind. The microstructure aspects of evolution under this type of wind component is different only in spatial scale from the barium cloud evolution illustrated in Section 2-5. The other dominant heave wind component is an axisymmetric radially directed wind. The investigation of microstructure evolution under the influence of this type of wind is presented in this section.

One interesting and useful facet of an axisymmetric radial wind which will be capitalized upon in this section is that if the bomb plasma statistics are also axisymmetric then the mean electrostatic potential is zero. This fact is a consequence of the property that the wind driven component of the current is divergence-free and consequently no electric fields are established. Solutions of the potential equation become unnecessary for following the evolution of the plasma.

Under the condition of axisymmetry in the wind and the plasma statistics the two-dimensional evolution problem may be reduced to a one-dimensional problem. The equations for the one-dimensional spatial evolution of $\langle N \rangle$ and Σ^2 through time which are produced using the SCENARIO approximation can be found from the results of Section 2-2 to be:

$$\frac{\partial \langle N \rangle}{\partial t} = - \nabla \cdot \langle N \rangle F_c V \tag{2.27}$$

$$\frac{\partial \Sigma^2}{\partial t} = - \nabla \cdot (\Sigma^2 - F_c \langle N \rangle^2) V - F_c V \cdot \nabla \langle N \rangle^2 \tag{2.28}$$

where $F_c = 1 - 1/(\langle N \rangle \langle 1/N \rangle)$

where the divergence and gradient operations are defined for the radial coordinate r through

$$\nabla \cdot A = \frac{1}{r} \frac{\partial}{\partial r} (r A_r) \tag{2.29}$$

$$\nabla q = \frac{\partial q}{\partial r} \tag{2.30}$$

Equations (2.27) and (2.28) together with the asymptotic closure approximation, i.e.,

$$F_c \simeq \Sigma^2/(\langle N \rangle^2 + \Sigma^2) \tag{2.31}$$

can be numerically time-stepped to simulate plasma and plasma structure evolution.

The evolution of plasma and plasma structure has been simulated using a generic wind model and representative wind conditions as illustrated in Figure 2-30. The initial plasma density is a constant background value of 1 plus a Gaussian of magnitude 4 which has a 100 kilometer e-fold radius. The standard deviation of the plasma structure has been set to be 3% of the initial mean density. The radial wind has a peak value of 1 km/sec at the 100 kilometer radius value with a linear inner dependence (from zero value) and a $1/r$ outer dependence. This wind profile is assumed to be constant throughout the simulation. The spatial sampling rate used in the simulation is 2 samples per kilometer.

The initial conditions have been advanced 15 minutes in time (900 seconds) using a .1 second time step. Figures 2-31 through 2-34 show plots of the mean and r.m.s. density at 2 1/2 minute intervals. Sturcture growth is seen to begin immediately. By 300 seconds the structure has become intense enough to significantly influence the motion of the

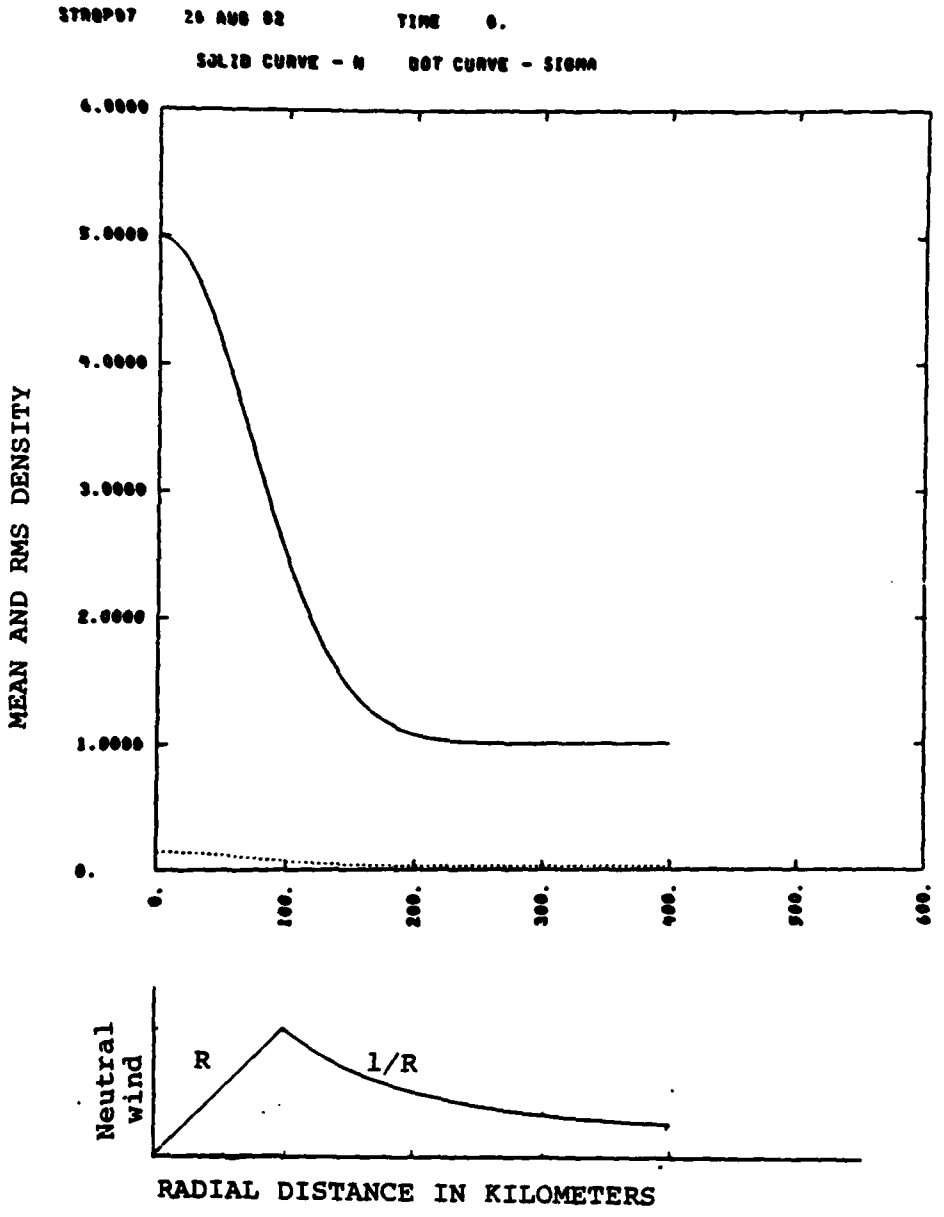

Figure 2-30. Initial and r.m.s. plasma density values and assumed initial wind.

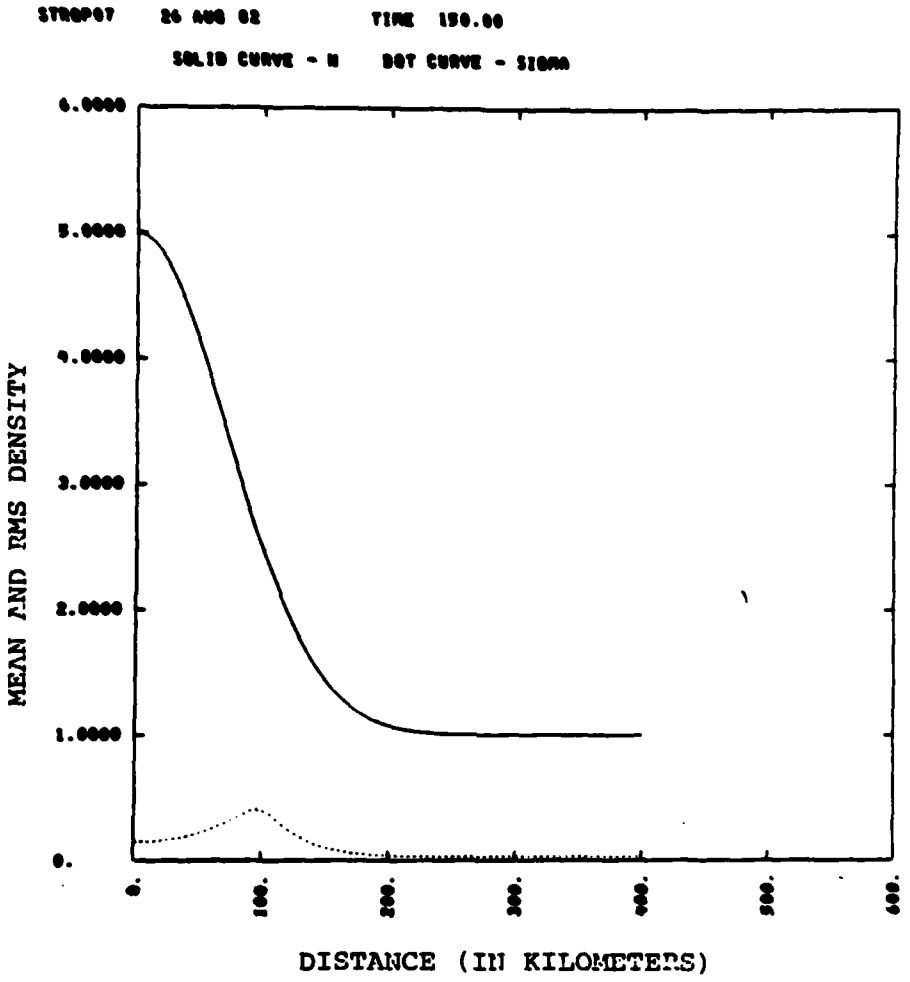

Figure 2-31. Plasma density and structure at 150 seconds.

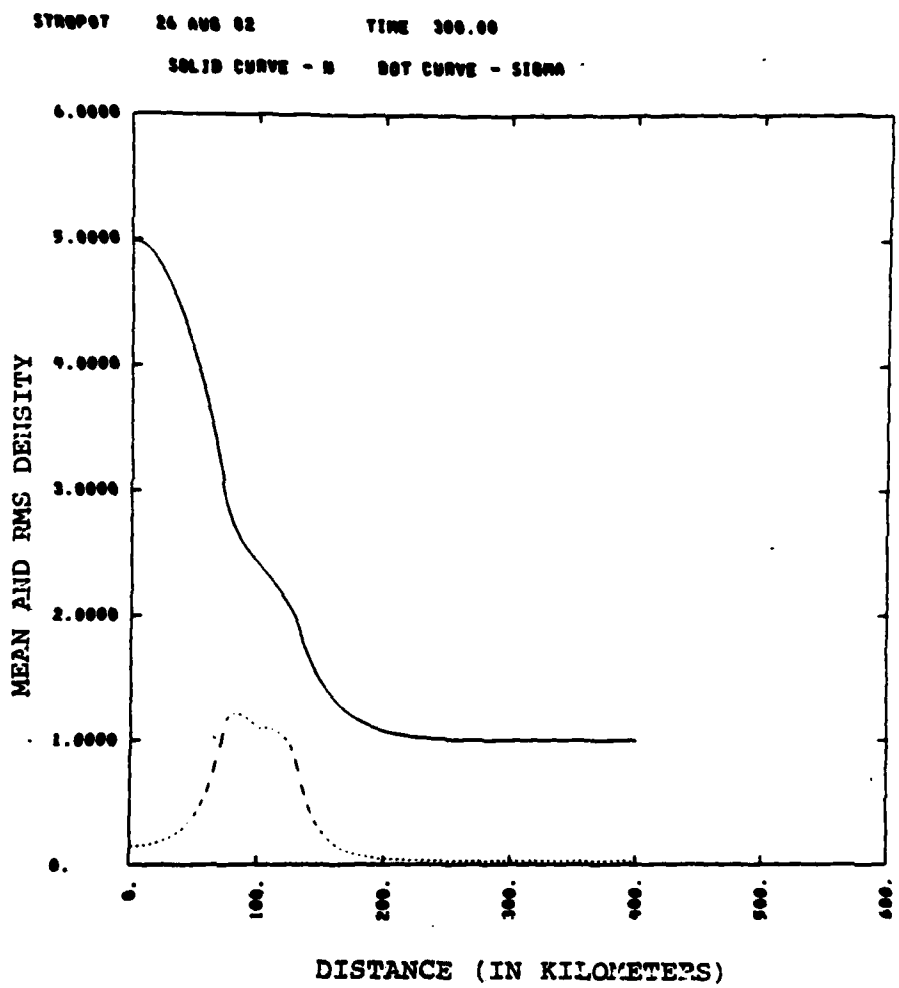

Figure 2-32. Plasma density and structure at 300 seconds.

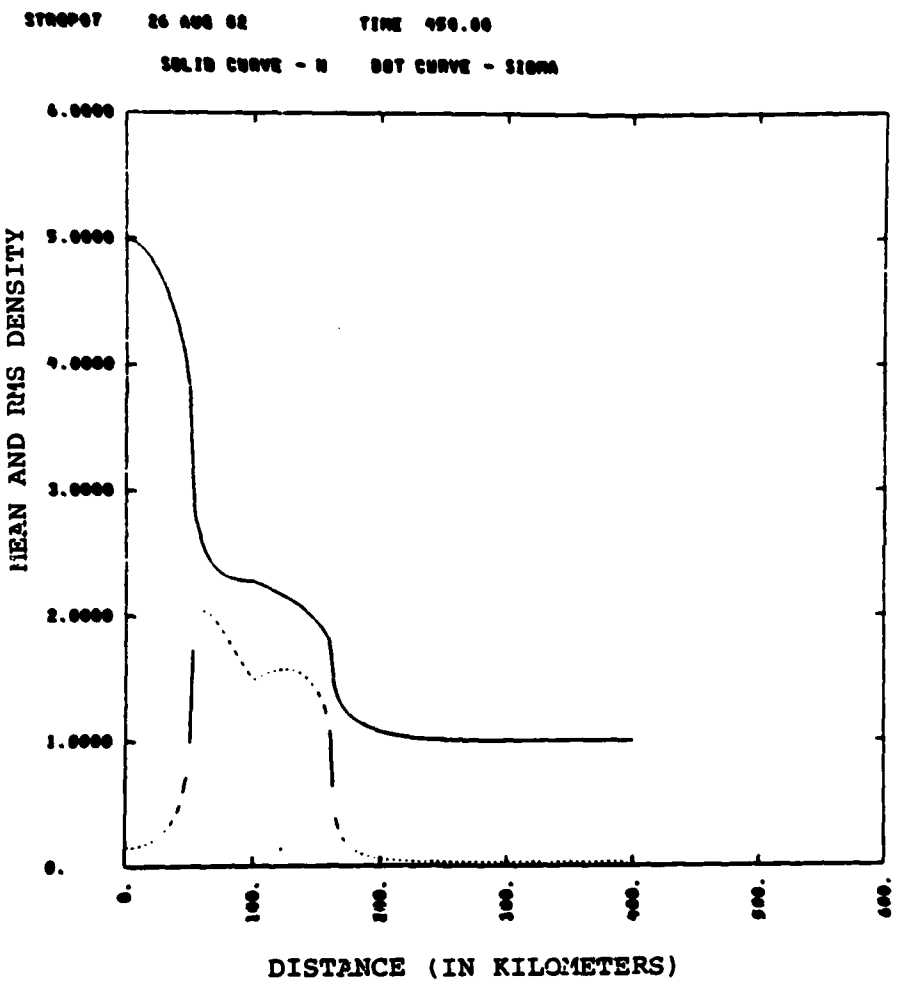

Figure 2-33. Plasma density and structure at 450 seconds.

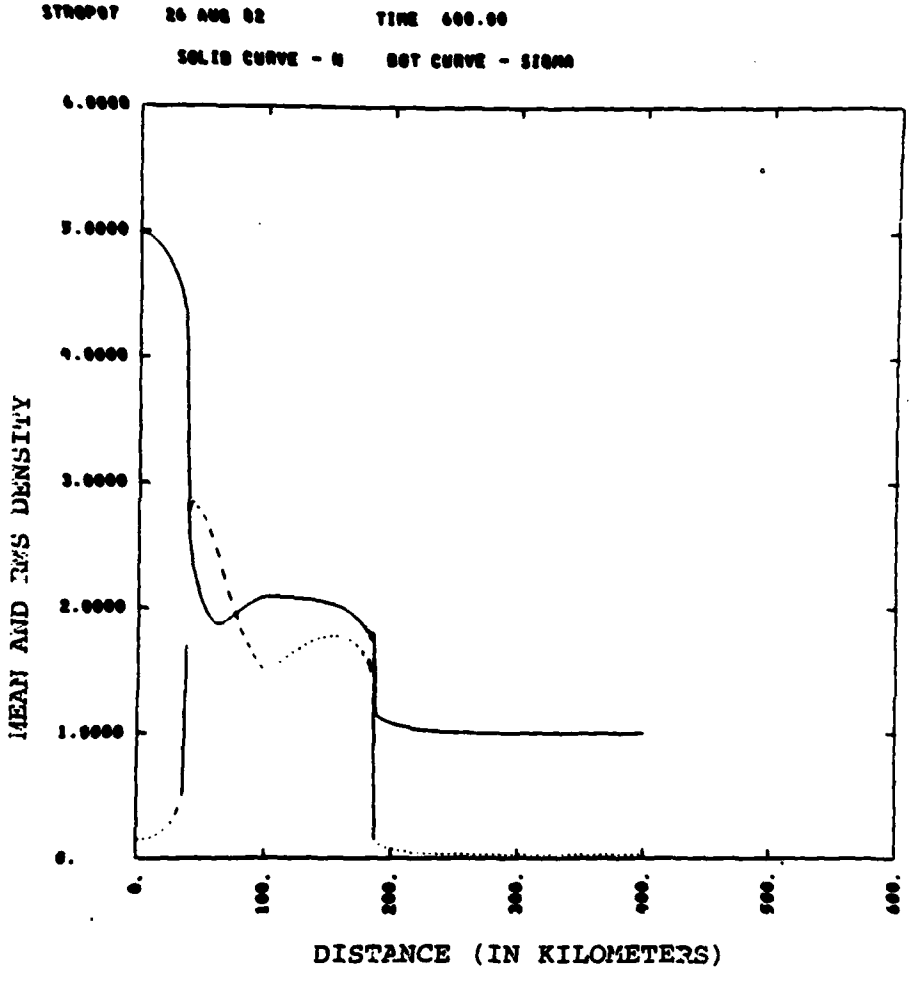

Figure 2-34. Plasma density and structure at 600 seconds.

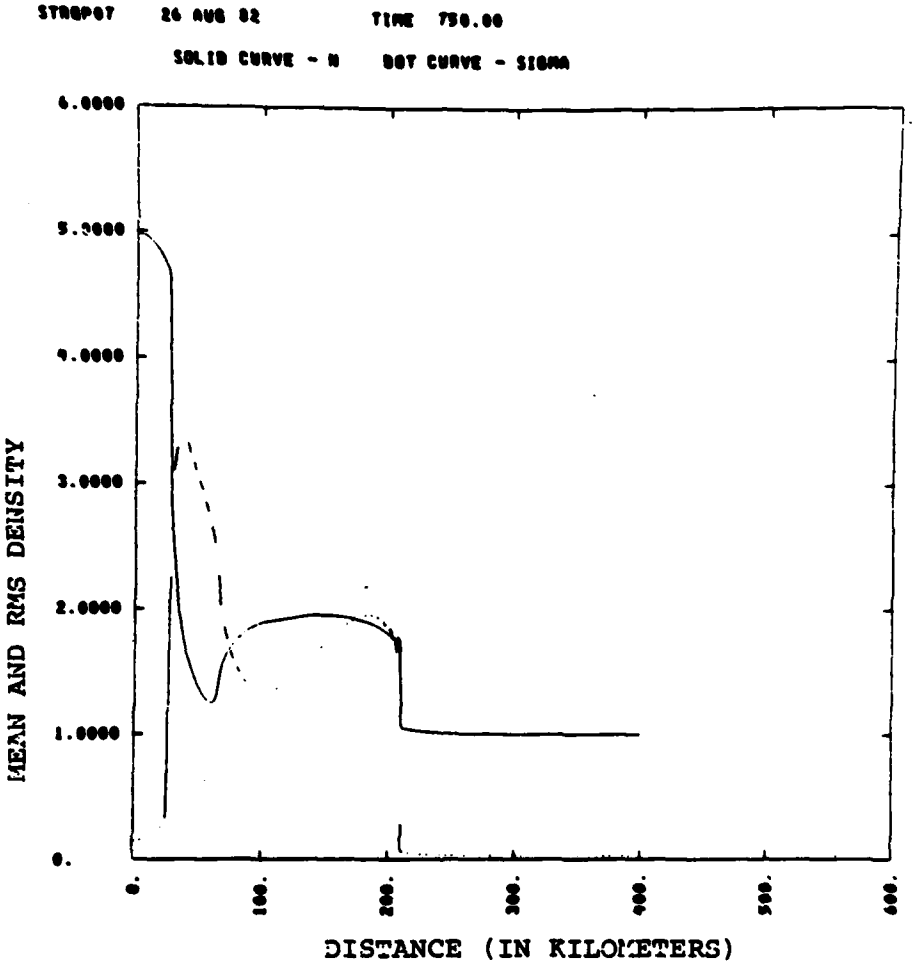

Figure 2-35. Plasma density and structure at 750 seconds.

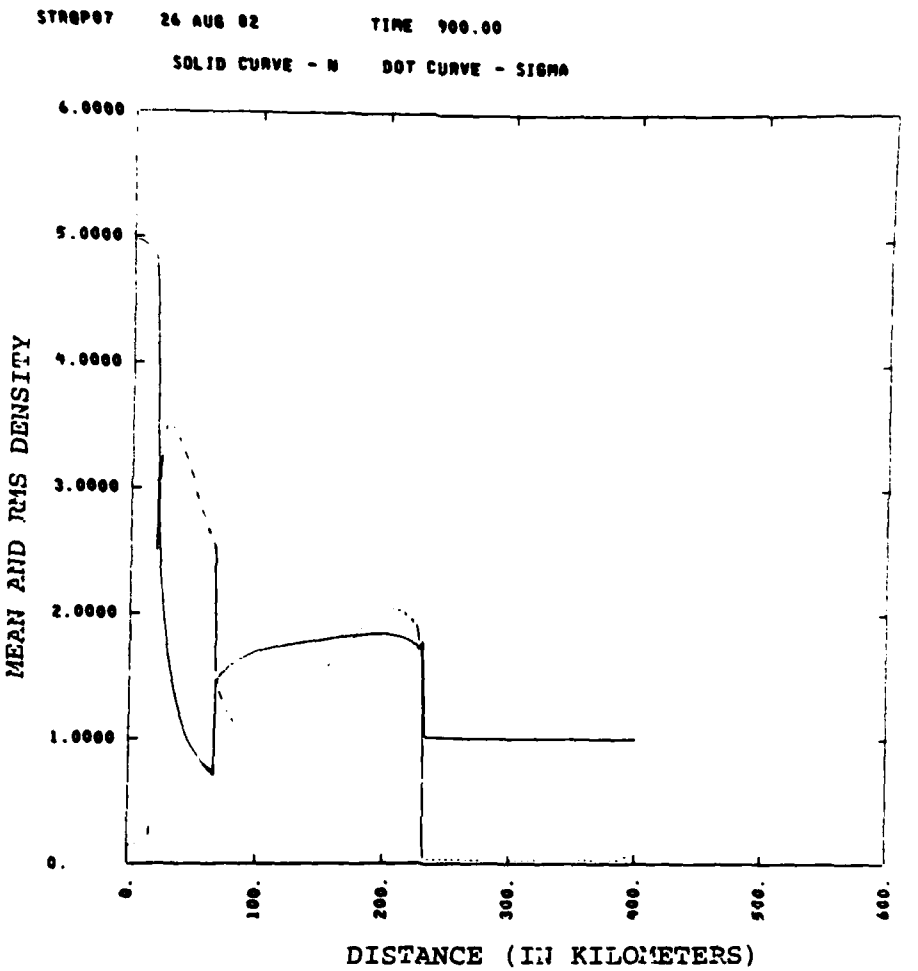

Figure 2-36. Plasma density and structure at 900 seconds.

mean plasma density. Very steep gradients in both density and structure occur by 600 seconds. By 900 seconds three of these steep gradient fronts have become established.

At 900 seconds the mean density has formed a ring around the interior peak. The exterior of the ring is at a radius of 230 kilometers. While this exterior radius indicates significant dispersal of the bomb plasma note that the dispersal is significantly less than Kilb's (Stoeckly and Kilb, 1981) free moving stick analysis would prescribe (≈ 400 kilometers).

At 900 seconds the plasma structure is intense both at the exterior of the mean density ring and at the exterior of the center peak intensity. The motion of the mean density with the enhancement of plasma structure at the exterior of the ring is physically suggestive of structure and density being carried by high density finger-like regions extending through the ring. The structure in the interior region of the plasma is suggestive of the complementary low density fingers extending into the interior plasma region.

The results of this microstructure evolution using the SCENARIO approximation is physically appealing. In contrast note that if classical conductivity and correlation assumptions were used then the plasma density and structure would not change from their initial values. The structure and density would be frozen to their initial location and no striation dispersal would be predicted.

Of numerical interest in this calculation are the fronts of steep gradients in mean density and structure. Special care must be taken in treating these gradients numerically to avoid Gibbs phenomena. Similar gradients would be expected if the problem is performed in two dimensions and similar Gibbs phenomena may result if care

is not taken. These fronts, thus, reinforce the points alluded to in Section 2-4 that the SCENARIO algorithms are somewhat more sensitive than classical algorithms and that care must be taken to reduce sources of numerical noise.

SECTION 3

MICROSTRUCTURE MODELLING OF TRANSVERSE TRANSPORT FOR SCENARIO

The development of microstructure transport techniques has been directed toward the implementation of transverse transport algorithms in the SCENARIO code. The SCENARIO code, in most aspects, is an engineering version of the MRC MELT code. The use of microstructure techniques is one aspect in which SCENARIO attempts to go beyond MELT. Its use is motived by the need to establish local structure intensities--quantities not directly given by MELT--for propagation effect calculation.

Like MELT, SCENARIO invokes the equi-potential approximation to reduce the three dimensional transport process to two simpler processes, namely, parallel-to-B transport and transport transverse to B. The parallel transport problem is basically one of calculating the compressible flow of the plasma in the direction of the geomagnetic field and is treated one-dimensionally with no interactions in the transverse direction. The algorithms for parallel transport in SCENARIO are basically approximations of and simplifications to MELT algorithms.

The problem of transverse transport in a three-dimensional geometry is closely related to the two-dimensional transport problem addressed in the previous section. In this section the microstructure techniques formulated in the previous section are extended to the three-dimensional transverse transport problem. First, the general theory is discussed in Section 3-1 and then in Section 3-2 the results of one set of algorithms which have been

implemented for SCENARIO are presented. Algorithms for alternative assumptions about the three-dimensional statistical characteristics are presented in Section 3-3.

3-1 EXTENSION OF MICROSTRUCTURE THEORY TO THREE DIMENSIONAL TRANSVERSE TRANSPORT

Classical algorithms for three-dimensional transverse transport numerically model the process in a two-step fashion similar to that discussed in Section 2. In one step, the convection step, the continuity equation is used with a known two-dimensional flow field to produce updated three-dimensional density values. In the second step, the potential solving step, an updated two-dimensional flow field is calculated from the updated three-dimensional density values. Microstructure influences the results of both steps--a fact which is ignored in classical techniques. In this section the general aspects of the extension of microstructure modelling techniques to this transport problem are discussed.

The microstructure three dimensional transverse transport split-step algorithm is outlined in Figure 3-1. It is basically an extension of the two-dimensional microstructure split-step algorithm seen in Figure 2-2 and has four basic steps. First the potential equation determines the transverse flow field from specified spatial dependences of the effective conductivity. Next, the flow fields are used to advance in time the statistics of the plasma density on each transverse layer. The statistics of the density are then field line integrated to determine the statistics of the field line integrated Pedersen conductivity. Finally, the spatial dependence of the effective conductivity is determined from the statistics of

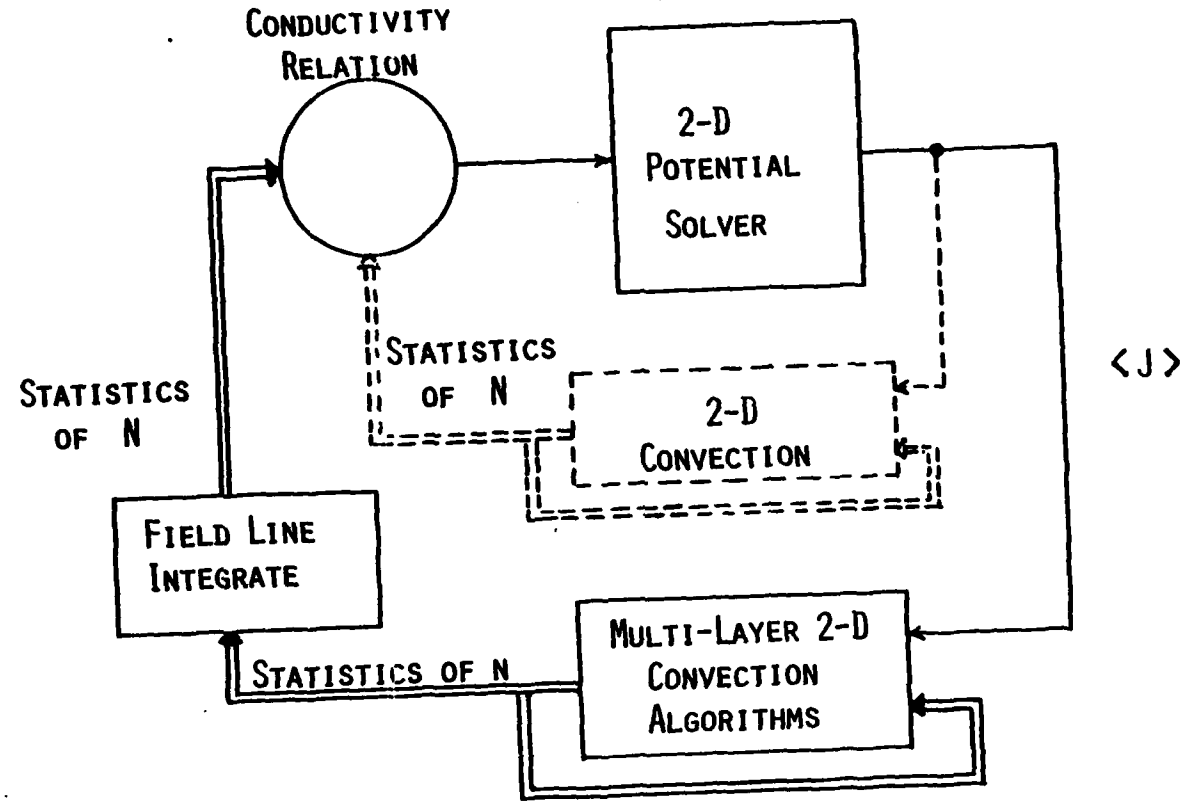

Figure 3-1. Microstructure split step algorithm for transverse transport.

the field line integrated Pedersen conductivity. If the plasma is not convected to regions of different neutral density and if the transverse wind on each layer is the same then the field line integrated Pedersen statistics are conserved and can be convected using the two-dimensional microstructure technique. As noted by the dotted line path in the figure, the two-dimensional calculation may in some instances serve as an alternative path for determining these field line integrated quantities and thereby allow consistency checks for the convection algorithm (Stagat, et al. 1982).

The central features of the three-dimensional microstructure approach are basically the same as those used to develop the two-dimensional microstructure algorithms of Section 2. For solving the potential step fluctuations in the cross-field conductivity are assumed to influence the mean conductivity through some specified relation, typically, the asymptotic closure relation. For solving the convection step the mean flux is calculated from the mean cross-field currents. As in the two-dimensional case, the cross-field currents are assumed to be uncorrelated with density related quantities. These features of the approach are basically the same as those described in Section 2. The primary issues involved in extending the theory to three dimensions focus on how to reduce the given three dimensional structure quantities to two-dimensional inputs to the potential equation and how to construct three-dimensional fluxes from its two-dimensional solutions. Currently these issues are resolved

through the use of fairly broad based assumptions based upon physical intuition.

With the parallels between the three-dimensional transverse transport problem and the two-dimensional evolution problem now established it is appropriate to review the derivation of the three-dimensional relations and to focus on the two issues of field integrated statistics and of relating the local flux to the plasma potential.

As noted above the issue of determining field line integrated statistics from local statistics arises in connection with the solution of the potential equation. The potential equation arises from the condition that the total transverse current at any field line be divergenceless to assure that charge will not accumulate. The field line integrated transverse current, J, is given by

$$J = \int j \, dz \tag{3.1}$$

where j is the local transverse current and where the magnetic field is assumed to be z-directed. Note that lower case quantities will be used throughout Section 3 to denote three-dimensional counterparts to upper case 2-dimensional quantities (with the exception of 'ϕ' which denotes a 2-dimensional quantity even though it is properly lower case). Also note that a constant magnitude z-directed magnetic field is assumed in order to simplify the discussion. The actual SCENARIO algorithms have been developed for a dipole coordinate system and include complicating coordinate scale factors.

From Section 2.1 the local transverse current can be expressed as (eq. 2.1).

$$j = \frac{en}{\mu B} \left(\frac{E}{B} + v \times i_z\right) \tag{3.2}$$

where n is the local plasma density, v is the local wind velocity, E is the electric field, μ is the ionic mobility in the neutrals and B is the magnitude of the magnetic field. The assumption that the field lines are equipotential implies that the electric field is a two-dimensional quantity. Performing the field line integration of this expression for the local current produces the following relation for J

$$J = N(E/B + V \times i_z) \tag{3.3}$$

where N and V are the field line integrated Pedersen conductivity and field line integrated neutral wind respectively defined by

$$N = \int \frac{en}{\mu B}\, dz \tag{3.4}$$

$$V = \int \frac{env}{\mu B}\, dz/N \tag{3.5}$$

The issue of determining the field line integrated statistics from the local statistics arises directly from these two integrals. Because of their importance some comments about them are appropriate. The values of N and V result from weighted field line integrals of the local plasma density and the wind velocity. For N the weighting function of most significance is the neutral density which enters strongly in the ionic mobility term. The neutral density weighting function varies rapidly with altitude. In the 300 kilometer altitude regime it

changes by a factor of ten every 100 kilometers. For V, as with N, the neutral density is also a significant weighting function but, unlike with N, the integral for V includes the local plasma density n as a weighting term. The field line averaged neutral wind, V thus will be correlated with the local density statistics.

The potential equation used in classical algorithms results from the assumptions that the electric field is irrotational and that the current J is divergenceless:

$$\begin{aligned} \nabla \cdot J &= \nabla \cdot (N(E/B + V \times i_z)) \\ &= \nabla \cdot (N(\nabla\phi + V \times i_z)) = 0 \end{aligned} \tag{3.6}$$

This relation is the same as the two-dimensional relation presented in Section 2 except that here N and V denote field line integrated quantities.

The potential equation used for microstructure theory is similar. It is derived from the assumption that the electric field is irrotational and that the mean current, <J>, is divergenceless yielding:

$$\begin{aligned} \nabla \cdot \langle J \rangle &= \nabla \cdot \langle N(E/B + V \times i_z \rangle \\ &= \nabla \cdot \langle N(\nabla\phi/B + V \times i_z) \rangle = 0 \end{aligned} \tag{3.7}$$

As in the two dimensional case approximations to the mean conductivity relation are needed to reduce the stochastic potential equation to a numerical equation. The requirement thus arises to define a relation for <J> in terms of the statistics of N, $\nabla\phi$, and V and to then determine these statistics from the local

statistics of the plasma density n. Determining the statistics of field line integrated quantities from the statistics of the local plasma density requires knowledge about the correlation properties of the plasma density along field lines.

The range of possible formulations can be exemplified by considering the possible expressions for the variance of N, denoted by Σ^2 in terms of the variance of the local plasma density n denoted by σ^2. For the case of uncorrelated structure between adjacent grid cells in the z-direction, the relation for the variance of the integrated Pedersen conductivity N is

$$\Sigma^2 = \int \left(\frac{e\sigma}{\mu B}\right)^2 dz \tag{3.8}$$

where the integration is understood to represent a summation over the grid cells in the z-direction. For the case of structure which is correlated or anti-correlated from cell to cell with correlation coefficient of 1 the relation would be

$$\Sigma = \int_{I_1} \frac{e\sigma}{\mu B} dz - \int_{I_2} \frac{e\sigma}{\mu B} dz \tag{3.9}$$

where I_1 is the region of the fluctuations positively correlated with the field line integrated content and where I_2 is the region of negatively correlated fluctuations. Note that if the value of σ in the I_2 region is assigned a negative value, the above relation can be expressed more compactly as

$$\Sigma = \int \frac{e\sigma}{\mu B} dz \tag{3.10}$$

Giving a positive or negative polarity to the value of σ has been found to be useful in developing the completely correlated algorithm discussed in Section 3.2. Since only σ^2 is required for propagation effects analysis, assuming negative values of σ does not alter any of the systems effects outputs. Different types of field line correlation models can thus lead to significantly different dependencies of the variance of N on the local plasma variance and correspondingly different algorithms as a result.

Assuming the issue of relating local quantities to field line integrated quantities has been resolved, solutions to the potential equation can be obtained numerically producing values of the mean potential, $\langle \nabla \phi \rangle$, and thereby precipitating the second issue. Given the mean potential, what is the flux field of the local plasma structure.

The mean flux of the local mean density and the mean flux of the mean square density are formally given by $\langle n\, U \rangle$ and $\langle n^2\, U \rangle$ respectively where U is the plasma velocity defined by $\nabla \phi \times i_z$. The current issue is basically how to express these quantities in terms of the known statistics of n and the result of the potential step $\langle \nabla \phi \rangle$ or equivalently $\langle U \rangle$. A first step in obtaining these relations may be taken as in Section 2 by investigating the expressions between the plasma velocity and the current:

$$U = \frac{J \times i_z}{N} + V \tag{3.11}$$

$$\langle n\ U \rangle = \left\langle \frac{n\ J \times i_z}{N} \right\rangle + \langle n\ V \rangle \tag{3.12}$$

$$\langle n^2\ U \rangle = \left\langle \frac{n^2\ J \times i_z}{N} \right\rangle + \langle n^2\ V \rangle \tag{3.13}$$

By invoking the assumption that the plasma density related quantities $1/N$, n/N, and n^2/N are uncorrelated with J, evaluating $\langle J \rangle$ in terms of $\langle U \rangle$, and then substituting; the following mean flux relations are obtained.

$$\langle n\ U \rangle = \left\langle \frac{n}{N} \right\rangle \frac{\langle U \rangle - \langle V \rangle}{\left\langle \frac{1}{N} \right\rangle} + \langle n\ V \rangle$$

$$\langle n^2\ U \rangle = \left\langle \frac{n^2}{N} \right\rangle \frac{\langle U \rangle - \langle V \rangle}{\left\langle \frac{1}{N} \right\rangle} + \langle n^2\ V \rangle$$

The basic problem which remains is how to evaluate the quantities

$$\left\langle \frac{n}{N} \right\rangle,\ \left\langle \frac{n^2}{N} \right\rangle,\ \langle V \rangle,\ \langle n\ V \rangle,\ \text{and}\ \langle n^2\ V \rangle$$

in terms of $\langle n \rangle$, σ, $\langle N \rangle$, Σ, and v. These quantities can be evaluated explicitly only if something is known about how the local quantity n is jointly distributed with the field line integrated quantity N. Once again the extension to the three-dimensional problem is focussed on its field line correlation aspects.

These quantities have been evaluated for the completely correlated situation as discussed in Section

3-2. For the uncorrelated situation, techniques for their evaluation are suggested in Section 3-3. The expressions arrived at are somewhat more complex than would initially be guessed. Neither does $\langle\frac{n}{N}\rangle$ equal $\frac{\langle n\rangle}{\langle N\rangle}$ for the completely correlated case nor does $\langle\frac{n}{N}\rangle = \langle n\rangle \langle\frac{1}{N}\rangle$ for the uncorrelated case. In both cases further assumptions about the fluctuation statistics are required. These assumptions and the resulting expressions are discussed more fully in the next two sections.

3-2 THREE-DIMENSIONAL TRANSPORT FOR COMPLETELY CORRELATED STRUCTURE

In order to reduce the three-dimensional transverse transport problem into a two-dimensional problem suitable for application of the techniques advanced in Section 2 it is necessary to know how the structure is correlated in the direction parallel to the geomagnetic field. In all current approaches to this problem the structure correlation properties are provided through assumption only. This section considers the case in which the structure is assumed to be coherently correlated along the geomagnetic field direction. Algorithms for use in SCENARIO are developed and selected results from a SCENARIO implementation are shown.

The coherent fluctuation approximation is explicitly that there exists a stochastic form function $\varepsilon(x,y)$ with zero mean and unit variance that describes the fluctuations of the integrated Pedersen conductivity through:

$$N = \langle N \rangle + \varepsilon(x,y)\ \Sigma \qquad (3.16)$$

as well as the fluctuations of the local density through the similar relations

$$n = \langle n \rangle + \varepsilon(x,y)\ \sigma \qquad (3.17)$$

Note that while the r.m.s. value of the integrated Pedersen conductivity Σ is defined in its usual positive sense, the r.m.s. values of the local density fluctuations are allowed to be either positive or negative. A negative value of σ denotes that fact that the local fluctuations n are coherently anti-correlated with the total electron content.

Coherent structure growth is produced when a structured two dimensional velocity field is imposed upon gradients of local density that may or may not be structured. This structure growth is correlated with a normalized correlation coefficient of plus or minus one according to the sign of an effective mixing velocity component in the direction of the local gradient, as will be detailed later in this section. The important point to note now is that this mechanism for the coherent growth of structure motivates the use of the sign of σ as well as its magnitude. Further, the important additional information carried by the sign of sigma imposes no added storage requirements to the algorithms. Its use can be construed as a more efficient use of available computational assets.

The basic quantities in the algorithm are $\langle n \rangle$ and σ. The two dimensional values used for input to the potential equation, $\langle N \rangle$ and Σ, are essentially the neutral density weighted sums of $\langle n \rangle$ and σ as discussed in the previous section. Explicity

$$\langle N \rangle = \frac{1}{N_o} \sum n_o \langle n \rangle \tag{3.18}$$

$$\Sigma = \frac{1}{N_o} \sum n_o \sigma \tag{3.19}$$

where N_o is the neutral density normalization quantity defined by:

$$N_o = \sum n_o \tag{3.20}$$

where the altitude variations of the magnetic field strength with position along the geomagnetic field have been dropped for simplicity of presentation, and where the sums are assumed to be along the geomagnetic field.

From Section 3-1, equation (3.6), the field line integrated transverse current J can be written as

$$J = N\ E/B + N\ V \times i_z \tag{3.21}$$

giving

$$\langle J \rangle = \langle N\ E/B \rangle + \langle N\ V \rangle \times i_z \tag{3.22}$$

While this expression is useful for determining the mean flux, essentially $\langle N\ E/B \rangle$; for solving the potential equation an expression for the mean current $\langle J \rangle$ in terms of the mean electric field and mean wind is needed. One method to obtain this needed expression is to divide the equation for J by N, to take the expectation and to then invoke the SCENARIO approximation that J is uncorrelated with $1/N$ giving:

$$\langle J \rangle \langle 1/N \rangle = \langle E/B \rangle + \langle V \rangle \times i_z \tag{3.23}$$

By invoking the asymptotic closure approximation to the effective conductivity, $\langle 1/N \rangle^{-1}$, the expression for the mean current becomes:

$$\langle J \rangle = \frac{\langle N \rangle^3}{\Sigma^2 + \langle N \rangle^2} \left(\left\langle \frac{E}{B} \right\rangle + \langle V \rangle \times i_z \right) \tag{3.24}$$

The potential equation which is solved numerically results from setting the divergence of this equation to zero. Note that $\langle N \rangle$ and Σ^2 are known from their field line integrations and that $\langle E/B \rangle$ is to be solved for. The neutral wind term $\langle V \rangle$ can also be expressed in terms of the local wind v and the local structure quantities through the form factor assumption as now discussed.

The expression for the field line integrated neutral wind V from Section 3-1 is:

$$V = \frac{\int n_o n v \, dz}{N N_o} \tag{3.25}$$

Note that V is a weighted integral of the neutral wind where the weighting functions are the local neutral density n_o and the local plasma density n. With the form factor assumption V can be written as

$$V = \frac{\int n_o \langle n \rangle v \, dz + \varepsilon \int n_o \sigma v \, dz}{N_o (\langle N \rangle + \varepsilon \Sigma)} \tag{3.26}$$

or for simplicity

$$V = \frac{F_n + \varepsilon F_\sigma}{\langle N \rangle + \varepsilon \Sigma} \tag{3.27}$$

where F_n and F_σ are weighted fluxes of plasma density and structure which have been defined through

$$F_n = \int n_o \langle n \rangle v \, dz / N_o \tag{3.28}$$

$$F_\sigma = \int n_o \sigma v \, dz / N_o \tag{3.29}$$

The above expression for the stochastic variation of V includes the ε form factor in both the numerator and the denominator. To find $\langle V \rangle$ long division is used to isolate ε into either the numerator or the denominator. This technique is also used frequently in the evaluation of many flux related quantities as discussed later. For evaluating the mean of V the long division technique produces

$$V = \frac{F_\sigma}{\Sigma} + \frac{F_n - F_\sigma \langle N \rangle / \Sigma}{\langle N \rangle + \varepsilon \Sigma} \tag{3.30}$$

Once the form factor is isolated to the denominator as above an expectation produces $\langle 1/N \rangle$, thus

$$\langle V \rangle = \frac{F_\sigma}{\Sigma} + \left\langle \frac{1}{N} \right\rangle F_n - \left\langle \frac{1}{N} \right\rangle \langle N \rangle F_\sigma / \Sigma \tag{3.31}$$

is the expression which results and which can be used directly in the potential equation.

For solving the convection equations for $\langle n \rangle$ and σ^2 the mean fluxes defined by $\langle n\, U \rangle$ and $\langle n^2\, U \rangle$ are required. As discussed in Section 3-1 these fluxes are derived through relations for the current with the assumption that both n/N and n^2/N are uncorrelated with J giving relations for the mean fluxes. Specifically for $\langle n\, U \rangle$ the expression obtained is

$$\begin{aligned} \langle n\, U \rangle &= \left\langle \frac{n}{N} \right\rangle \langle J \rangle \times i_z + \langle n\, V \rangle \\ &= \left\langle \frac{n}{N} \right\rangle \frac{\langle U \rangle - \langle V \rangle}{\left\langle \frac{1}{N} \right\rangle} + \langle n\, V \rangle \end{aligned} \tag{3.32}$$

where $\langle J \rangle \langle 1/N \rangle = \langle E/B \rangle + \langle V \rangle \times i_z$ and $\langle V \rangle = \langle E/B \rangle \times i_z$ have been used to substitute for $\langle J \rangle$. The quantity

$\langle n/N \rangle$ is found from the form factor assumption and the factorization provided by one long division:

$$\left\langle \frac{n}{N} \right\rangle = \frac{\langle n \rangle + \varepsilon\, \sigma}{\langle N \rangle + \varepsilon\, \Sigma}$$

$$= \left(\langle n \rangle - \frac{\sigma\, \langle N \rangle}{\Sigma} \right) \left\langle \frac{1}{N + \varepsilon\, \Sigma} \right\rangle + \frac{\sigma}{\Sigma}$$

$$= (\langle n \rangle - R\, \sigma)\ \langle 1/N \rangle \qquad (3.33)$$

where R is defined by

$$R = \frac{\langle N \rangle}{\Sigma} - \frac{1}{\Sigma\ \langle 1/N \rangle} = \frac{\langle N \rangle}{\Sigma}\, F_c \qquad (3.34)$$

where $F_c = 1 - \dfrac{1}{\langle 1/N \rangle\, \langle N \rangle}$

The quantity $\langle n\, V \rangle$ can be found similarly to be

$$\langle n\, V \rangle = \left\langle \frac{1}{N} \right\rangle \left(\langle n \rangle\, F_n - \left(\sigma F_n + F_\sigma \langle n \rangle - \frac{\sigma F_\sigma \langle N \rangle}{\Sigma} \right) R \right) \qquad (3.35)$$

When these quantities are substituted into the expression for $\langle n\, U \rangle$ considerable cancelling occurs giving the following result

$$\langle n\, U \rangle = \langle n \rangle\, \langle U \rangle + \sigma\, W \qquad (3.36)$$

where W is the velocity vector defined by:

$$W = R(F_\sigma/\Sigma - \langle U \rangle) \qquad (3.37)$$

This result is physically appealing in that it says the flux of the local plasma is determined by the classical term $\langle n \rangle\, \langle U \rangle$ plus a correction dependent upon the amount

of local structure. The presence of structure locally can cause convection in the direction of the mixing velocity W. The term F_σ/Σ can be recognized to be a weighted field-line integral of the neutral wind when the weighting function is the local structure amplitude. Thus W can be considered to be R times an effective structured wind force slip velocity. Note that with the asymptotic closure approximation R also takes on a simple form, namely,

$$R = \frac{\Sigma \ \langle N \rangle}{\langle N \rangle^2 + \Sigma^2} \tag{3.38}$$

which ranges from zero to a maximum value of 1/2.

In order to derive an equation for the convection of σ the mean flux of n^2 is needed. This quantity, $\langle n^2 \ U \rangle$, can be found in a fashion similar to the above with the relation

$$\begin{aligned} \langle n^2 \ U \rangle &= \langle \frac{n^2}{N} \ J \times i_z \rangle + \langle n^2 \ V \rangle \\ &= \langle \frac{n^2}{N} \rangle \ \frac{\langle U \rangle - \langle V \rangle}{\langle \frac{1}{N} \rangle} + \langle n^2 \ V \rangle \end{aligned} \tag{3.39}$$

In addition to $\langle V \rangle$ which was evaluated above, expressions for $\langle n^2/N \rangle$ and $\langle n^2 \ V \rangle$ are required and can be found using the long division technique. The algebra is considerably more complicated but as with $\langle n \ U \rangle$ considerable cancellation occurs in the derivation to produce

$$\langle n^2 \ U \rangle = \langle n \rangle^2 \ \langle U \rangle + 2 \ \sigma n W - \sigma^2 \ \frac{N}{\Sigma} \ W + \frac{\sigma^2 \ F_\sigma}{\Sigma} \tag{3.40}$$

The convection equation for the standard deviation of the local density can be expressed in terms of the mean flux of the density and density squared by the following

$$2\sigma \frac{\partial \sigma}{\partial t} = \frac{\partial \langle n^2 \rangle}{\partial t} - \frac{\partial \langle n \rangle^2}{\partial t} \tag{3.41}$$

or

$$\frac{\partial \sigma}{\partial t} = \frac{\langle n \rangle}{\sigma} \nabla \cdot \langle n\, U \rangle - \frac{1}{2\sigma} \nabla \cdot \langle n^2\, U \rangle \tag{3.42}$$

Substituting the above relations for $\langle n\, U \rangle$ and $\langle n^2\, U \rangle$ and performing further cancellation of terms yields a relation which is physically appealing, namely

$$\frac{\partial \sigma}{\partial t} = - \frac{1}{2\sigma} \nabla \cdot (\sigma^2 Q) - W \cdot \nabla n \tag{3.43}$$

where Q is a velocity given by

$$Q = \frac{F_\sigma}{\Sigma} - \frac{N}{\Sigma} W \tag{3.44}$$

If the local density gradients are zero this equation reverts to a relation for the conservation of structure variance moving with velocity Q, namely

$$\frac{\partial \sigma^2}{\partial t} = - \nabla \cdot (\sigma^2\, Q) \tag{3.45}$$

Thus local structure moves in a conservative manner according to the two-dimensional flow field given by Q, a sum of effective structured wind flow field and the mean plasma flow field with each of these velocity terms weighted by structure related values. This flow is independent of the sign of σ and does not alter it.

If the local density gradients are not zero then structure can grow according to the $W \cdot \nabla n$ term. This term demonstrates the growth expected to be produced by a structured flow field in a smooth density gradient. As noted earlier in this section the growth term can be

positive or negative according to the relationship between the local density gradient direction and the velocity W. Positive structure growth denotes structure growing in a manner correlated with fluctuations in the total electron content. Negative growth denotes growth toward anti-correlated structure. Note that the growth term can exist even if the local structure $\sigma = 0$; however, in order to assure a non-zero value of W structure must exist somewhere along the field line, $\Sigma \neq 0$, in order for structure to grow. As with the two dimensional case an initially smooth, $\sigma = 0$ everywhere, plasma will produce no structure. All of these features which are evident in the convection equations very nicely characterize the features of gradient drift structure growth and are intuitively appealing from a physical standpoint.

The potential and convection algorithms have been coded into SCENARIO and results from a single burst Cheyenne Mt. run are available. Figures 3-2 and 3-3 summarize the Cartesian form of these relations for easy reference. Shown in Figures 3-4 and 3-5 are the mean plasma density and the standard deviation of the microstructure used to initialize the SCENARIO plasma grid. The mean plasma density is determined by the MHD initializer module. The standard deviation has been simply chosen to be 25% of the mean density. Figure 3-6 shows a constant altitude view of the mean density near the bottom of the bomb density enhancement. Of specific interest in this plot is the depletion of mean density near the center and an almost ring-like distribution of the peak value of mean density. On the interior of the ring are density gradients which would be stable to the heave winds in a two-dimensional problem; however, in the subsequent evolution of this 3-d problem the gradients are the source of important structure growth that is anti-correlated with the total electron content fluctuations.

- Given n, σ, v (three-dimensional quantities) algorithm advances n, σ through time.

- Define

  - Field line integrated density

$$N = \int \frac{en}{\mu B}\, dz$$

  - Field line integrated structure

$$\Sigma = \int \frac{e\sigma}{\mu B}\, dz$$

  - Field line integrated mean wind flux vector

$$F_n = \int \frac{env}{\mu B}\, dz$$

  - Field line integrated structured wind flux vector

$$F_\sigma = \int \frac{en\sigma}{\mu B}\, dz$$

  - Structure Strength Parameter

$$R = \frac{\Sigma N}{\Sigma^2 + N^2}$$

  - Mixing Velocity Vector

$$W = R(F_\sigma/\Sigma - U)$$

    where U is result of potential calculation.

Figure 3-2. Transverse transport algorithm for completely correlated structure--definitions in terms of elemental parameters.

- Convection of Mean

$$\frac{\partial n}{\partial t} = -\nabla \cdot \underbrace{(n\,U}_{\substack{\text{classical}\\ \text{term}}} + \underbrace{\sigma W)}_{\substack{\text{structure}\\ \text{correction}}}$$

- Convection of Structure

$$\frac{\partial \sigma}{\partial t} = -\frac{1}{2\sigma} \underbrace{\nabla \cdot (\sigma^2\, Q)}_{\substack{\text{structure}\\ \text{convection}\\ \text{with velocity}\\ Q}} - \underbrace{W \cdot \nabla n}_{\substack{\text{structure}\\ \text{growth!}}}$$

$$Q = \frac{F_\sigma}{\Sigma} - \frac{N}{\Sigma} W$$

- Potential Eq. (two dimensional)

$$\nabla \cdot J = 0$$

$$J = \frac{N^3}{N^2 + \Sigma^2} (-U \times i_z) + (F_n - R\, F_\sigma) \times i_z$$

Figure 3-3. Transverse transport algorithm for completely correlated structure--equations.

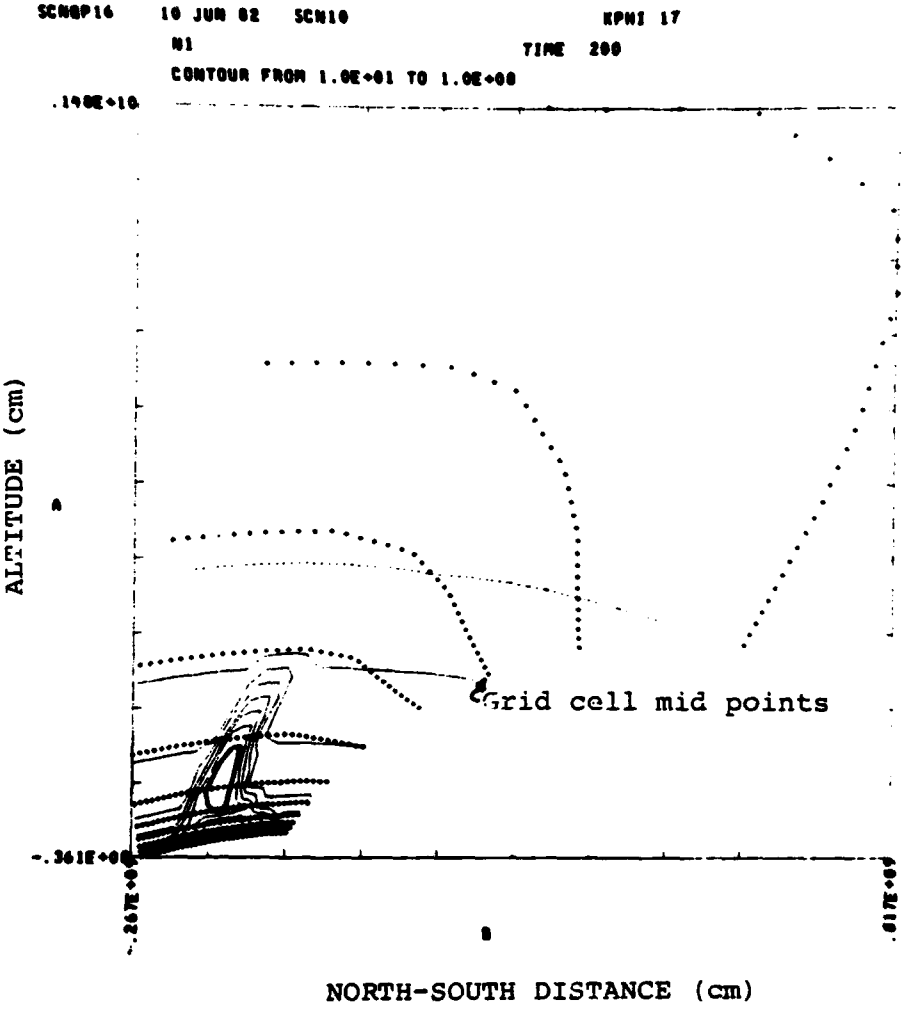

Figure 3-4. Initial density for SCENARIO plasma grid calculation for Cheyenne Mt. calculation.

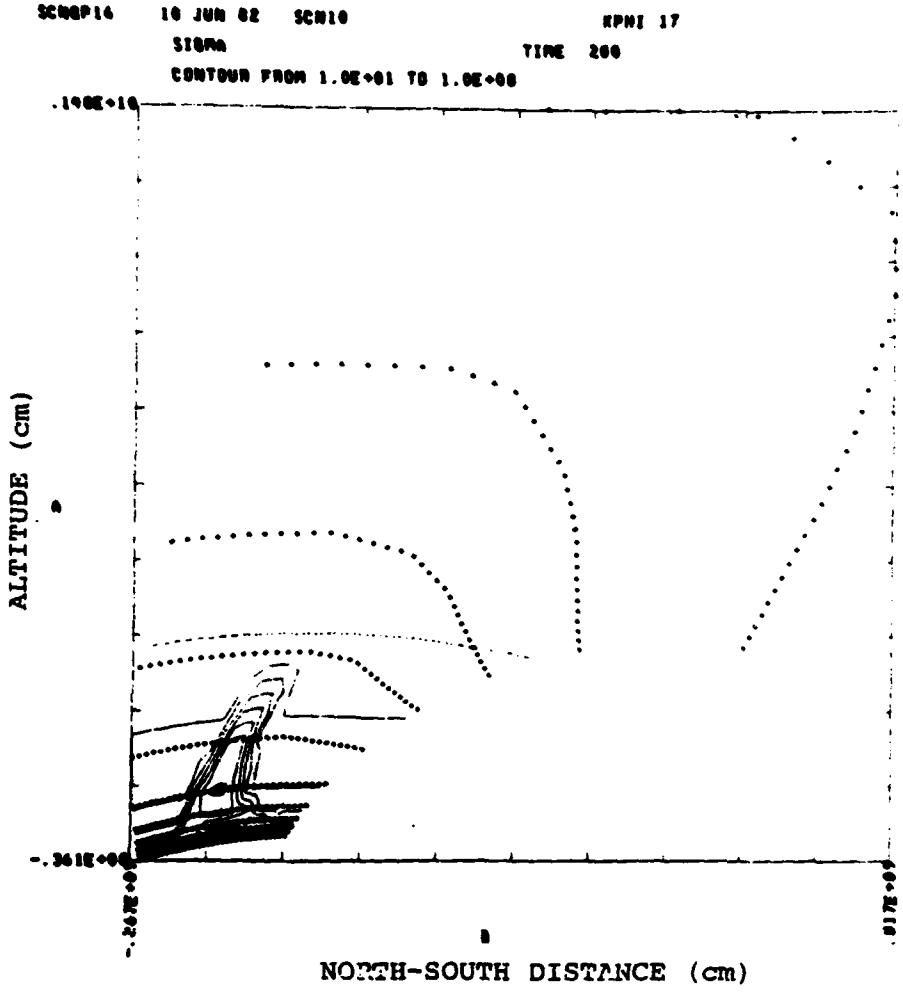

Figure 3-5. Initial standard deviation of plasma density. The initial value is arbitrarily set at 25% of the mean density with all fluctuations assumed to be coherently correlated with the total electron content fluctuations. Crosses denote grid cell centers.

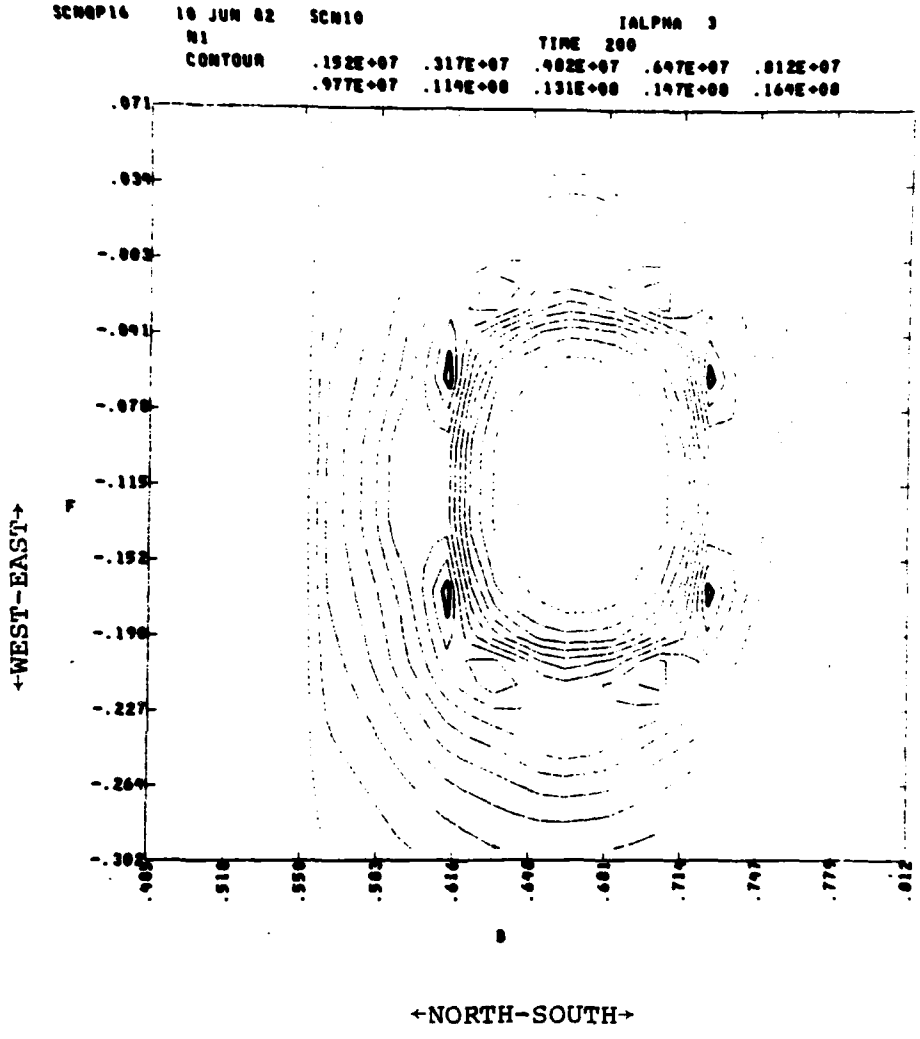

Figure 3-6. Initial density on a constant altitude layer. The layer shown is the third layer of cells from the bottom. On all plots the bold and dotted contours are respectively the maximum and minimum valued contours.

Figures 3-7 and 3-8 show the mean plasma density and the standard deviation of the microstructure at 450 seconds after 250 seconds of further plasma evolution. During this interval the peak density has decreased below 10^8 electrons per cc as a result of the rapid expansion of plasma along field lines. Note that a comparison with the MRC MELT Cheyenne Mountain calculations indicates that in this version of SCENARIO the parallel transport algorithm probably overestimates this expansion.

The transverse transport during this interval on the constant altitude layer shown in Figure 3-4 is illustrated in Figures 3-9 and 3-10. The transverse motion has been governed by a field line averaged neutral wind with a 1-2 kilometer per second northward velocity (as referred to the earth's surface). In response to the wind the structure has moved across the gradients on the north side of the density ring. The initial value of σ of +.25 times the mean decreased through zero to a negative value indicating anti-correlated structure growth. At this time its magnitude begins to approach the mean density.

Figures 3-11 thru 3-14 show the mean plasma density and standard deviation for the results corresponding to Figures 3-7 thru 3-10 obtained at 900 seconds. Continued parallel dynamics are discernible in Figures 3-11 and 3-12. Of interest is the enhanced transverse transport visible in the constant altitude plots of Figures 3-13 and 3-14. Structure has grown to a level of order five times the mean density and has moved toward the north. The mean plasma density has moved with it. The enhanced northward mean density transport is even visible at lower altitudes in the plot of Figure 3-11.

It is evident from the above results that three-dimensional transverse transport algorithms that produce physically appealing results and that have a sturdy

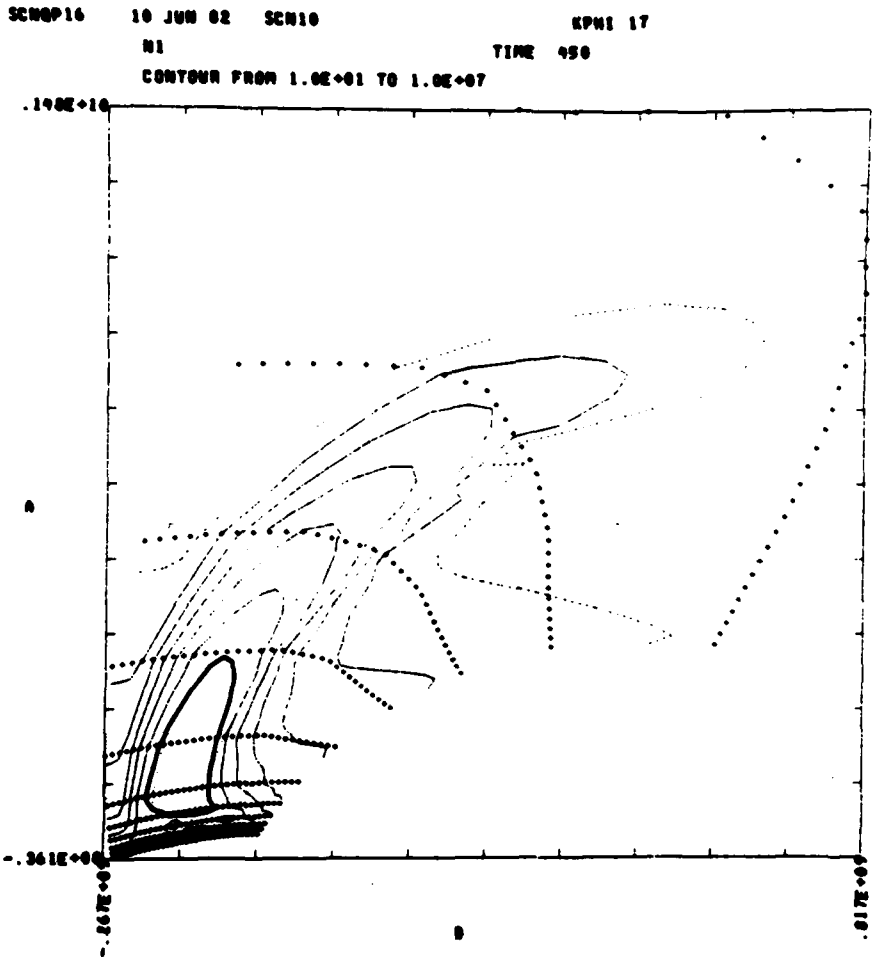

Figure 3-7. Density at 450 seconds. The parallel transport dynamics prominently affect the plasma density.

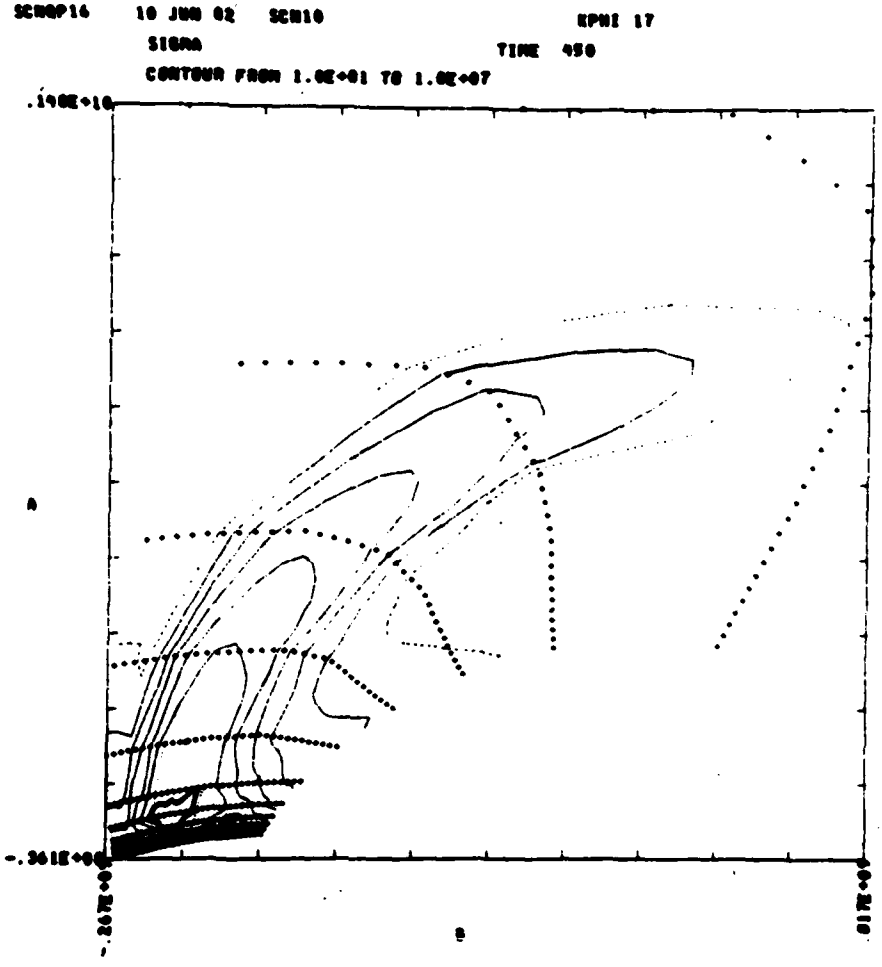

Figure 3-8. Standard deviation at 450 seconds.

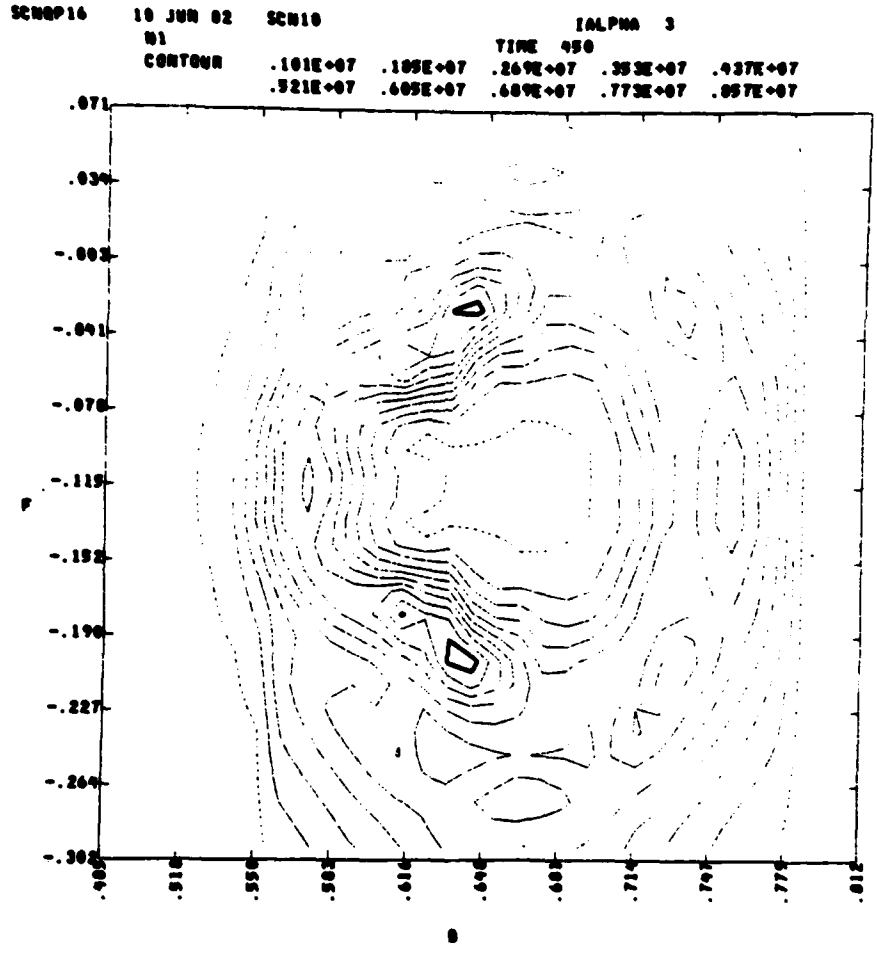

Figure 3-9. Plasma density on constant altitude layer at 450 seconds. This layer is the same layer as shown in Figure 3-6.

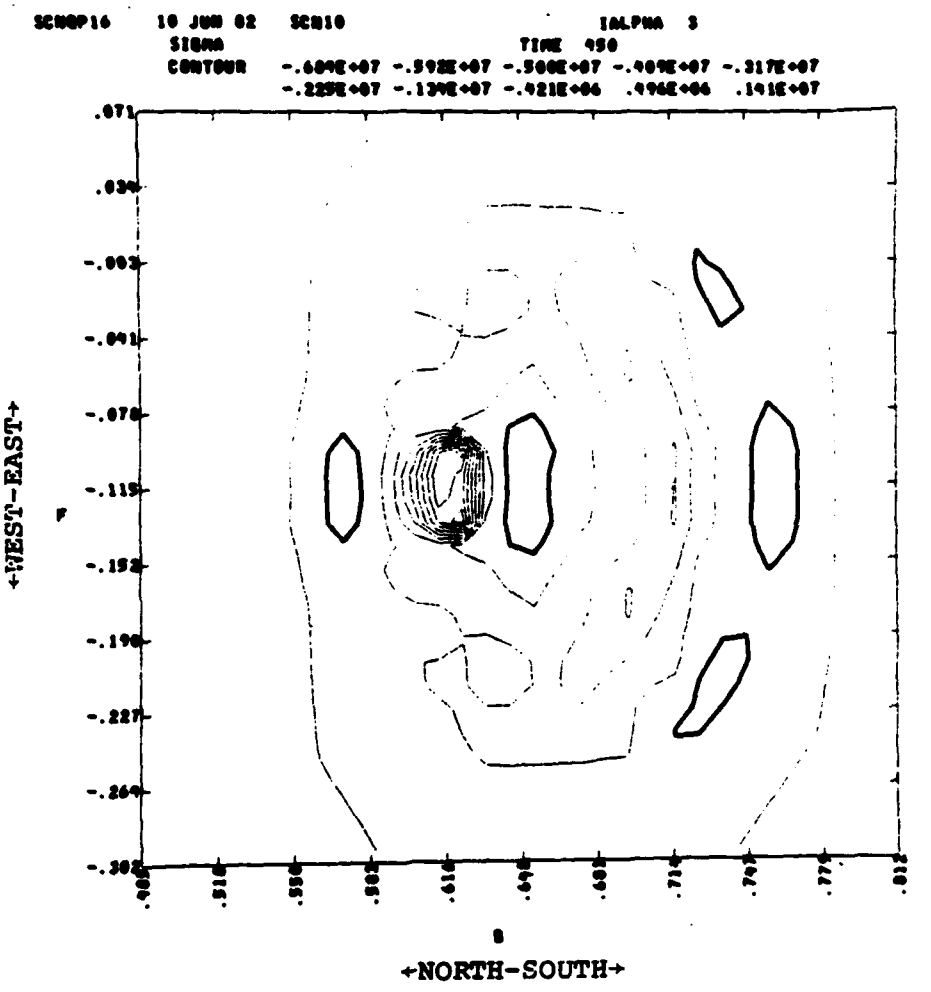

Figure 3-10. Standard deviation of plasma density on constant altitude layer. This layer is the same layer as shown in Figure 3-6. Note the region of negative values which indicate anti-correlated structure growth.

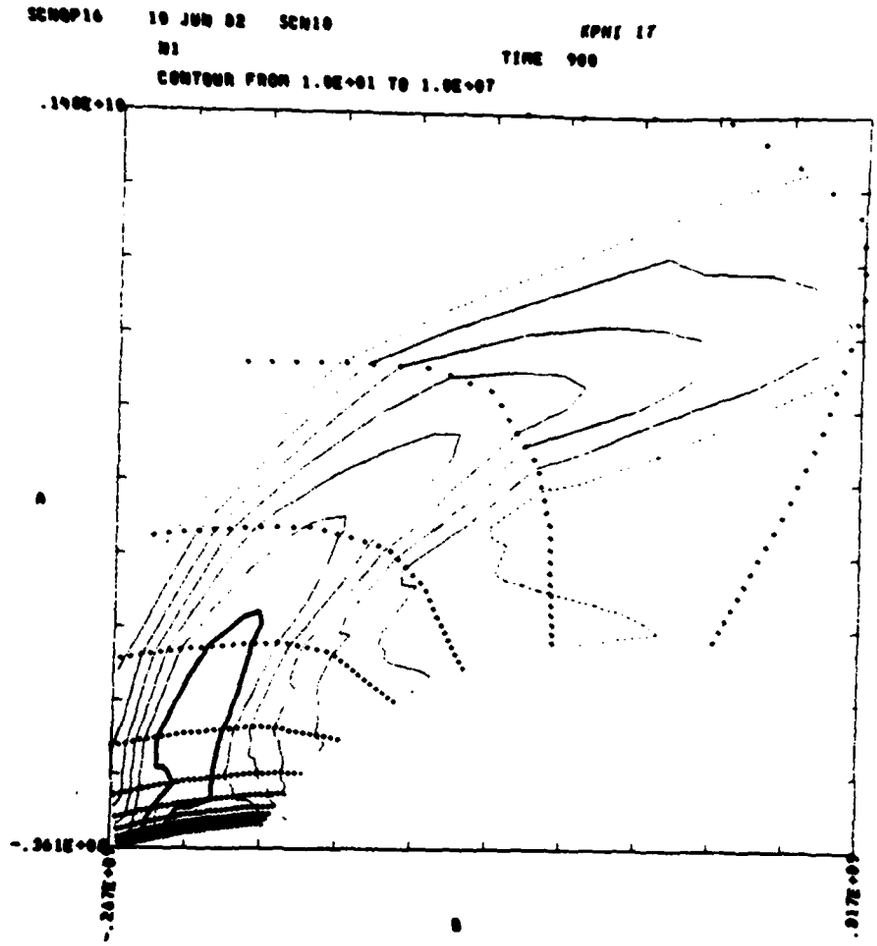

Figure 3-11. Plasma density at 900 seconds.

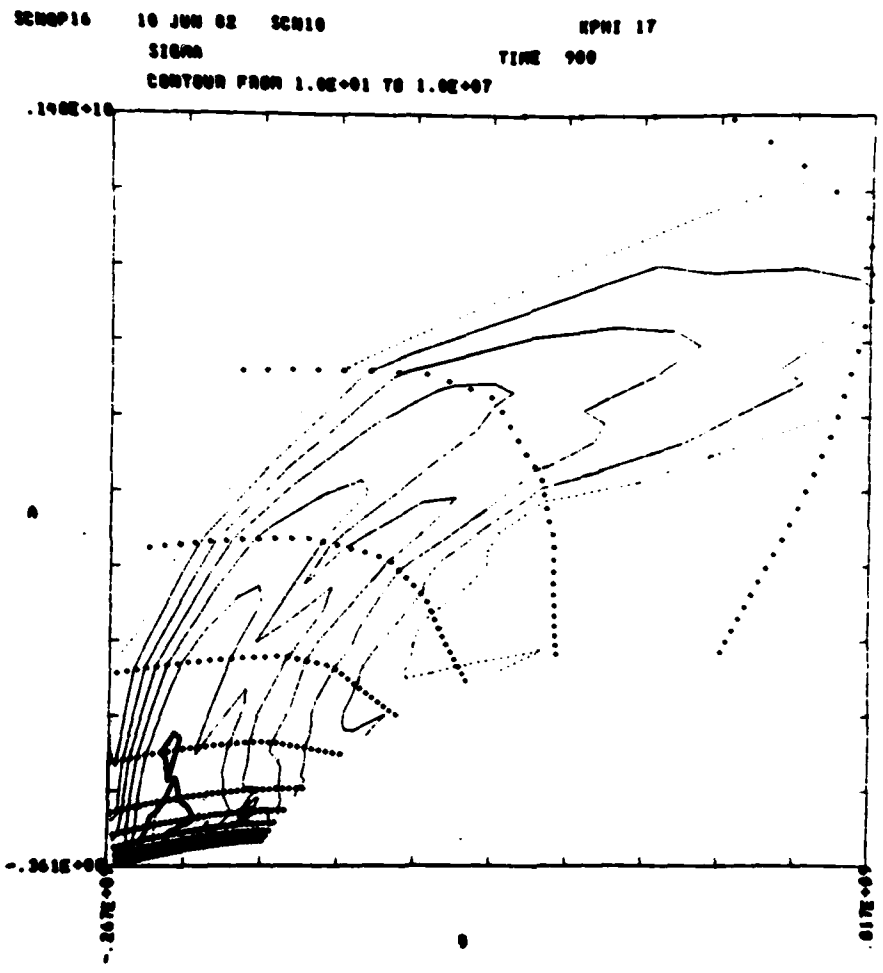

Figure 3-12. Standard deviation of plasma density at 900 seconds.

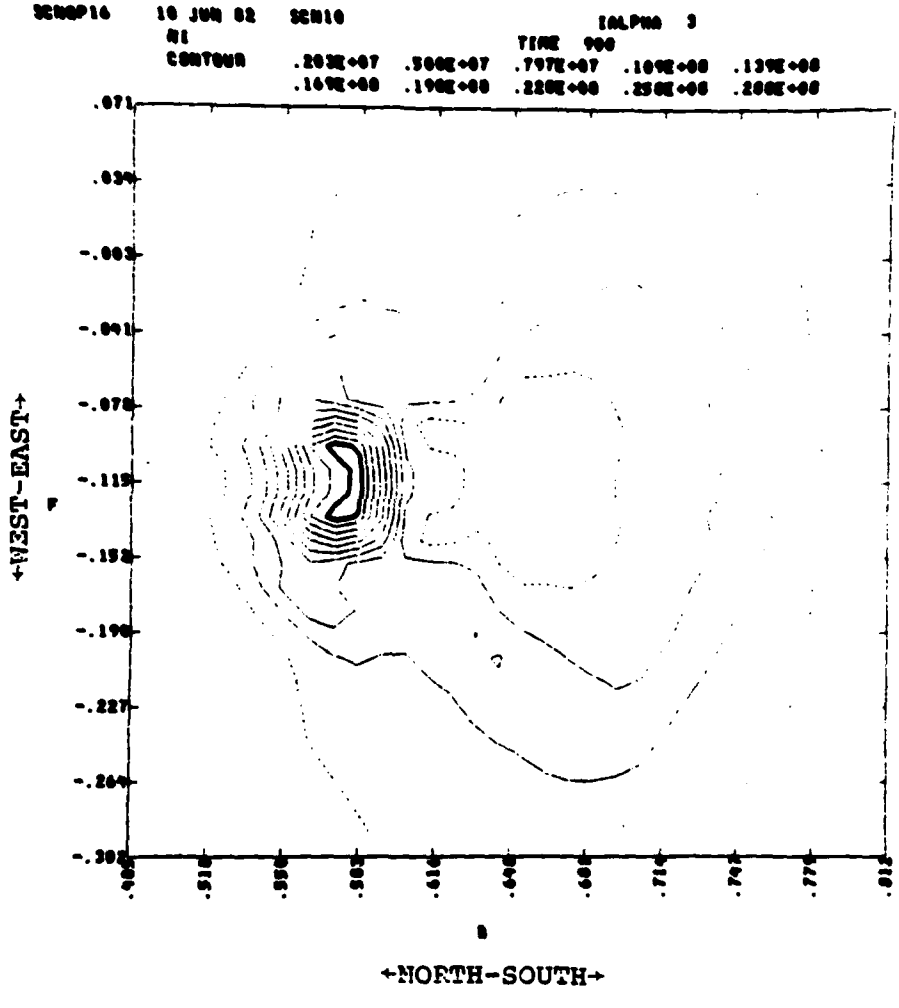

Figure 3-13. Plasma density on a constant altitude layer at 900 seconds. The layer is the same as shown in Figure 3-6. Note the enhanced density convection associated with the enhanced structure seen in Figure 3-14.

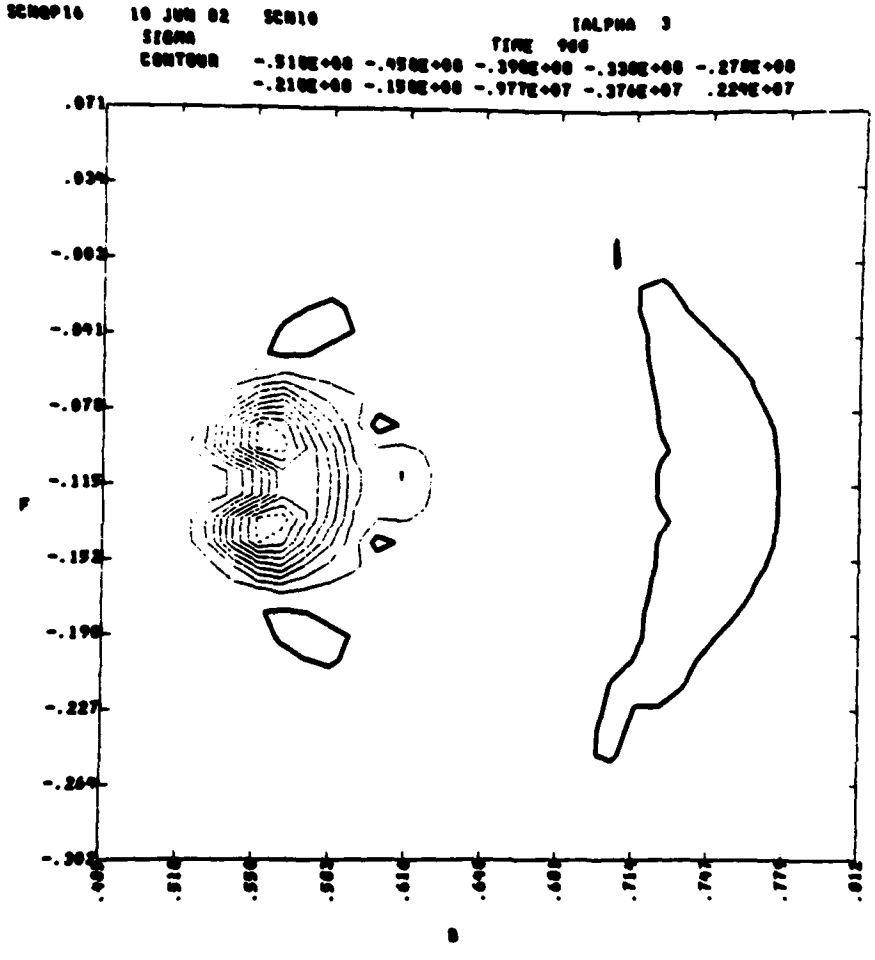

Figure 3-14. Plasma standard deviation on a constant altitude layer at 900 seconds. The layer is the same layer shown in Figure 3-6. Intense structure growth is forming on the north side of the burst because of neutral wind effects.

microstructure theory foundation can be developed for SCENARIO. In this section a set of transport algorithms have been developed under the assumption that structure along field lines is coherently correlated or coherently anti-correlated. Because they allow the structure to be coherently anti-correlated as well as coherently correlated, the algorithms developed herein represent a significant advancement over previously described three-dimensional transverse transport for correlated structure (Stagat, 1982). When the structure is not allowed to grow in an anti-correlated fashion unreliable results are obtained especially in situations where anticorrelated structure growth would have occurred. The numerical results for a Cheyenne Mountain burst SCENARIO run with these algorithms have been seen to produce physically appealing results.

3-3 THREE-DIMENSIONAL TRANSPORT ALGORITHMS FOR UNCORRELATED STRUCTURE

Nuclear structure is believed to be field aligned over distances that are large with respect to their cross-field dimensions. It may be the case, however, that over the very large SCENARIO grid lengths in the direction of the geomagnetic field the fine scale structure may significantly decorrelate. At least two physical processes could cause structure to lose field line coherence, namely, finite parallel conductivity and image growth. Thus while the investigation of uncorrelated microstructure transport algorithms is not only motivated from the standpoint of evaluating both extremes of field line coherence; it is also motivated from a physical standpoint.

This section develops the theory for an algorithm for three-dimensional microstructure transport which could be implemented into SCENARIO. The basic quantities for the algorithm are the local mean density $\langle n \rangle$ and the local microstructure variance σ^2.

Two approaches are available for calculating the structure related conductivity modifications necessary for solution of the two dimensional potential problem. One approach is to calculate the variance of the integrated Pedersen conductivity, Σ^2 and to use this value with the asymptotic closure approximation discussed in Section 2-4 to estimate $\langle 1/N \rangle$. To calculate Σ^2 an approximation which is appropriate for the incoherently aligned structure is

$$\Sigma^2 = \sum (n_o \sigma)^2 / N_2 \tag{3.46}$$

where N_2 is a neutral density normalization quantity with

$$N_2 = \sum n_o^2 \tag{3.47}$$

and where n_o is the local neutral density. Once Σ^2 is determined the asymptotic closure approximation gives $\langle 1/N \rangle$ as $(\Sigma^2 + \langle N \rangle^2)/\langle N \rangle^3$. The potential equation can then be solved to find $\langle U \rangle$.

As discussed in Sections 3-1 and 3-2 $\langle U \rangle$ can be used to find the mean flux of the density and density squared if the five quantities $\langle n/N \rangle$, $\langle n^2/N \rangle$, $\langle V \rangle$, $\langle n\ V \rangle$ and $\langle n^2\ V \rangle$ are known:

$$\langle n\ U \rangle = \left\langle \frac{n}{N} \right\rangle \frac{\langle U \rangle - \langle V \rangle}{\langle 1/N \rangle} + \langle n\ V \rangle \tag{3.48}$$

$$\langle n^2\ U \rangle = \left\langle \frac{n^2}{N} \right\rangle \frac{\langle U \rangle - \langle V \rangle}{\langle 1/N \rangle} + \langle n^2\ V \rangle \tag{3.49}$$

In order to evaluate the five quantities it is necessary to make assumptions about the joint statistics of n and N. In Section 3-2 the form function approximation allowed evaluation of these quantities for coherently aligned structure. For incoherently aligned structure the key assumption is that the two stochastic quantities n and $N - n$ are mutually independent. For this approximation evaluation of $\langle n/N \rangle$ and $\langle n^2/N \rangle$ reduces to the evaluation of

$$\left\langle \frac{n}{n + y} \right\rangle \quad \text{and}$$

$$\left\langle \frac{n^2}{n + y} \right\rangle$$

where y is defined to be $N - n$. Evaluating the expressions in this format accounts for the fact that even though the structure in any layer is uncorrelated with all other layers it is still partially correlated with the field line integrated Pedersen conductivity. Note that $\langle n/N \rangle$ is not being assumed to be $\langle n \rangle \langle 1/N \rangle$.

The next step in the evaluation is to make assumptions regarding the statistics of the local density. Of the possible candidates of Gaussian, log normal, two-level and others, the two-level distribution is numerically attractive and reproduces many of the physical characteristics believed to be present. The main problem with the two level approximation is that for any given pair of structure and mean variance, the chosen levels must both be positive to assure physically realistic quantities. This condition cannot be met with an equally weighted two-level distribution and

consequently the probability density at the two levels must be variably weighted according to an assumed function of the mean and variance. Note that this condition also rules out straightforward use of Gaussian probability densities. While the choice of the two-level density weighting function is somewhat arbitrary, it is felt that the choice which makes the local probability densities satisfy the asymptotic closure relation is an appropriate choice.

Thus it is assumed that on each layer n is distributed according to

$$p(n) = \begin{cases} 1 - \varepsilon; & \text{if } n = n_L \\ \varepsilon; & \text{if } n = n_H \\ 0; & \text{otherwise} \end{cases} \tag{3.50}$$

where n_L, n_H, and ε are functions of the mean value $\langle n \rangle$ and variance σ^2 such that

$$\left\langle \frac{1}{n} \right\rangle = \frac{\sigma^2 + \langle n \rangle^2}{\langle n \rangle^3} \tag{3.51}$$

Explicitly these relations are

$$n_L = \langle n \rangle - \sqrt{\frac{\varepsilon}{1 - \varepsilon}}\,\sigma \tag{3.52}$$

$$n_H = \langle n \rangle + \sqrt{\frac{1 - \varepsilon}{\varepsilon}}\,\sigma \tag{3.53}$$

$$\varepsilon = \frac{1}{2} - \frac{1}{2}\sqrt{\frac{\sigma^2}{\sigma^2 + 4\langle n \rangle^2}} \tag{3.54}$$

Given these local density functions, evaluation of the quantities $\langle n/(n+y)\rangle$ and $\langle n^2/(n+y)\rangle$ at each layer is straightforward. For example

$$\langle n/n+y\rangle = \varepsilon_H\, n_N \int \frac{f(y)\, dy}{n_H + y} + \varepsilon_L\, n_L \int \frac{f(y)\, dy}{n_L + y} \qquad (3.55)$$

where $f(y)$ is the density of y. The density of y is known if the local densities are assumed to be jointly independent. Explicitly the quantity $f(y)$ is a multiple convolution of the two-level density function over all the other layers and is thus comprised of $2^L - 2$ Dirac delta functions of unequal weight where L is the number of SCENARIO cells along the geomagnetic field. The term $\langle n/(n+y)\rangle$ is thus explicitly the sum of 2^L terms that can be straightforwardly evaluated computationally. The values of $\langle n^2/(n+y)\rangle$, $\langle V\rangle$, $\langle n\ V\rangle$ and $\langle n^2\ V\rangle$ can be evaluated similarly.

Given $\langle n/N\rangle$, $\langle n^2/N\rangle$, $\langle V\rangle$, $\langle n\ V\rangle$, and $\langle n^2\ V\rangle$ the mean flux of the density and the density squared can be determined. In a manner similar to that used in Sections 2-4 and 3-2 the n and n^2 continuity equations can be manipulated into an equation for the convection of σ^2. The approach has as yet not been fully developed for SCENARIO algorithms for various reasons. The most important reason is that extensive computation time is required for evaluating the terms like $\langle n/(n+y)\rangle$ over the multi-layer multi-level density function. Future extension of this approach most likely will need to consider approximations to $f(y)$ in these evaluations. It is fair to conclude now, however, that a technique for calculating three-dimensional transverse transport of uncorrelated structure has been set upon a firm theoretical footing.

It is appropriate at this time to mention the other approach available for the evaluation of the mean conductivity $1/\langle 1/N \rangle$. The probability density function for N can be found in a manner similar to that used for finding $f(y)$ in the above evaluation. That is, the probability density of N could be expressed as the convolution of L two-level local plasma density probability densities yielding a function with as many as 2^L unequally weighted Dirac delta functions. Using this probability density function an alternative evaluation for $\langle 1/N \rangle$ for use in the potential equation is possible. Using this approach in an algorithm might also be considered more consistent than using the asymptotic closure assumption approach. It should be noted in the defense of the asymptotic closure approximation to $\langle 1/N \rangle$ in the potential equation that to a large extent the consistency between it and the approximation to $\langle n/N \rangle$ in the convection equation is unimportant in comparison with the other approximations involved. Clearly though, if $\langle 1/N \rangle$ is available in the self-consistent form by using the multi-layer multi-level statistics, its use would seem to be preferable. Both approximations should be considered during any algorithm verification.

SECTION 4

CONCLUSIONS

Numerical simulations of high altitude nuclear explosions cannot be gridded fine enough to spatially resolve the structure in the plasma density. Classical techniques ignore the presence of structure that cannot be resolved.

The importance of the location and intensity of plasma structure for the evaluation of RF propagation effects motivates the application of stochastic theory to the HANE evolution problem. The transport of plasma and plasma structure transverse to the magnetic field is closely related to the problem of the evolution of a two-dimensional plasma. In Section 2 stochastic theory is applied to the 2-d problem and modifications to the classical 2-d split-step evolution algorithm are developed which include micro-structure effects. In Section 3 the 2-d algorithms are extended to the HANE 3-d transverse transport problem for implementation in the SCENARIO code.

Numerical calculations presented in Section 2 demonstrate that structured plasma has a lower effective conductivity than unstructured plasma with the same mean density. Thus, classical algorithms which ignore structure calculate somewhat erroneous current patterns and plasma flow fields. Microstructure algorithms attempt to correct this deficiency by convecting plasma density structure statistics as well as the mean plasma density and by using structure statistics to estimate the local conductivity.

The difference between the classical convection algorithms and the algorithms implemented for convection

in SCENARIO can be understood on a stochastic basis as which quantities are assumed uncorrelated. In the classical algorithms fine scale density fluctuations are assumed to be uncorrelated with the electric field fluctuations. In the SCENARIO algorithms the inverse of the density fluctuations are assumed to be uncorrelated with the fluctuations in the current. The former tends to be the case when structure gradients are parallel with the wind while the latter applies both to the case where the gradients are predominantly perpendicular to the wind and to the case of isotropic structure.

A split-step algorithm which convects the mean plasma density and the r.m.s. density fluctuation level is developed in Section 2. This algorithm is applied to the problem of 2-d evolution of a barium cloud. The results obtained can be considered to be in agreement with observed barium cloud structuring times. The algorithm is also applied to the problem of radial winds through an axisymmetric 2-d structured plasma.

In Section 2 the choice of which statistical parameter should be used in convection algorithms is discussed. Algorithms which use statistical parameters which are not independent of each other, e.g., mean density and mean square density, can produce unphysical results and should be avoided.

The 2-d microstructure theory is extended to the 3-d transverse problem in Section 3. A key consideration in this extension is the correlation of the fluctuations in the direction parallel to the field. The correlation properties are currently specified by assumption. Two orthogonal assumptions have been used to develop convection algorithms. One is the assumption of completely coherent structure along the magnetic field. The other is the assumption of structure that is independent from grid cell to grid cell in the magnetic field direction.

The completely correlated algorithms have been programmed for use in SCENARIO and some SCENARIO results are presented. The results demonstrate the convection of structure and the enhanced convection of the mean density associated with the structure. The growth of coherently anti-correlated structure is also demonstrated. The algorithms presented represent a significant advance over previously used algorithms because they allow for anti-correlated structure growth.

Microstructure theory is a powerful tool which has not as yet been fully exploited. It is perhaps appropriate to point out areas where further application may prove useful.

Image growth of fine scale structure is currently not modelled. Image growth is a consequence of the fact that transverse currents are carried by ions and parallel currents are carried by electrons. This fact leads to plasma enhancements and depletions associated with structure convection. The growth of these regions could be modelled based on calculated values of the divergence of the local transverse current. Note that image growth produces uncorrelated structure.

A natural extension of the algorithms of Section 3 is the development of an algorithm for a field line correlation function with a fixed dependence. It is believed currently that a decomposition of the multi-layer density fluctuations into a basis set of uncorrelated functions through a Gram-Schmidt orthonormalization could be used to extend the uncorrelated algorithms to this special case. The convection algorithms would then be used to advance the statistics of the basis functions.

Given that algorithms for a fixed but arbitrary correlation function along the field line can be developed

a still more ambitious extension is suggested. By accounting for the correlated nature of gradient drift growth and the uncorrelated nature of image growth, the correlation properties along the field could be dynamically altered. This sophisticated approach could then produce structure correlation along the field as a function of time in contrast to merely relying on assumption. While this type of calculation might be of interest on a one-of-a-kind investigation of field line correlation; because of its probable complexity, it would most likely not be suited for use in engineering codes such as SCENARIO. It is mentioned here primarily to point out the advances possible through the application of microstructure theory to the HANE simulation problem.

REFERENCES

Anthanasios Papoulis, Probability, Random Variables, and Stochastic Processes, San Francisco, McGraw-Hill, 1965.

M. Pongratz and T.J. Fitzgerald, "Growth and Decay of km Size Structures on an Ionospheric Barium Cloud," EOS, vol. 62, November 10, 1981, page 988.

R.W. Stagat, D.S. Sappenfield and J.P. Incerti, The SCENARIO Code: Modifications in Version II and the Striation Convection Theory, Mission Research Corporation, Air Force Weapons Laboratory Final Report AFWL-TR-80-124, April 1982.

Robert Stoeckly and Ralph Kilb, Striation Dispersal after Nuclear Burst, Mission Research Corporation, Defense Nuclear Agency Final Report #DNA 5960F, March 1981.

J.B. Workman, S.Y.F. Chu and J.R. Ferrante, A Power Model for Plasma Convection, Berkeley Research Associates, Defense Nuclear Agency, Final Report, DNA 4927F, April 1979.

J.B. Workman and S.Y.F. Chu, Nuclear Environment Models for Communication Analysis, Berkeley Research Associates, Final Report to Mission Research Corporation under contract to USAF Kirtland AFB, NM, PD-BRA-79-215, December 1979.

J.B. Workman and S.T.F. Chu, A Gradient Drift Microstructure Model, Berkeley Research Associates, Defense Nuclear Agency Topical Report DNA 4539T, February 1978.

DISTRIBUTION LIST

DEPARTMENT OF DEFENSE

Defense Nuclear Agency
ATTN: NAFD
ATTN: RAAE, P. Lunn
ATTN: STNA
ATTN: RAEE
ATTN: NATD
3 cy ATTN: RAAE
4 cy ATTN: TITL

Defense Technical Information Center
12 ATTN: DD

DEPARTMENT OF THE ARMY

BMD Advanced Technology Ctr
ATTN: ATC-R, D. Russ
ATTN: ATC-T, M. Capps
ATTN: ATC-O, W. Davies
ATTN: ATC-R, W. Dickinson

BMD Systems Command
ATTN: BMDSC-HLE, R. Webb
2 cy ATTN: BMDSC-HW

DEPARTMENT OF THE NAVY

Naval Ocean Systems Ctr
ATTN: Code 532
ATTN: Code 5323, J. Ferguson
ATTN: Code 5322, M. Paulson

Naval Research Lab
ATTN: Code 4780
ATTN: Code 4780, S. Ossakow
ATTN: Code 4187
ATTN: Code 7500, B. Wald
ATTN: Code 4700
ATTN: Code 4720, J. Davis
ATTN: Code 7950, J. Goodman
ATTN: Code 6700

DEPARTMENT OF THE AIR FORCE

Air Force Geophysics Lab
ATTN: OPR, H. Gardiner
ATTN: OPR-1
ATTN: LKB, K. Champion
ATTN: CA, A. Stair
ATTN: PHY, J. Buchau
ATTN: R. Babcock
ATTN: R. O'Neil

Air Force Weapons Lab
ATTN: SUL
ATTN: NTYC
ATTN: NTN

DEPARTMENT OF ENERGY CONTRACTORS

Los Alamos National Labs
ATTN: MS 670, J. Hopkins
ATTN: P. Keaton
ATTN: MS 664, J. Zinn
ATTN: T. Kunkle, ESS-5
ATTN: R. Jeffries
ATTN: D. Simons
ATTN: J. Wolcott

DEPARTMENT OF ENERGY CONTRACTORS (Continued)

Sandia National Labs
ATTN: D. Thornbrough
ATTN: Tech Lib 3141
ATTN: D. Dahlgren
ATTN: Space Project Div
ATTN: Org 4231, T. Wright
ATTN: Org 1250, W. Brown

DEPARTMENT OF DEFENSE CONTRACTORS

BDM Corp
ATTN: T. Neighbors
ATTN: L. Jacobs

Berkeley Research Associates, Inc
ATTN: S. Brecht
4 cy ATTN: C. Prettie
4 cy ATTN: J. Workman
4 cy ATTN: S. Chu

Cornell University
ATTN: D. Farley Jr
ATTN: M. Kelly

EOS Technologies, Inc
ATTN: B. Gabbard

General Electric Co
ATTN: A. Steinmayer
ATTN: C. Zierdt

GTE Communications Products Corp
ATTN: J. Concordia
ATTN: I. Kohlberg

Institute for Defense Analyses
ATTN: J. Aein
ATTN: E. Bauer
ATTN: H. Wolfhard
ATTN: H. Gates

JAYCOR
ATTN: J. Sperling

Kaman Tempo
ATTN: B. Gambill
ATTN: K. Schwartz
ATTN: DASIAC
ATTN: J. Devore
ATTN: W. McNamara

Kaman Tempo
ATTN: DASIAC

Pacific-Sierra Research Corp
ATTN: H. Brode, Chairman SAGE

Physical Dynamics, Inc
ATTN: E. Fremouw

Physical Research, Inc
ATTN: R. Deliberis
ATTN: T. Stephens

R&D Associates
ATTN: B. Yoon

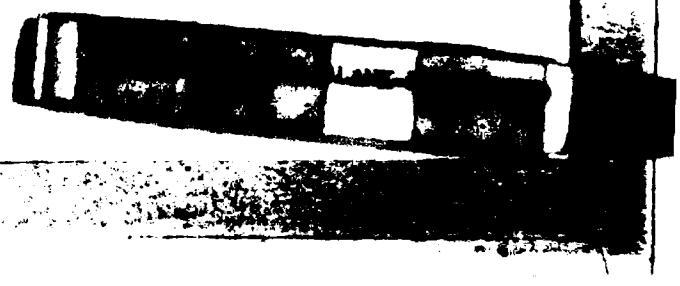

DEPARTMENT OF DEFENSE CONTRACTORS (Continued)

Mission Research Corp
ATTN: C. Lauer
ATTN: Tech Library
ATTN: F. Fajen
ATTN: R. Kilb
ATTN: S. Gutsche
ATTN: R. Bigoni
ATTN: R. Bogusch
ATTN: F. Guigliano
ATTN: G. McCartor
ATTN: D. Knepp
ATTN: R. Hendrick

R&D Associates
ATTN: R. Turco
ATTN: W. Karzas
ATTN: H. Ory
ATTN: C. Greifinger
ATTN: P. Haas
ATTN: M. Gantsweg
ATTN: F. Gilmore
ATTN: W. Wright

Rand Corp
ATTN: E. Bedrozian
ATTN: C. Crain
ATTN: P. Davis

Rand Corp
ATTN: B. Bennett

Toyon Research Corporation
ATTN: J. Ise
ATTN: J. Garbarino

DEPARTMENT OF DEFENSE CONTRACTORS (Continued)

Science Applications, Inc
ATTN: L. Linson
ATTN: D. Hamlin
ATTN: C. Smith
ATTN: E. Straker

SRI International
ATTN: R. Tsunoda
ATTN: J. Vickrey
ATTN: W. Chesnut
ATTN: R. Leadabrand
ATTN: R. Livingston
ATTN: D. McDaniels
ATTN: M. Baron
ATTN: G. Price
ATTN: D. Neilson
ATTN: A. Burns
ATTN: W. Jaye
ATTN: J. Petrickes
ATTN: C. Rino
ATTN: V. Gonzales
ATTN: G. Smith

Stewart Radiance Lab
ATTN: J. Ulwick

Technology International Corp
ATTN: W. Boquist

Visidyne, Inc
ATTN: G. Humphrey
ATTN: O. Shepard
ATTN: W. Reidy
ATTN: J. Carpenter